THE IDENTIFICATION OF *DICTYOSTELIUM* PHOSPHOPROTEINS ALTERED IN RESPONSE TO THE ACTIVATION OF RASG

By

DAVID MATTHEW SECKO

B.Sc. (Hons), Queen's University, 1998

A THESIS SUBMITTED IN PARTIAL FULFILLMENT OF THE REQUIREMENTS FOR THE DEGREE OF

DOCTOR OF PHILOSOPHY

In

THE FACULTY OF GRADUATE STUDIES

(Department of Microbiology and Immunology)

We accept this thesis as conforming to the required standard

THE UNIVERSITY OF BRITISH COLUMBIA

June 2004

THE INDENTIFICATION OF *DICTYOSTELIUM* PHOSPHOPROTIENS ALTERED IN RESPONSE TO THE ACTIVATION OF RASG

By

DAVID MATTHEW SECKO

B.Sc. (Hons), Queen's University, 1998

A THESIS SUBMITTED IN PARTIAL FULFILLMENT OF THE REQUIREMENTS FOR THE DEGREE OF

DOCTOR OF PHILOSOPHY

In

THE FACULTY OF GRADUATE STUDIES

(Department of Microbiology and Immunology)

We accept this thesis as conforming to the required standard

THE UNIVERSITY OF BRITISH COLUMBIA

June 2004

ABSTRACT

Dictyostelium RasG has been implicated in the regulation of a variety of cellular processes, including the initiation of development, cell movement, and cytokinesis, but the molecular components of the signaling pathways involved are largely unknown. This thesis describes the search for putative downstream targets of the RasG signaling pathway through the identification of proteins whose level of phosphorylation were changed in response to the induction of a gene encoding an activated form of RasG, RasG(G12T).

Two expression systems were tested to increase the level of RasG(G12T) in the cell. One system used the *rasG*(G12T) gene fused to the ribonucleotide reductase (*rnrB*) promoter. Induction of RasG(G12T) expression from this promoter was accompanied by a decrease in *discoidin* mRNA levels, a proposed negatively regulated target of RasG. Regulation of Discoidin expression was also down regulated in *rasG* null cells under all experimental conditions, but the response to well established *discoidin* regulators still occurred in this strain. These results revealed a role for RasG in modulating *discoidin* gene expression. A tetracycline-regulated expression system was used to study the effect of increasing the level of RasG(G12T) on the phosphorylation state of *Dictyostelium* proteins. Over 70 phosphorylated proteins in vegetative cells were resolved by 2D immunoblot analysis and thirteen proteins, which reproducibly changed in response to RasG(G12T) expression, were recovered from 2D gels and identified by mass spectrometry. The proteins identified were: the signaling proteins RasGEF-R and protein kinase B (PKB), the adhesion protein DdCAD-1, the cytoskeletal protein actin, the mitochondrial division protein FtsZA, as well as several proteins involved in protein translation or metabolism. An additional set of experiments showed that phosphorlyation of the vacuolar H+-ATPase component VatA upon folate stimulation was modulated by RasG.

Two of the proteins whose phosphorylation levels were affected by RasG(G12T), DdCAD-1 and PKB, were analyzed further. Cells expressing RasG(G12T) exhibited increased cohesion and this increase correlated with DdCAD-1 localization and dephosphorylation. Induction of RasG(G12T) was also found to up-regulate both the basal and folate-induced level of phosphorylation of PKB, and cells expressing RasG(G12T) contained slightly more membrane bound PKB. Together the presented work has identified several proteins whose phosphorylation state was affected by RasG(G12T) and additional regulatory roles for RasG.

TABLE OF CONTENTS

LIST OF TABLES

LIST OF FIGURES

LIST OF ABBREVIATIONS

2D	two-dimensional
AC	adenylyl cyclase
aleA	*aimless* gene – RasGEF homologues
BSA	bovine serum albumin
cAMP	adenosine 3′,5′-cyclic monophosphate
cAR	cAMP receptor
CHAPS	3-[3-cholamidopropyl)dimethylammonio]-1-propanesulfonate
CMF	conditioned media factor
DdCAD-1	*Dictyostelium discoideum* calcium-dependent adhesion molecule-1
DMSO	dimethyl sulfoxide
DTT	dithiothreitol
EDTA	disodium ethylenediamine tetraacetic
EGF	epidermal growth factor
EGFR	epidermal growth factor receptor
ERK	extracellular regulated protein kinase
FITC	fluorescein isothiocyanate
GAP	GTPase activating protein
GDI	guanine nucleotide dissociation inhibitor
GDP	guanosine 5′-diphosphate
GEF	guanine nucleotide exchange factor
GPCR	G-protein coupled receptor
GTP	guanosine 5′-triphosphate
HEPES	N-[2-hydroxyethyl]piperazine-N′-[2-]ethanesulfonic acid
HL5	nutrient rich axenic growth media
HPLC	high pressure liquid chromatography
hrs	hours
IEF	isoelectric focusing
kDa	kilodalton
KK2	potassium phosphate buffer

LRR	leucine-rich repeat
MAPK	mitogen activated protein kinase
min	minutes
MMS	methyl methanesulfonate
MS	mass spectrometry
MSV	murine leukaemia virus
PAGE	polyacrylamide gel electrophoresis
PBS	phosphate-buffer saline
PDK	phosphoinositide dependent kinase
PEG	polyethylene glycol
PH	pleckstrin homology
pI	isoelectric point
PI3K	phosphoinositide 3-kinase
PKA	protein kinase A
PKB	protein kinase B
PSF	pre-starvation factor
PTB	phosphotyrosyl binding
PtdIns(3,4,5)P_3	phosphatidylinositol 3,4,5-bisphosphate
PTEN	phosphatase and tensin homologue
PTK	protein tyrosine kinase
PVDF	polyvinylidene difluoride
REMI	restriction enzyme-mediated integration
RIP	Ras-interacting protein
RTK	receptor tyrosine kinase
SDS	sodium dodecyl sulfate
sec	seconds
SH2	Src homology 2
Sos	Son of sevenless
t	time
TBS	Tris-buffered saline
TEMED	N,N,N′,N′-tetramethyl-ethylenediamine

ACKNOWLEDGEMENTS

I would like to acknowledge the work and the play of those that I have spent anywhere from hours to days to years alongside while working towards this degree. In a room, lodged away in the middle of Wesbrook, time has flown and folks have come and gone, to each of you, my salutations. Specifically, I would like to thank Meenal Khosla for her help and collaboration on the *discoidin* project and for teaching me how to keep amoebae happy. My appreciation to James Lim for his insight on assays and what a dusty piece of lab equipment, long forgotten, might be useful for. Thanks to Helmut Kae for his ability to ask and answer the question: "what would happen if we did this?" To Michelle Wyse, the last of a wandering Weeks flock, I raise my glass to your inquisitive thinking and drive to understand science. To Parvin, Zahara, Shiv, Rujun, and all my other colleagues, I appreciate your time and effort. To my supervisors, Gerry Weeks and George Spiegelman, I express gratefulness and joy. Gerry you taught me to organize my thoughts and how to design my endeavors. George you taught me how to solve problems and think critically. Together you have taught me what I desired to learn and opened my mind to the possibilities.

Dedicated to my father

Who taught a boy that knowledge is astounding

Bought him a plane ticket to B.C.

And never tires of science

1 INTRODUCTION

1.1 A historical introduction to Ras research

This thesis is part of an endeavor to further understand the role that Ras proteins play in regulating cellular functions. Research on Ras can be traced back 40 years to a murine leukaemia virus (MSV) and Jennifer Harvey, who showed this virus to be capable of inducing sarcomas in newborn rodents (Harvey, 1964). Viruses similar to the Harvey (Ha-MSV) strain were soon discovered, including Kirsten-MSV (Kirsten and Mayer, 1967), but their molecular characterization would wait some years due to a self-imposed ban on molecular cloning that was lifted in 1977 (Malumbres and Barbacid, 2003). Nonetheless, during this time it was becoming clear that these viruses were recombinant and that their oncogenic properties were due to their possession of genomic rat sequences (Scolnick *et al.*, 1973). This came as an enormous shock and interest quickly shifted to these cellular 'oncogenes'. In 1979, reports appeared that genomic DNA from human tumor cell lines could transform NIH-3T3 cells, revealing that cellular genetic elements were capable of inducing these transformations (Shih *et al.*, 1979; Perucho *et al.*, 1981). Channing Der made the definitive connection three years later (Der *et al.*, 1982), revealing that the Harvey and Kirsten viral oncogenes, which were given the acronym *ras* for *ra*t *s*arcoma, were the same as the cellular oncogenes that had been used to transform NIH-3T3 cells. The study of human H-*ras* and K-*ras* was born and shortly thereafter a third highly related *ras* oncogene, N-*ras*, was identified (for review see Barbacid, 1987). This pioneering work on tumor inducing viruses, which many had originally thought to be "irrelevant", has sparked an extensive research field directed towards better understanding how Ras proteins regulate cell function (Malumbres and Barbacid, 2003).

1.2 An overview of Ras biology

Ras proteins are undoubtedly important: the numerous biological functions to which they have been linked (e.g. proliferation, transformation, differentiation and apoptosis) and the fact that 20-30% of human cancers involve Ras mutations (Bos, 1989; Shields *et al.*, 2000) should leave no question of this. In addition, all eukaryotic organisms thus far studied contain at least one highly conserved Ras protein (Barbacid, 1987; Bourne *et al.*, 1991). This widespread distribution has been an asset to the goal of understanding Ras function, with information being

garnered from a variety of organisms, such as yeasts (*Saccharomyces cerevisiae* and *Schizosaccharomyces pombe*), *Drosophila*, *Caenorhabditis elegans*, *Dictyostelium discoideum* and mammalian cells (Egan and Weinberg, 1993; Wassarman *et al.*, 1995; Campbell *et al.*, 1998; Sternberg and Han, 1998; Weeks and Spiegelman, 2003). In the early 1990s, a synthesis of observations from these diverse organisms indicated a role for Ras in the transmission of signals from the cell surface to the nucleus (Egan and Weinberg, 1993).

Since this time, the known physiological functions of Ras proteins have grown and for mammalian H-, K- and N-Ras proteins can be summarized into the five following categories. Firstly, it is well established that Ras proteins are involved in the transmission of mitogenic signals and proliferation (Campbell *et al.*, 1998). In fact, Ras has been linked to cell cycle progression potentially through cyclin D1 (Pruitt and Channing, 2001). Secondly, Ras proteins play essential roles in development; for example, mammalian K-*ras* is essential for mouse embryogenesis (Johnson *et al.*, 1997). Thirdly, Ras has been linked to apoptosis and senescence, a process that may occur through the activation of the proteins such as $p27^{Kip1}$, $p21^{Cip1}$, $p19^{Arf}$ and $p16^{INK4a}$ (Ehrhardt *et al.*, 2002). Fourthly, H-Ras has been linked to the regulation of cell adhesion through effects on integrin activation (Hughes *et al.*, 1997). Lastly, Ras proteins have been implicated in regulating the actin cytoskeleton potentially through effects on Rac activation (Burridge and Wennerberg, 2004). This section will briefly review our current understanding of how Ras is thought to function in these roles.

1.2.1 The Ras superfamily of proteins

Ras proteins comprise one subfamily of a large superfamily of proteins referred to as the Ras superfamily (Takai *et al.*, 2001). This superfamily already numbers over 100 members that are divided in five subfamilies based on sequence relatedness: Rho, Rab, Sar1/Arf, Ran and Ras. All the members of the superfamily are small (20-40 kDa), monomeric proteins that bind guanine nucleotides (resulting in them often being referred to as GTP-binding proteins). Each subfamily appears to regulate distinct functions within the cell (reviewed in Takai *et al.*, 2001); Rho subfamily proteins regulate cytoskeletal organization and gene expression; Rab and Sar1/Arf subfamily members regulate intracellular vesicle trafficking; Ran subfamily proteins regulate nuclear cytoplasmic transport and microtubule organization during the cell cycle; and Ras proteins integrate cell surface signals to cellular processes like proliferation, transformation,

differentiation and apoptosis. A great deal has been learned about each of the five subfamilies (reviewed by Bourne *et al.* 1991; Takai *et al.*, 2001), but the rest of this section will deal solely with the Ras subfamily.

1.2.2 The GTP/GDP switch

All members of the Ras superfamily function as nucleotide-dependent molecular switches (*Figure 1*). This function relies on the ability of these proteins to switch between two conformations: an active GTP-bound form and an inactive GDP-bound form (Bourne *et al.*, 1991). The switch has been most extensively studied for Ras subfamily proteins, where the modulation between these two conformations requires three types of regulatory proteins. The first are guanine nucleotide exchange factors (GEFs) that promote the formation of active Ras-GTP, the second are GTPase activating proteins (GAPs) that promote the hydrolysis of Ras-GTP to Ras-GDP and the last are guanine nucleotide dissociation inhibitors (GDIs) that keep Ras in the GDP-bound form (Boguski and McCormick, 1993; Geyer and Wittinghofer, 1997). As depicted in Figure 1, the concerted action of these proteins can be considered a cycle, which regulates the "on" (Ras-GTP) and "off" (Ras-GDP) states of Ras, ultimately allowing Ras to act as a switch in signal transduction pathways. The importance of the Ras cycle is emphasized by the perturbations that occur as a result of various mutations of Ras. Single amino acid substitution at position 12 or 61 results in the locking of Ras in the active GTP-bound form, while substitution at position 17 prevents GTP binding and thus Ras activation (Barbacid, 1987). These mutations prevent normal Ras function by interfering with the GDP/GTP cycle. In fact, mutations that lock Ras in the active GTP-bound form are often found in human tumor cells (Bos, 1989).

1.2.3 Ras activation

In mammalian cells, Ras is activated, i.e. stimulated to switch GDP for GTP, in response to the stimulation of receptor tyrosine kinases (RTKs), receptor-associated protein tyrosine kinases (PTKs) or G-protein coupled receptors (GPCRs) (reviewed in Schlessinger, 2000; Genot and Cantrell, 2000; Marinissen and Gutkind, 2001).

Epidermal growth factor (EGF) mediated activation of Ras provides an example of the process with regard to RTK stimulation (Schlessinger, 2000; Carpenter, 2000). EGF stimulation of the EGF receptor (EGFR) promotes the autophosphorylation of various tyrosine residues in

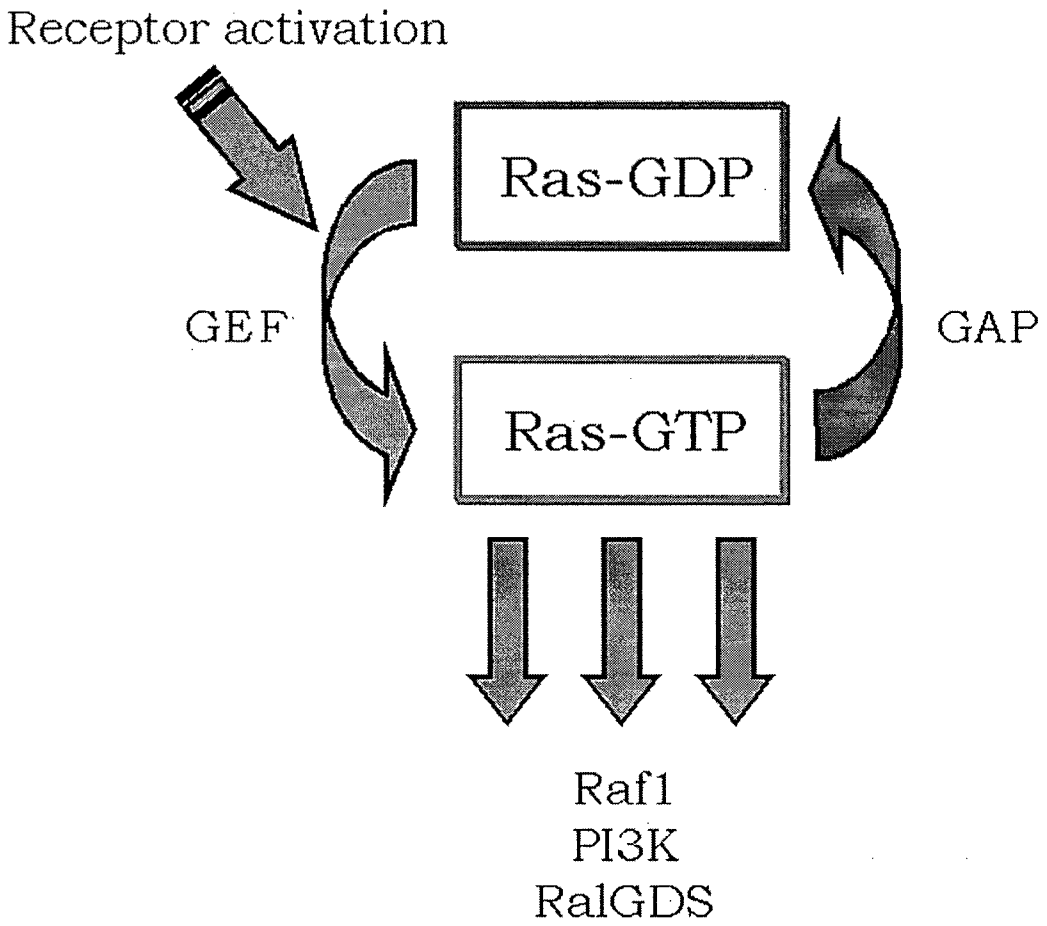

Figure 1. **A model of the Ras GTP/GDP switch.** Cell receptor stimulation results in a guanine nucleotide exchange factor (GEF) facilitating the displacement of GDP and the binding of GTP to Ras. Ras-GTP then interacts and activates downstream effector molecules, such as Raf1, phosphatidylinositide 3-kinase (PI3K) and RalGDS. A GTPase activating protein (GAP) promotes the hydrolysis of Ras-GTP to RasGDP terminating Ras activity.

the cytoplasmic domain of EGFR. This tyrosine phosphorylation leads to the association of the adaptor proteins Shc and Grb2 through their Src homology 2 (SH2) and/or phosphotyrosyl binding (PTB) domains (Pawson and Scott, 1997). Grb2 and a RasGEF, Son of sevenless (Sos), then associate through an interaction between the C-terminus of Sos and the SH3 domains of Grb2 (Pawson and Schlessinger, 1993), bringing Sos into close proximity with Ras at the plasma membrane and allowing Ras activation through GDP/GTP exchange (Downward, 1996).

Ras activation can also occur through the stimulation of receptor-associated PTKs, as in the case of ligand binding to immunoreceptors in B- and T-lymphocytes (Genot and Cantrell, 2000). In contrast to RTKs, these receptors possess no intrinsic tyrosine kinase activity and instead recruit PTKs to the membrane. Once recruited upon receptor stimulation, these PTKs phosphorylate tyrosine residues on immunoreceptors, which serve to further recruit Syk/Zap70 and adaptor proteins such as LAT and Shc (Genot and Cantrell, 2000). This results in the recruitment of the Grb2/Sos complex and the activation of Ras. The mechanism of Ras activation upon GPCRs stimulation has remained more elusive, but is believed to involve the Gß? subunits of heterotrimeric G-protein and Src kinase acting to allow the transactivation of RTKs and thus Ras activation (Marinissen and Gutkind, 2001).

The above paradigms represent an over-simplification and in reality other components also regulate the activation process. Thus, there are additional RasGEFs in mammalian cells, for example the Ras-guanine-nucleotide-releasing factor 1 (Ras-GRF1; also known as $CDC25^{Mm}$) and closely related protein Ras-GRF2 that act as Ca^{2+}-regulated Ras exchange factors (Cullen and Lockyer, 2002), the Ras guanine nucleotide-releasing protein (Ras-GRP; also known as CalDAG-GEFII) that acts as Ca^{2+}- and diacylglycerol-regulated Ras exchange factors (Cullen and Lockyer, 2002), and three RasGEFs (MR-GEF, PDZ-GEF and GRP3) (Rebhun *et al.*, 2000). Furthermore, 173 human genes have been identified whose encoded proteins are related to Ras superfamily GAPs and it has been suggested that at least 14 of these genes are RasGAPs (Bernards, 2003).

1.2.4 Ras Effectors

Activated Ras interacts with a variety of effector proteins to transmit the activation signal downstream, a process that occurs through multiple cascades of cytoplasmic proteins (Marshall, 1996). Ras effectors preferentially interact with active Ras-GTP, as opposed to Ras-

GDP, through the Switch 1 and Switch 2 regions of Ras, with the Switch 1 comprising amino acids 30-38 (which includes the Ras effector domain) and Switch 2 comprising amino acids 60-76 (Milburn *et al.*, 1990; Marshall, 1996; Boriack-Sjodin *et al.*, 1998; Herrmann, 2003). The Ras effectors bear little sequence homology but contain a structurally similar Ras binding domain (RBD) that is responsible for the interaction with Ras (Herrmann, 2003).

Kinases of the Raf family, phosphoinositide 3-kinase (PI3Ks) and RalGEFs are three classes of proteins that have been sufficiently investigated to be considered as definite Ras effectors (Marshall, 1996; Campbell and Der, 2004). Other proteins have been implicated as Ras effectors, although their involvement is currently less well defined (Campbell *et al.*, 1998; Cullen, 2001). Therefore, Ras effectors can be generalized into three groups: kinases, GEFs for other Ras Superfamily proteins and effectors with uncertain functions (*Figure 2*) (Ehrhardt *et al.*, 2002).

The first Ras effector to be identified was the serine/threonine kinase Raf (Vojtek *et al.*, 1993). Shown to be recruited to the plasma membrane upon the activation of Ras and subsequently itself activated, the Raf kinase is an important transducer of biological signals (Morrison and Cutler, 1997; Takai *et al.*, 2001). A cascade of cytoplasmic protein phosphorylation results from Ras activation of Raf (Morrison and Cutler, 1997), which begins with Raf phosphorylating and activating MEK, which in turn, phosphorylates and activates ERKs. Further transmission of the signal is achieved by the translocation of ERKs into the nucleus where they activate several transcription factors (e.g. Jun and Elk-1). Thus, the coupling of Ras to gene expression is mediated by the activation of kinase cascades that stimulate the phosphorylation and activation of transcription factors.

The next-best-characterized Ras effector is phosphoinositide 3-kinase (PI3K) (Rodriguez-Viciana *et al.*, 1997), which when activated in mammalian cells regulates apoptosis and rearrangements of the actin cytoskeleton (Shields *et al.*, 2000). Activated PI3K catalyzes the formation of phosphatidylinositol 3,4,5-bisphosphate (PtdIns(3,4,5)P_3) (Katso *et al.*, 2001). PtdIns(3,4,5)P_3 acts as a membrane docking site for the recruitment of pleckstrin homology (PH) domain containing proteins, such as PKB, also known as AKT (Cozier *et al.*, 2004). The presence of PtdIns(3,4,5)P_3 in the membrane causes PKB and phosphoinositide dependent kinase 1 (PDK1) to localize to the membrane. PDK1 then directly phosphorylates one of two sites on PKB that are required for PKB activation (Fresno Vara *et al.*, 2004). The kinase responsible for

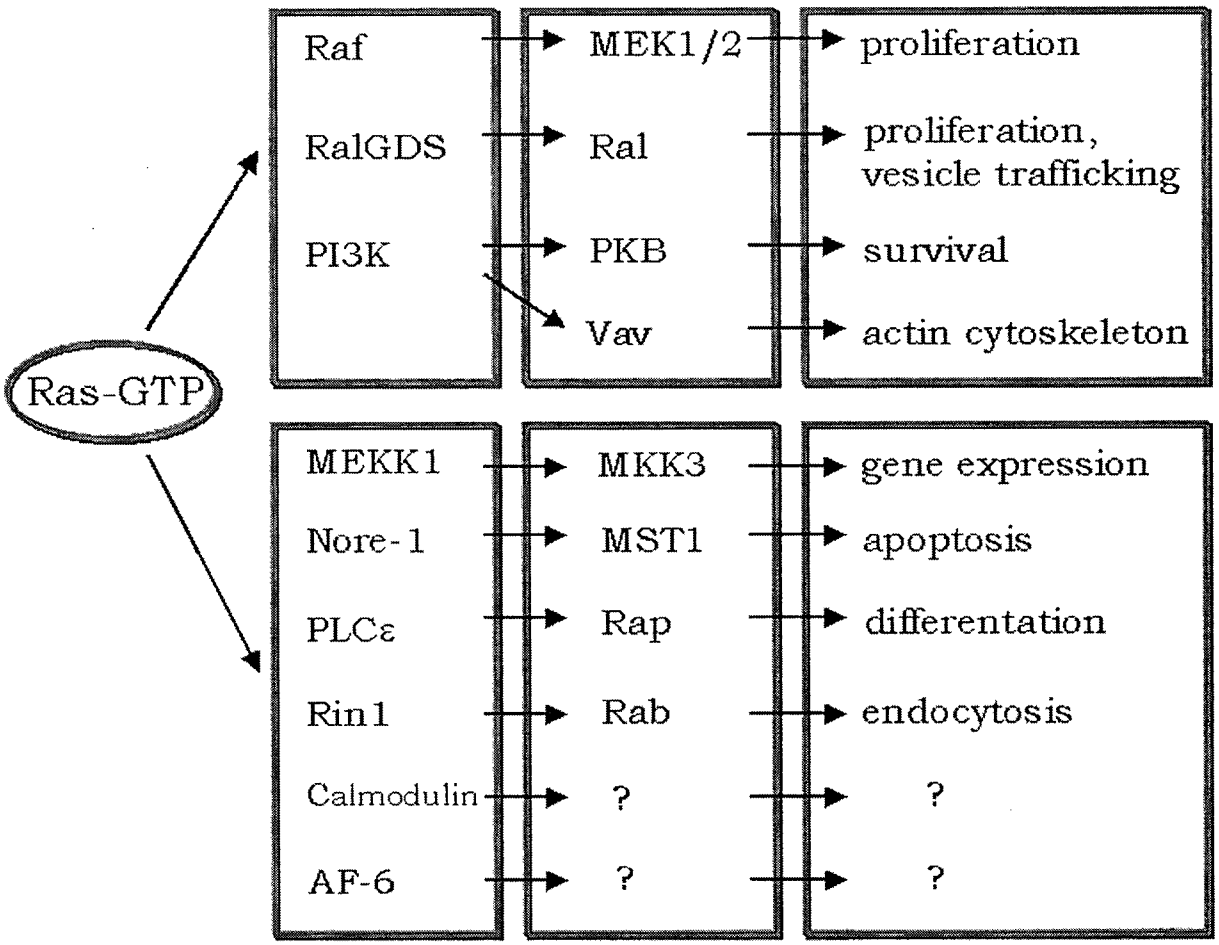

Figure 2. **Downstream effectors of Ras proteins and their functions.** Ras-GTP interacts with numerous effectors to regulate several cellular functions. Some Ras/effectors interactions, downstream components and subsequent cellular response are well characterized (top boxes), while others have yet to be critically tested or are unknown (bottom boxes). Adapted from Ehrhardt *et al.*, 2002.

phosphorylating the second site is still unidentified, but it has been speculated that integrin-linked kinase (ILK) may be responsible (Persad *et al.*, 2001). In mammalian cells, activated PKB then phosphorylates various downstream targets, including the apoptotic protein BAD, forkhead transcription factors and glycogen synthase kinase 3 (Cross *et al.*, 1995; Datta *et al.*, 1997; Biggs *et al.*, 1999). In addition, Ras activation of PI3K can lead to the activation of Sos1/2, Vav, and Tiam-1, which are all capable of activating Rac, thereby regulating rearrangements of the actin cytoskeleton (Ehrhardt *et al.*, 2002).

Four RalGEFs (RalGDS, Rgl, Rlf, Rgr) have been described that also interact with Ras-GTP and subsequently function in the promotion of Ral activation (Wolthuis and Bos, 1999). Initially discovered as Ras interacting proteins in yeast two-hybrid assays (Hofer *et al.*, 1994; Peterson *et al.*, 1996), these proteins have since been confirmed to be *in vivo* effectors of Ras. Two additional RalGEFs, RalGPS/RalGEF2 and Rsc, have recently been described, but whether they interact with Ras proteins is not yet clear (Ehrhardt *et al.*, 2002). Rapid activation of endogenous Ral is observed after the stimulation of a variety of receptors (e.g. receptor-associated tyrosine kinases and GPCRs) (Feig, 2003). The downstream consequence of this activation is less well defined, but some putative Ral targets have been described, including phospholipase D, RalBP1 and Cdc42 (Wolthuis and Bos, 1999).

Additional molecules have been described but still need to be critically tested as physiologically relevant Ras effectors (Campbell *et al.*, 1998; Cullen, 2001; Ehrhardt *et al.*, 2002). For example, phosphoinositide-specific phospholipase Ce (PLCe) was recently identified as a novel Ras effector (reviewed in Cullen, 2001), generating renewed speculation that Ras may be linked to the formation of diacylglycerol and inositol 1,4,5-triphosphate, which are known to regulate protein kinase C (PKC) and Ca^{2+} signaling respectively (Williams, 1999). Another example is Rin1, a Ras subfamily protein that can form a stable complex with Ras *in vivo* (Campbell *et al.*, 1998) and has been suggested to facilitate Ras-mediated endocytosis (Tall *et al.*, 2001). The serine/threonine kinase MEKK1 has been shown to bind directly to the effector domain of Ras (Russell *et al.*, 1995) and be an upstream activator of the Jun N-terminal kinase cascade (Campbell *et al.*, 1998). Examples of other candidate effectors include AF-6, calmodulin and Nore-1 (Ehrhardt *et al.*, 2002). Through these, it has been suggested that Ras regulates cell-cell junctions, Ca^{2+} signaling and apoptosis respectively (Campbell *et al.*, 1998; Cullen, 2001;

Ehrhardt *et al.*, 2002). This growing number of Ras effectors reveals that much is still to be learned.

1.3 A broader understanding of Ras function through model organisms

Much of the information described above has been obtained using *in vitro* approaches and transfected mammalian cell lines. However, the conservation of Ras proteins throughout eukaryotes provides the potential to broaden of our understanding of Ras function. In fact, studies with the model organisms *C. elegans* and *Drosophila* have already made a significant impact on our understanding of Ras. For example, the *C. elegans* Ras homologue Let60 has been linked to the formation of the vulva during larval development (Sternberg and Han, 1998) and *Drosophila* Ras1 activation is associated with the differentiation of the R7 photoreceptor cell during development of the compound eye (Wassarman *et al.*, 1995). In addition, studies in *Dictyostelium* have uncovered an unusually large Ras subfamily of proteins, several of which have already been genetically disrupted, uncovering novel Ras functions (Weeks and Spiegelman, 2003). Thus, the conservation of signaling strategies throughout eukaryotic evolution has been particularly useful in furthering our understanding of the role of Ras in signal transduction.

1.4 *Dictyostelium* as a model organism

Dictyostelium has proved to be an excellent system for the study of signaling networks and parallel pathways (Parent and Devreotes, 1996). Many of the proteins involved in mammalian signaling (e.g. GSK-3 and STAT) are conserved in *Dictyostelium* (Harwood *et al.*, 1995; Kawata *et al.*, 1997) but not in other unicellular organisms like yeast. In addition, the study of these proteins is greatly facilitated by the availability of a genetic approach that allows the analysis of novel genes and pathways (Parent and Devreotes, 1996; Guerin and Larochelle, 2002). This includes high-efficiency transformation with extrachromosomal and integrating vectors, the ability to disrupt or replace genes by homologous recombination, and insertional mutagenesis using restriction enzyme-mediated integration (REMI). The near completion of the *Dictyostelium* genome is quickening the pace of this research through the further identification of unique and conserved genes (Eichinger and Noegel, 2003). In fact, the *Dictyostelium* genome sequence has already predicted at least five new and as yet uncharacterized *ras* genes (M. Wyse, *unpublished observations*).

One of the appeals of *Dictyostelium* as a model organism is its life cycle, which allows growth and differentiation to be studied as separate processes (reviewed in Kessin, 2001). This solitary amoeba generally feeds on bacteria during its vegetative phase, or in case of axenically created laboratory strains ingests liquid media. Upon nutrient deprivation, *Dictyostelium* initiates a developmental program where free-living amoebae chemotax towards cAMP and aggregate into a multicellular organism (*Figure 3*). Within the aggregate different cell-types (prespore and prestalk) begin to emerge and spatially organize. Prestalk cells sort to the top of the aggregate where a single tip forms and the structure subsequently elongates to produce a migrating slug or pseudoplasmodium. Later, culmination results in the formation of a mature fruiting body, in which prestalk cells produce a fibrous stalk that supports a prespore-derived spore mass. The entire process is rapid, occurring within 24 hours.

cAMP is a key chemoattractant during *Dictyostelium* aggregation, and signaling pathways that regulate this process have been well documented (reviewed in Aubry and Firtel, 1999). cAR1, a seven transmembrane glycoprotein belonging to the GPCR superfamily, is central to this process (Kessin, 2001). cAR1 is one of a group of four receptors (the others are cAR2, 3 and 4) whose ligand is cAMP. These receptors are associated with heterotrimeric G-proteins. The genes for eight Gα, one Gβ and one Gγ protein, capable of forming these complexes, have been cloned (Kessin, 2001; Zhang *et al.*, 2001). The binding of cAMP to cAR1 results in adenylyl cyclase A (ACA) activation, the transcriptional activation of aggregation specific genes and the mobilization of the cytoskeleton (e.g. the accumulation of actin and myosin II in the cytoskeleton) (Aubry and Firtel, 1999). The activation of ACA is a requirement for the relay of the cAMP signal during aggregation and requires the release of the G$\beta\gamma$ subunit from cAR1 upon reception of a cAMP signal. At least two additional proteins are required for ACA activation: CRAC and PiaA (Insall *et* al., 1994; Chen *et al.*, 1997). Mutations in genes encoding potential Ras pathways components: ERK2, AleA (a RasGEF), and RasC (discussed below), all cause defects in aggregation (Segall *et al.*, 1995; Insall *et al.*, 1996; Lim *et al.*, 2001). Furthermore, a PI3K dependent pathway has been described that is activated in response to cAMP (Zhou *et al.*, 1995), since cells lacking both PI3K1 and PI3K2 (*pi3K1*$^-$*/pi3k2*$^-$) show defects in chemotaxis and aggregation, and the PH-domain containing proteins PKB and PhdA require PI3K1/2 activity for their localization in response to cAMP (reviewed in Firtel and Chung, 2000).

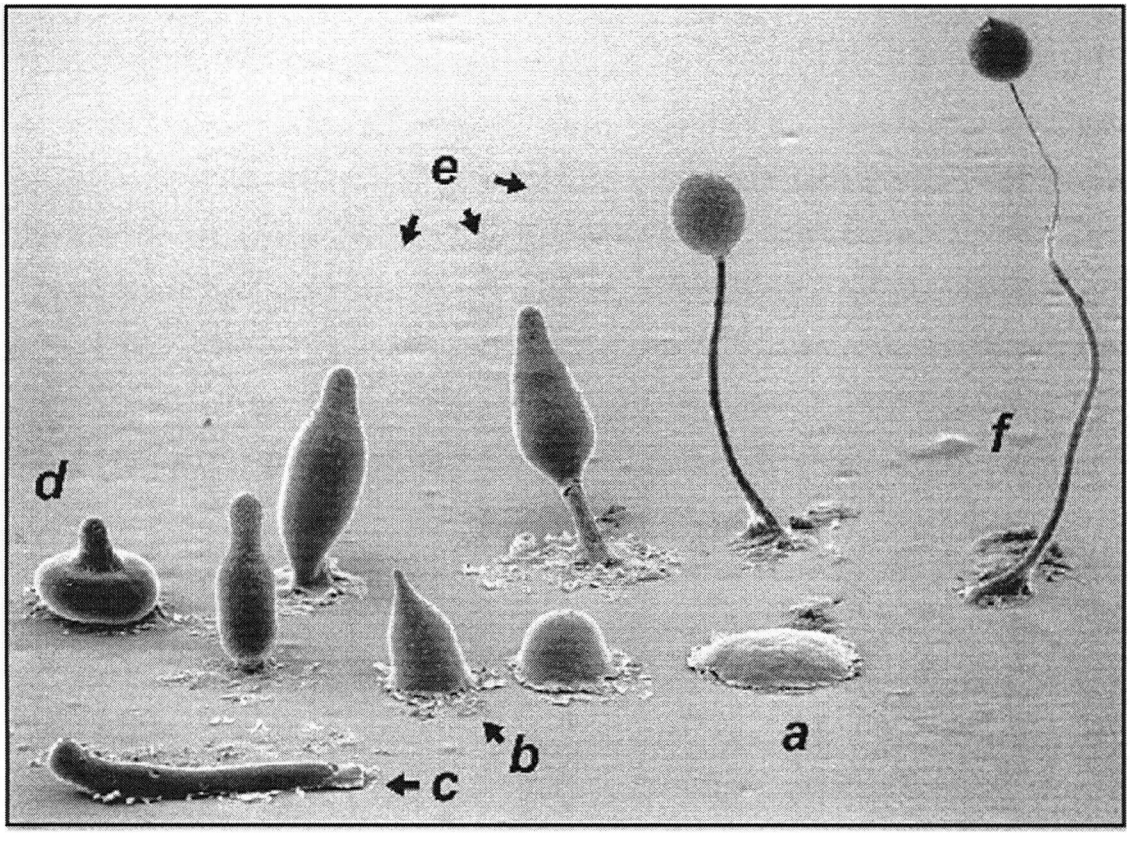

Figure 3. **Multicellular development of *Dictyostelium discoideum*.** *Dictyostelium discoideum* developmental structures are shown in a clockwise pattern beginning with (*a*) an aggregating mound of cells, (*b*) standing slug or finger, (*c*) migrating slug, (*d*) 'mexican hat', (*e*) culminating structures, and (*f*) a terminal fruiting body. The process from *a* to *f* takes approximately 24 hours to complete. Electron micrograph image by M. G. Grimson and R. L. Blanton, Texas Tech University, Lubbock, Texas.

At later stages of development, morphogens including differentiation-inducing-factor (DIF), adenosine, and ammonia, are important for cell-type decisions (Parent and Devreotes, 1996; Kay *et al.*, 1999). DIF-1, the most extensively studied, induces stalk cell formation, while inhibiting prespore cell formation (Kessin, 2001). Several other molecules have also been shown to influence cell-type decisions, including glycogen synthetase kinase-3 (GSK-3), Wariai and MEKKa (Weeks, 2000). Extracellular cAMP, through cAR3, regulates the activity of GSK-3 and the protein tyrosine kinase ZAK1 has been implicated as an intermediate in this process (Plyte *et al.*, 1999; Kim *et al.*, 1999).

Less is known about signaling in vegetative cells and the transition from growth to development, although a few processes have been examined in some detail. For example, growing cells chemotax towards bacteria, attracted by secreted chemoattractants including folic acid and pterin (Kuwayama *et al.*, 1993; Parent and Devreotes, 1996). In the chemotactic response to folate, the binding of folic acid to its unknown receptor results in the activation of guanylyl cyclases and alteration of the cytoskeleton (Kuwayama *et al.*, 1993; Blusch and Nellen, 1994). In addition, growing cells secrete various factors, including pre-starvation factor (PSF) and conditioned media factor (CMF) (Clarke and Gomer, 1995). PSF is continually secreted by growing cells and triggers the expression of genes whose products are required for aggregation, although it is not known how this is mediated (Burdine and Clarke, 1995). CMF is secreted upon starvation, where it participates in regulating aggregation (Jain *et al.*, 1992; Yuen *et al.*, 1995). One pathway involved in the transition from growth to development that has been partially characterized involves the protein kinase YakA (Souza *et al.*, 1998). *yakA* null cells are smaller, have a cell cycle that is accelerated, do not turn off genes expressed during growth when starved and do not initiate development (Souza *et al.*, 1998). The use of REMI on *yakA* null cells revealed that the disruption of the gene encoding the translational regulator PufA reversed their developmental block (Souza *et al.*, 1999). The disruption of *pufA* in *yak*A null cells restores the synthesis of PKA-C and PufA can bind to PKA-C, suggesting a pathway where PufA inhibits PKA-C synthesis and YakA inhibits PufA (Souza *et al.*, 1999). In addition, YakA has recently been implicated in the folate-stimulated activation of guanylyl cyclases and alteration of the cytoskeleton (van Es *et al.*, 2001).

1.5 *Dictyostelium* Ras proteins

Six distinct Ras subfamily proteins, encoded by the genes *rasG*, *rasD*, *rasB*, *rasS*, *rasC* and *rapA*, have thus far been characterized in *Dictyostelium* (reviewed in Daniel *et al.*, 1995). The five Ras proteins listed above are well conserved relative to the human H-, N-, and K-Ras proteins, sharing between 54 and 68% amino acid identity with H-Ras. The only *Dictyostelium* Rap protein thus far identified, encoded by *rapA*, is even more conserved, sharing 76% amino acid identity to human Rap1. Several novel *ras* genes have emerged from analysis of the *Dictyostelium* database, and although these Ras proteins are less well conserved, they are clearly members of the Ras subfamily (M. Wyse, *personal communication*).

Investigation into the specific functions of the individual Ras proteins has been centered on *ras* gene ablation studies, but studies on the overexpression of activated or dominant negative forms of *Dictyostelium* Ras proteins have also provided insight. The first *Dictyostelium* Ras protein to be studied in this way was RasD. Transformants overexpressing an activated version of RasD, RasD(G12T), were found to form multi-tipped aggregates that were blocked in further development (Reymond *et al.*, 1986). These transformants express enhanced levels of two prestalk cell-specific markers and decreased levels of a prespore cell-specific marker (Louis *et al.*, 1997), suggesting that RasD influences cell fate. Activated Ras expression from a prespore promoter was sufficient to reproduce the multi-tipped phenotype (Jaffer *et al.*, 2001), suggesting that activated protein exerts its influence in the prespore cell population. It was thus surprising when the only observable phenotype of a *ras*D null strain was defective phototaxis and thermotaxis of the slug (Wilkins *et al.*, 2000b). However, it has been suggested that RasG, which share 82% overall amino acid identity and identical effector regions with RasD, might be compensating for RasD function in these cells (Weeks and Spiegelman, 2003).

Aggregation was recently shown to require RasC, since *rasC* null cells are unable to produce cAMP upon receptor stimulation (Lim *et al.*, 2001). Thus, although *rasC* null cells do not normally aggregate, this phenotype can be circumvented by exogenously applying cAMP to the cells. In addition to its requirement for adenylyl cyclase activation, RasC is also required for wild type levels of PKB activity (Lim *et al.*, 2001; Lim, 2002). Starved *ras*C null cells also have motility defects and chemotax poorly to cAMP, but interestingly, cAMP-pulsed *rasC* null cells move more rapidly toward cAMP (Lim *et al.*, 2001). Cells expressing an activated version of

RasC, RasC(G13T), have also been created and exhibit reduced motility and defects in aggregation (Lim, 2002).

Disruption of *rasS* resulted in cells that were unable to grow in axenic culture due to impairments in fluid phase endocytosis (Chubb *et al.*, 2000). *rasS* null cells also move rapidly, are highly polarized and exhibit increased F-actin localization to their pseudopods. Based on these observations it was suggested that RasS regulates the balance between feeding and movement, with competition for the cytoskeletal components required for both feeding and motility (Chubb *et al.*, 2000). Thus, the rapid movement of *rasS* null cells would impact their ability to feed. A strain null for a RasGEF protein, RasGEF-B, also show reduced endocytosis and enhanced motility. While it was initially suggested that RasGEF-B regulates RasS (Wilkins *et al.*, 2000a), the motility defects in *rasS* and *gefB* null cells have been shown to rely on different mechanisms (Chubb *et al.*, 2002), even though *rasS/gefB* double null strain shows phenotypes similar to each single null strain (King and Insall, 2004).

Both *rasB* and *rapA* appear to be essential for growth (Sutherland *et al.*, 2001b; Kang *et al.*, 2002). All presumptive *rasB* null cells grew very slowly but contained at least two copies of the disrupted gene and eventually reverted to a wild type phenotype (Sutherland *et al.*, 2001b). RasB has been shown to be localized to the nucleus in cell cycle specific manner and RasB(G12T) expression has been shown to produce multinucleate cells (Sutherland, 2001a; Sutherland *et al.*, 2001b). Attempts to disrupt the *rapA* have been unsuccessful. The reduction of Rap1 levels by antisense reduces growth and viability, suggesting the *rapA* is an essential gene (Kang *et al.*, 2002). Rap1 is activated in response to osmotic stress (Kang *et al.*, 2002).

The most studied *Dictyostelium* Ras protein has been RasG. This gene was identified using low stringency hybridization with the only other *Dictyostelium ras* gene that had been identified at the time, *rasD*, as a probe (Robbins *et al.*, 1989). RasG was subsequently found to be the major Ras species present in vegetative cells, with its expression down regulated to negligible levels by the aggregation stage (Robbins *et al.*, 1989; Khosla *et al.*, 1990). This suggested a role for RasG during growth, although, the overexpression of an activated form of RasG, RasG(G12T), and the creation of a *rasG* null strain indicated a possible role for the protein in early development (Khosla *et al.*, 1996; Tuxworth *et al.*, 1997).

Cell expressing RasG(G12T) exhibit several phenotypes. These cells were unusually flattened with numerous filopodia and prominent dorsal and peripheral membrane ruffles that

contained large amounts of F-actin (Zhang *et al.*, 1999), suggesting the possibility that RasG(G12T) expression affects the actin cytoskeleton. These cells also showed impaired motility and chemotaxis compared to wild type strains (Khosla *et al.*, 1996). However, although the effects of RasG(G12T) expression on the cytoskeleton and motility were conspicuous, the most noteworthy phenotype of cells expressing RasG(G12T) was their inability to aggregate, with these cells producing less cAMP than a wild type strain in response to a pulse of 2?–deoxy-cAMP (Khosla *et al.*, 1996). This last phenotype suggested that constitutive RasG signaling blocked the initiation of development and implicated RasG in potentially regulating the transition from growth to development.

The *rasG* null cells also exhibited a complex phenotype. Vegetative *rasG* null cells displayed multiple elongated filopodia, aberrant lamellipodia and unusual punctate polymerized actin structures (Tuxworth *et al.*, 1997). These cells lacked cell polarity and it was thus not surprising that they also exhibit both reduced motility and chemotaxis (Tuxworth *et al.*, 1997; Khosla *et al.*, 2000). The growth of these cells in shake suspension is very slow, and growth was to a much lower final density than parental control strains. Suspension grown cells were multinucleate, being defective in the completion of cytokinesis due to an inability to sever the cleavage furrow (Tuxworth *et al.*, 1997). This cytokinesis defect was not observed in *rasG* null cells grown on plastic dishes, presumably due to the ability of *Dictyostelium* cells to overcome cytokinesis defects on surfaces by traction-mediated cytofission (Fukui *et al.*, 1990). The loss of RasG appears to be partially compensated for by other Ras proteins, in that *rasG* null cells contained increased levels of RasD, RasB and RasC (Khosla *et al.*, 2000; Weeks and Spiegelman, 2003).

The first downstream signaling protein linked to RasG was ERK2, a MAP kinase activated in response to cAMP (Segall *et al.*, 1995). Use of antibodies that react with phosphorylated ERK2 (Kosaka *et al.*, 1997) revealed that cells expressing RasG(G12T) exhibited decreased ERK2 phosphorylation in response to cAMP (Aubry *et al.*, 1997; Kosaka *et al.*, 1998), whereas cells expressing a dominant negative *rasG* gene exhibited increased ERK2 phosphorylation (Aubry *et al.*, 1997).

RasG has also been shown to interact with *Dictyostelium* PI3K1 and PI3K2 in yeast two-hybrid assays (Lee *at al.*, 1999; Funamoto *et al.*, 2002). Cells lacking both PI3K1 and PI3K2 exhibit defects in aggregation and chemotaxis (Buczynski *et al*, 1997; Funamoto *et al.*, 2001)

and these proteins are required for the translocation PH-domain containing proteins to the membrane (Meili *et al.*, 1999; Funamoto *et al.*, 2001). In addition, PI3K activity, which results in the generation of PtdIns(3,4,5)P_3 and PtdIns(3,4)P_2 (Katso *et al.*, 2001), has been shown to be activated by chemoattractant stimulation and confined to the leading edge of chemotaxing cells (Huang *et al.*, 2003). Since RasG binds to PI3Ks, it could well play a role in regulating these processes.

Ras-interacting protein 3 (RIP3) was also identified in a yeast two-hybrid assay as a putative RasG interacting protein (Lee *at al.*, 1999). *rip3* null cells are unable to aggregate or activate adenylyl cyclase upon receptor activation (Lee *at al.*, 1999). Unfortunately, RIP3 lacks a recognizable homolog in other organims (Lee *at al.*, 1999) and it is not clear as yet how RasG binding to RIP3 affects its function. Nonetheless, the identification of this protein suggests a potential role for RasG in regulating aggregation and receptor-stimulated adenylyl cyclase activity.

1.6 Thesis Objectives

1.6.1 Background

Following on from studies on the expression of RasG(G12T) under the control of the folate-repressible *discoidin* promoter in a *pVEII-rasG*(G12T) transformant (Khosla *et al.*, 1996), it was found that levels of RasG(G12T) increased as growth progressed in the absence of folate. However, the expression of RasG(G12T) from the *discoidin* promoter reached a maximum at a cell density of approximately 7 x 10^5 cells/ml and then declined dramatically (Secko *et al.*, 2001). Discoidin expression is known to decrease at high cell density (Wetterauer *et al.*, 1995), but the observed decline in RasG(G12T) expression (Secko *et al.*, 2001) was more dramatic and occurred at a considerably lower cell density than had been previously reported. A possible explanation for the difference was that the elevated level of RasG(G12T) dramatically inhibited expression from the *discoidin* promoter.

To further investigate the possible link between RasG(G12T) levels and *discoidin* expression, the levels of Discoidin in the *pVEII-rasG*(G12T) transformant was compared with those in the Ax2 parental strain at various stages during growth after the removal of folate. As cell density increased there was the anticipated increase in Discoidin in response to the removal of folate for both the parental Ax2 cells and the *pVEII-rasG*(G12T) transformant and this

increase occurred at similar cell densities in the two strains. However, considerably more Discoidin was produced in the Ax2 parental cells than in the *pVEII-rasG*(G12T) transformant and the levels of Discoidin in the *pVEII-rasG*(G12T) transformant declined at a lower cell density as growth progressed. These results are consistent with the idea that elevated levels of RasG(G12T) repressed *discoidin* expression. However, since RasG(G12T) was expressed on the *discoidin* promoter, it was difficult to definitively interpret the results.

1.6.2 Objectives

The first objective of this thesis was to confirm that activated RasG inhibited *discoidin* expression. This required the development of an alternative inducible expression system, which was accomplished through the use of the inducible *rnrB* promoter. The second objective was use an expression system to rapidly express activated RasG to allow the consequences of the RasG activation signal to be monitored. The development of a system to rapidly express activated RasG provided a method to investigate the virtually unknown RasG signaling pathway and this investigation comprised the third objective of this thesis. This objective relied on Ras proteins making extensive use of phosphorylation cascades involving multiple kinases and phosphatases in many other organisms (see Section 1.2; Campbell *et al.*, 1998; Shields *et al.*, 2000). Thus, the third objective was to monitor the changes in the phosphorylation of proteins that occurred upon RasG(G12T) expression and to identify these proteins using proteomic techniques.

2 MATERIALS AND METHODS

2.1 Materials

2.1.1 Reagents

Chemicals were acquired from Sigma, Fisher Scientific, ICN, Bio-Rad, BDH or Invitrogen, unless otherwise stated. Restriction enzymes, DNA polymerases and other DNA modifying enzymes were obtained from New England Biolabs or Invitrogen. Growth media reagents were from Oxoid, BBL, or Difco. Chemical or electro-competent *Escherichia coli* strain XL1-Blue MRF′ (Stratagene) was used for all cloning and sub-cloning procedures. Immobiline DryStrips, PVDF membranes, enhanced chemiluminescence assay and secondary antibodies were from Amersham Pharmacia Biotech. Blasticidin S was from Calbiochem. Modified sequencing grade trypsin and complete protease inhibitor cocktail were from Roche Diagnostics. Siliconized microcentrifuge tubes were from Diamed. 40% Acrylamide/Bis Solution (19:1, electrophoresis grade) and D_C Protein Assay were from Bio-Rad Laboratories. Reagents used for 2D electrophoresis and mass spectroscopy (MS) analysis (except acrylamide/bis solution) were of HPLC quality.

Phospho-p44/42 MAP kinase polyclonal antibody (Cat # 9101), phosphothreonine polyclonal antibody (Cat # 9381), phosphotyrosine monoclonal antibody (Cat #9419), Myc-tag polyclonal antibody (Cat # 2272) were from Cell Signaling Technology. Monoclonal actin-specific antibody was from Chemicon (Cat # MAB1501). The *Dictyostelium* specific antibodies were generously provided as follows: the PKB-specific polyclonal antibody by Dr. Robert Dottin (Hunter College, New York), the DdCAD-1-specific polyclonal antibody by Dr. Chi-Hung Siu (University of Toronto, Toronto), the *Dictyostelium* VatA-specific N4 antibody and the Discoidin I antibody by Dr. Margaret Clarke (Oklahoma Medical Research Foundation, Oklahoma City). The RasG and RasC specific antibodies were generated in the Weeks laboratory (Khosla *et al.*, 1994; Lim, 2002).

2.1.2 Services

DNA sequencing was performed at the University of British Columbia Nucleic Acid and Protein Services (NAPs) unit (www.biotech.ubc.ca/services/naps/index.html).

Oligonucleotides for PCR were generated at Alpha DNA (www.alphadna.com). Mass spectral analysis was performed at the UVic–Genome BC Proteomics Centre (www.proteincentre.com). Indirect immunofluorescence was performed at the University of British Columbia BioImaging Facility (www.emlab.ubc.ca).

2.1.3 *Dictyostelium* strains

Ax2 is the parental strain used for all transformations and this strain was originally obtained from Dr. Barry Coukell (York University, Toronto). Ax2 is an axenic derivative of the wild type strain NC-4 (for a discussion of strain history please see: dictybase.org/strain_history.htm). The *pVEII-rasG*(G12T) strain was generated in the Weeks Laboratory (Khosla *et al.*, 1996). The *rasG* null and *gefR* null strains were obtained from Dr. Robert Insall (University of Birmingham, England). The *cadA* null strain was obtained from Dr. Chi-Hung Siu (University of Toronto, Toronto). The *lrrA* null strain was obtained from Dr. Wen-Tsan Chang (National Cheng Kung University Medical College, Taiwan). The *vatA-oe* strain was obtained from Dr. Margaret Clarke (Oklahoma Medical Research Foundation, Oklahoma City).

2.1.4 Plasmids

Plasmids were obtained from the indicated sources: the tetracycline expression vectors, MB-35 and MB-38, from M. Blaauw (University of Groningen, Groningen), ptz-*rasG*(G12T) from Meenal Khosla (UBC), RnrB-ubi-S65TGFP6 from Dr. Harry MacWilliams (Ludwig-Maximilians-Universität, Munich), *discoidin* Iγ gene fragment from Dr. Margaret Clarke (Oklahoma Medical Research Foundation, Oklahoma City).

2.2 Methods

2.2.1 *Dictyostelium* cell culture

Dictyostelium discoideum cells were grown axenically in HL5 medium (14.3 g peptone, 7.15 g yeast extract, 15.4 g glucose, 0.96 g $Na_2HPO_4 \cdot 7H_2O$ and 0.486 g KH_2PO_4 per liter of water) supplemented with 50 μg/ml streptomycin (Sigma) at 22°C, either on tissue culture dishes (Nunc) or in rotatory agitated suspension (175 rpm) (Watts and Ashworth, 1970). Transformed strains were selected and maintained in HL5 media supplemented with the either: 5 μg/ml

blasticidin S (Calbiochem) or 10 μg/ml G418 (Gibco-BRL) as appropriate. *rasG* null strains were grown and maintained on Nunc tissue culture dishes, since this strain grows poorly in rotatory agitated suspension (Tuxworth *et al.*, 1997), unless otherwise stated. Ax2::MB, AX2::MB-*rasG*(G12T) and Ax2::MB-LrrA^{MYC} strains were additionally maintained and grown in 5 μg/ml tetracycline (Sigma) until their use and the *pVEII-rasG*(G12T) strain was maintained in 1 mM folate until required. Cells grown in shake suspension were passaged by diluting between 20-50 fold in fresh media upon reaching a cell density of approximately 2-3 x 10^6 cells/ml. Cells numbers were determined using a hemocytometer. Cells grown on Nunc plates were passaged by diluting 10-30 fold into fresh media/plates when they research confluent density. All cells were maintained for no more than 7 passages before being re-derived from cryo-preserved stocks or spores. For cryo-preservation, approximately 2.5 x 10^7 cells/ml in 1.0 ml aliquots were frozen at –70°C in HL5 containing 10% DMSO.

2.2.2 Dictyostelium growth in bacterial suspension

Axenically grown cells were inoculated into a suspension of *Klebsiella oxytoca* in KK2, OD_{600} of 8 (Rathi and Clarke, 1992; Primpke *et al.*, 2000) and allowed to grow for approximately seven to eight generations before being transferred to a fresh suspension of bacteria. *Dictyostelium* cells were collected by centrifugation at 500 x g for 3 minutes, then washed exhaustively to remove residual bacteria before being used for further analysis.

2.2.3 Dictyostelium development

Vegetative cells were axenically grown to a density of 2-3 x 10^6 cells/ml in shake suspension or to confluence on Nunc plates, washed twice in 20 mM potassium phosphate buffer, pH 6.5 (KK2), and resuspended in KK2 to a density of 5.0 x 10^6 cells/ml. Cells were then shaken at 160 rpm for the indicated periods at 22°C. Cells were also grown in association with bacteria to a density of approximately 2-3 x 10^6 cells/ml, exhaustively washed with KK2 to remove bacteria, plated at 1 x 10^6 cells/cm^2 on non-nutrient agar (2% agar buffered in KK2, 1mM $MgCl_2$, 0.1 mM $CaCl_2$) and allowed to develop for the indicated periods.

2.2.4 Vector constructions and Polymerase Chain Reaction (PCR)

To generate the *rnrB-rasG*(G12T) construct, a vector containing the *rnrB* promoter, RnrB-ubi-S65TGFP6 (Gaudet *et al.*, 2001), was digested with *Xho*I to remove *gfp*, treated with

Klenow polymerase and deoxynucleoside triphosphates to generate blunt ends and then subsequently digested with *Bgl*II. A *rasG*(G12T) insert (Khosla *et al.*, 1996) was then sequentially digested with *Bgl*II and *Sma*I and ligated to the above vector fragment. To generate the MB-*rasG*(G12T) vector, the tetracycline responsive vector MB-38 (Blaauw *et al.*, 2000) and the *rasG*(G12T) insert described above (Khosla *et al.*, 1996) were both digested with *Bgl*II and *Mlu*I and ligated together. The MB-*rasG*(G12T) and *rnrB-rasG*(G12T) constructs were transformed into *Escherichia coli* strain XL1-MRF' (Stratagene) and their sequences confirmed by DNA sequencing.

The *lrrA* (# SLG759) and *vatA* (# VHD171) cDNAs were obtained from the Japanese *Dictyostelium* cDNA project (http://www.csm.biol.tsukuba.ac.jp/cDNAproject. html). The primer lrrAF1 (5′ - GAATTCATGGGAGGAAATTTATCAT - 3′) and lrrARmyc (5′ - TTAAAGATCCTCTTCTGAAATAAGTTTTTGTTCTGCTGCTTTTTCATTATCTTGTTGAA TACC - 3′) were used for PCR to amplify the *lrrA* cDNA while adding the c-myc epitope EQKLISEEDL (Lim, 2002) before the termination codon of the *lrr*A cDNA. The primers vatF1 (5′ - GAGCTCTGCACGAGAAATGTCAAAAAATTC-3′) and vatRmyc (5′ - TCTAGATTAA AGATCCTCTTCTGAAATAAGTTTTTGTTCTGCTGCAACTAAATCACTAAAGTTTC - 3′) were used for PCR to amplify the *vatA* cDNA, adding the same c-myc epitope as above. All PCR reactions were performed using an Idaho RapidCycler (Idaho Technologies). The quantities of template DNA used per reaction were 0.1 – 0.5 ng plasmid DNA. A standard PCR reaction to test primers was done in 10 μl mixtures in glass capillary tubes containing 5.38 μl ddH_2O, 1.0 μl 10x Idaho PCR buffer (500 mM Tris, pH 8.3, 2.5 mg/ml BSA, 20% (w/v) sucrose, 1 mM cresol red, 30 mM $MgCl_2$), 0.5 μl 2.5 mM dNTPs (Pharmacia), 1.0 μl of each 2.5 μM oligonucleotide, 1.0 ng DNA and 0.125 μl *Taq* DNA polymerase (5 U/ μl) (Gibco-BRL). High fidelity PCR with the proof reading enzyme *Pfu* Turbo DNA polymerase (Stratagene) was used to construct all expression vectors after testing the primers. High fidelity PCR reactions were done in 10 μl mixtures in plastic capillary tubes containing 4.7 ng ddH_2O, 1.0 μl 10x Cloned *Pfu* DNA polymerase reaction buffer, 1.0 μl 2.5 mM dNTPs (Pharmacia), 1.0 μl of each 2.5 μM oligonucleotide, 1.0 μl DNA and 0.3 μl *Pfu* DNA polymerase (2.5 U/ μl).

For both standard and high fidelity PCR the cycling parameters were as follows: (i) 2 cycles of D = 92°C for 60 sec, $A = x$°C for 7 sec, E = 72°C for 90 sec; (ii) 36 cycles (*Taq*) or 30 cycles (*Pfu*) of D = 92°C for 1 sec, $A = x$°C for 7 sec, E = 72°C for y sec; hold at 72°C for 120

sec. (Where *D* is denaturation, *A* is annealing, *E* is extension, *x* is the temperature optimized for a particular pair of primers, and *y* is 60 sec for every 1000 bp of amplification target.) The temperature ramping rate for all cycling was set at 6.0.

Amplified PCR fragments for *lrrA* and *vatA* were ligated into pGEM-T Easy (Promega) to generate the vectors pGEM-*lrrAmyc* and pGEM-*vatAmyc*. These vectors were subsequently digested with *Sph*I and *Mlu*I and ligated into the *Sph*I/*Mlu*I digested MB-38 vector to generate the vectors MB-*lrrAmyc* and MB-*vatAmyc*.

2.2.5 Dictyostelium transformations

To generate the tetracycline-responsive Ax2::MB, AX2::MB-*rasG*(G12T) and Ax2::MB-LrrA^{MYC} strains, the MB38, MB38-*rasG*(G12T), MB38-*lrrAmyc* and MB35 vectors were first purified by PEG precipitation (Sambrook *et al.*, 1989). Ten μg of the MB38, MB38-*rasG*(G12T) and MB38-*lrrAmyc* vectors were then mixed with ten μg of MB-35 and incubated with 1 x 10^7 Ax2 cells that had been previously washed and resuspended in 0.8 ml electroporation buffer (10 mM $NaPO_4$, pH 6.1, 50 mM sucrose). This suspension was incubated on ice for 10 min, pulsed with a Bio-Rad GenePulser set at 0.9 kV, 3 μF, and then incubated on ice for 10 min. HL5 media supplemented with 5 μg/ml tetracycline was added and the cells were plated in Nunc tissue culture dishes at 22°C. 24 hours later the media was replaced with fresh HL5 media supplemented with 5 μg/ml blasticidin S, 10 μg/ml G418 and 5 μg/ml tetracycline. Transformants were grown for 10 days, before stable transformants were selected by clonal growth in HL5 containing G418, blasticidin S and tetracycline at the previously indicated concentrations.

The *rnrB-rasG*(G12T) transformant was obtained by the $CaPO_4$ DNA precipitation method (Nellen *et al.*, 1987). This involved precipitating 10 μg of plasmid DNA for 0.5 hr in a mixture containing 375 μl ddH_2O, 125 μl 0.125 M $CaCl_2$ and 500 μl 2X HBS (42 mM HEPES, 270 mM NaCl, 10 mM KCL, 1.4 mM Na_2HPO_4, 10 mM glucose, pH 6.1). Precipitates were then added drop wise to *Dictyostelium* cells cultured in Nunc dishes in Bis-Tris buffered HL5 (2.1 g Bis-Tris, 10 g peptone, 5 g yeast extract, 10 g glucose per 1 liter of dH_2O) and incubated at 22°C for 4 hr. Cells were then exposed to a solution of 15% glycerol/1X HBS for 2 min, followed by replacement of HL5 media. 24 hours later this media was replaced with HL5 medium supplemented with 10 μg/ml of G418. Colonies were visible after 10-14 days and stable

transformants were selected by clonal growth in HL5 medium containing G418 and streptomycin at the previously indicated concentrations and were maintained in the same medium.

2.2.6 Induction conditions for protein overexpression

A *pVEII-rasG*(G12T) cell population was centrifuged at 700 x g for 4 min, washed once in HL5 media and resuspended in HL5 media containing no folate. The *rnrB-rasG*(G12T) strain was treated as above and then incubated with 5 or 10 mM methyl methanesulfonate (MMS) (Sigma) to induce protein expression. All tetracycline repressible strains were centrifuged as above, washed three times in HL5 media, and then resuspended in HL5 media containing no tetracycline to induce protein expression. For all strains, incubation was performed in rotatory agitated suspension (175 rpm) at 22°C.

2.2.7 RNA analysis

Total cytoplasmic RNA was isolated from 1 x 10^7 cells using a modified protocol employing the TRIzol Reagent (Gibco-BRL). Pelleted cells were lysed in 1.0 ml TRIzol and incubated for 5 mins at 22°C, then mixed with 200 µl chloroform and incubated a further 5 min. Sample were centrifuged at 16,000 x g for 15 min and the upper aqueous phase (~ 600 µl) was then transferred to a new microcentrifuge tube. The upper aqueous phase was mixed with 500 µl of iso-propanol, incubated 10 min and centrifuged at 16,000 x g for 15 min. The pelleted RNA was further washed with 1.0 ml 75% ethanol, air dried, dissolved in DEPC-treated ddH_2O. Dissolved RNA was quantitated by absorbance spectrophotometry at 260 nm. Samples were size fractionated by electrophoresis on 1% formaldehyde-agarose gels as previously described (Khosla *et al.*, 1996). Equal loading of samples was verified by observing the intensities of 28S and 18S rRNAs following ethidium bromide staining. The RNA was transferred to a nylon membrane (Hybond N+, Amersham) and the filters were prehybridized for 3 to 4 h at 42°C in a mixture containing 30% formamide, 5x Denhardt's solution (1x Denhardt's solution is 0.02% Ficoll, 0.02% bovine serum albumin, and 0.02% polyvinylpyrrolidone), 5x SSC (1x SSC is 0.15 M NaCl plus 0.015 M sodium citrate), 20 mM sodium phosphate buffer (pH 6.5), 0.5 % sodium dodecyl sulfate (SDS), and 30 µg of polyadenylic acid per ml. A 330 bp *Hind*III/*Eco*RI *discoidin* Iγ gene fragment (Rathi *et al.*, 1991) that had been first gel purified using the QIAquick Gel Extraction Kit (Qiagen) was labeled with [α-^{32}P]dCTP by the random primer method as

previously described (Sambrook *et al.*, 1989). This probe was added to the prehybidization mixture and hybridization at 42°C was allowed to proceed for 12 to 16 hrs. The filters were then washed once sequentially in 2x SSC, 0.1% SDS at 50°C for 20 min, then 1x SSC, 0.1% SDS at 55°C for 30 min, and then finally in 0.1x SSC, 0.1% SDS at 60°C for 30 min. The filters were exposed to X-ray film (X-OMAT XK-1, Kodak).

2.2.8 One dimensional (1D) immunoblot analysis

Cells were pelleted by centrifugation and lysed directly in 1x Laemmli SDS-PAGE loading buffer (6x Laemmli SDS-PAGE is 350 mM Tris-Cl, pH 6.8, 10% SDS, 600 mM DTT, 0.012% w/v bromophenol blue, 30% glycerol, 12 mM NaF, 12 mM Na_3VO_4, 12 mM EDTA, and complete protease inhibitor cocktail (Roche)). Alternatively, cells in suspension in KK2 buffer were directly lysed by mixing with 6X Laemmli SDS-PAGE loading buffer in a volume ration of 5:1. All samples were boiled at 100°C for 5 min and used for SDS-polyacrylamide gel electrophoresis (Laemmli, 1970) or stored –20°C. Equal loading of proteins was ensured through two methods: (i) determining protein concentrations using a D_C Protein Assay and (ii) through subjecting test samples to SDS-polyacrylamide gel electrophoresis followed by staining the gels with Coomassie blue solution (0.025% w/v Coomassie G-250, 50% methanol, 5% v/v acetic acid) and visual inspection.

SDS-polyacrylamide gels consisted of an upper protein stacking gel (3.9% bis-acrylamide (1:19), 125 mM Tris-Cl, pH 6.8, 0.1% SDS, 0.03% ammonium persulphate, 0.1% TEMED) and a lower protein resolving gel (11% bis-acrylamide (1:19), 375 mM Tris-Cl, pH 8.8, 0.1% SDS, 0.03% ammonium persulphate, 0.07% TEMED). A 20 µg protein aliquot of each sample and 2.0 µl of low-range pre-stained SDS-PAGE molecular weight standards (Cat # 161 0305, Bio-Rad) were loaded in each well and electrophoresed at 90V. The electrophoresis buffer was 25 mM Tris, 192 mM glycine, 0.1% SDS, pH 8.3. For electrophoresis prior to the immunoblot analysis of DdCAD-1 phosphorylation, 180 mm x 160 mm x 1 mm size SDS-polyacrylamide gels as above were used. These gels were run at a constant current of 25 mA/gel for 3 hrs with cooling.

After electrophoresis, the proteins were transferred to nitrocellulose (Hybond C, Amersham) or PVDF (Hybond P, Amersham) membranes using a Bio-Rad electroblot apparatus (Mini Protean II) submerged in ice-cold transfer buffer (25 mM Tris, 192 mM glycine, 20%

methanol) for 1 hr at 90 V (Towbin *et al.*, 1979). The membranes were incubated in 5% powdered milk in Tris-buffered saline (TBS)-Tween (25mM Tris-Cl [pH 8.0], 1.0% NaCl, 0.1% Tween 20) for 1 hr at room temperature and were then washed twice for 5 min with TBS-Tween. Alternatively, all membrane that were to be probed with phospho-specific antibodies were incubated in 3% BSA in TBS-Tween 1 hr at room temperature and were then washed three times for 5 min with TBS-Tween. Membranes were then probed with primary antibodies in 1% w/v powdered milk (Carnation)/TBS-Tween (1/1000 dilutions for phospho-specific antibodies and 1/2000 dilutions for all others) overnight at room temperature or according to the manufacturer's instructions. The membranes were washed three times for 5 min in TBS-Tween and exposed to a secondary antibody (Donkey anti-rabbit or sheep anti-mouse conjugated to horseradish peroxidase, as appropriate) diluted 1/10,000 in TBS-Tween containing 1% powdered milk. Membranes were then washed three times for 5 min with TBS-Tween and bound antibody was detected by an enhanced chemiluminescence assay (ECL, Amersham) using X-ray film (X-OMAT XK-1, Kodak). Immunoblots that were directly compared were detected on the same sheet of film to account for differences in exposure time. Where desired, probed membranes were stripped by incubation in 0.2 M NaOH for 10 min, followed by three washes in ddH_2O and reblocked as above, before being re-probed with another primary antibody. Blots were scanned using an UMAX-II scanner (UMAX, Dallas, Tx, USA) and densitometry was then performed using GeneQuant Analysis software (Molecular Dynamics).

2.2.9 Two dimensional (2D) electrophoresis and immunoblot analysis

Cells were lysed in a buffer (Soskic *et al.*, 1999) containing 25 mM Tris-HCl (pH 8.0), 0.3% SDS, 100 mM DTT, 1 mM Na_3VO_4, 1 mM NaF, 2 mM EDTA, 1 mM sodium pyrophosphate, complete protease inhibitor cocktail (Roche), 25 μg/ml DNAse I, and 7 μg/ml RNAse A and centrifuged at 16000 x g for 15 min at 4°C. The supernatant was removed and 80% (v/v) cold acetone added to the supernatant. Proteins were allowed to precipitate on ice for 30 min and then pelleted by centrifugation at 16000 x g for 15 min at 4°C. The protein pellet was dissolved in isoelectric focusing (IEF) sample buffer (8 M urea, 4% (w/v) CHAPS, 1% (v/v) Triton X-100, 1% DTT, 20 mM Tris, 0.5% (v/v) IPG buffer [pH3-10]) and proteins concentrations were determined using a D_C Protein Assay.

Ready-to-use Immobiline DryStrips (13 cm, pH 3-10) were re-hydrated overnight in 250 µl of protein solution (750 µg for staining and 250 µg for immunobloting) and IEF was then carried out up to a total of 75 kVh on an IPGphor isoelectric focusing system (Amershan). Prior to SDS gel electrophoresis, focused strips were equilibrated first in SDS equilibration buffer (50 mM Tris-Cl [pH 8.8], 6M urea, 30% (v/v) glycerol, 2% (w/v) SDS) containing 10 mg/ml DTT for 15 min, and then in the same buffer containing 25 mg/ml iodoacetamide instead of DTT for 15 min. SDS-PAGE was performed on 11% polyacrylamide gels (180 mm x 160 mm x 1 mm) at a constant current of 25 mA/gel for 3 hrs with cooling. Gels were stained with brilliant blue G-colloidal concentrate (Sigma) or silver (Shevchenko *et al.*, 1996). Although some proteins were lost as a result of the acetone treatment, the resolution of components was greatly enhanced by including this step as part of the procedure.

For immunoblot analysis, gels were transferred (Towbin *et al.*, 1979) to PDVF membranes, blocked in 3% BSA for 1 hr, and then incubated with either anti-phosphothreonine (1/1000 dilution) or anti-phosphotyrosine (1/1000 dilution) primary antibodies in 3% BSA in TBS-Tween (25mM Tris-Cl [pH 8.0], 1.0% NaCl, 0.1% Tween 20) at 4°C overnight. Membranes were washed in TBS-Tween before being exposed to secondary antibody (donkey anti-rabbit or -mouse IgG conjugated to horseradish peroxidase) diluted 1/5000 in TBS-Tween. Bound antibody was detected by an enhanced chemiluminescence assay (ECL, Amersham) using X-ray film (X-OMAT XK-1, Kodak). When comparing levels of phosphoprotein between samples, the chemiluminescence signal on the immunoblots was detected on the same film to prevent differences in exposure time for affecting image analysis.

Stained gels and immunoblots were scanned using a UMAX-II scanner and image analysis/spot matching was performed using Amersham ImageMaster 2D Elite Software or programs available from the proteome 2D-PAGE database web site (http://www.mpiib-berlin.mpg.de/2D-PAGE/). Computer-aided spot matching was performed through the overlaying of the image of an immunoblot, the same immunoblot membrane stained with silver (Sorensen *et al.*, 2002), and a corresponding stained gel. For each phosphoprotein detected on an immunoblot, surrounding landmark proteins were identified from the above overlays and used to locate the position of phosphoproteins on stained gels through the measurement of distances between landmark spot patterns and phosphoprotein spots. A phosphoprotein spot was considered matched if three independent repeats of this process overlaid the phosphoprotein spot

to a single resolved protein on the stained gel. pI values were determined relative to the values specified by the manufacturer of the pI strips (Amersham).

2.2.10 In-gel tryptic protein digestion

All reagents used for in-gel tryptic digestion (Wilm *et al.*, 1996; Gharahdaghi *et al.*, 1999) were prepared immediately prior to use. Excised protein spots were placed in 1.5 ml siliconized microcentrifuge tubes, which were rinsed with HPLC quality methanol before use. All gel pieces were washed in 50% (v/v) methanol and 5% (v/v) acetic acid overnight, after which, the wash solution was removed and the wash repeated for 2 hr. In the case of silver stained spots, gel pieces were destained prior to the wash procedure as described in Gharahdaghi *et al.* (1999).

Following the wash procedure, gel spots were digested with trypsin essentially using standard procedures as described in Wilm *et al.* (1996). Briefly, gel pieces were dehydrated in 200 µl acetonitrile for 5 min and then dried at ambient temperature in vacuum centrifuge for 3 min. 30 µl of 10 mM DTT in 100 mM ammonium bicarbonate was added to the dried gel pieces and incubated for 30 min. After removal of the DTT solution, 30 µl of 100 mM iodoacetamide in 100 mM ammonium bicarbonate was added to the gel pieces and incubated for an additional 30 min. Samples were then dehydrated in 200 µl of acetonitrile for 5 min, then washed in 200 µl of 50 mM ammonium bicarbonate for 10 min, before being dehydrated in acetonitrile and dried. Trypsin was dissolved in ice-cold 50 mM ammonium bicarbonate to a concentration of 25 ng/µl and 30 µl of this solution was then used to re-hydrate the dried gel pieces on ice for 10 mins. Once re-hydrated the excess trypsin solution was removed and the gel pieces were covered with 50 mM ammonium bicarbonate and digested overnight at 37°C.

After digestion, peptides were extracted by the addition of 30 µl of 50 mM ammonium bicarbonate and incubation at room temperature for 10 min, followed by centrifugation at 13,000 x g to pellet insoluble material. The supernatant was removed and the procedure repeated two additional times with 30 µl of 50% (v/v) acetonitrile, 5% (v/v) formic acid. The pooled supernatants were reduced to approximately 20 µl by vacuum centrifugation and stored at –80°C

2.2.11 Mass spectral identification and analysis

Extracted peptides were analyzed by the UVic–Genome BC Proteomics Centre (http://www.proteincentre.com/) on an Applied Biosystems Voyager DE-STR MALDI-TOF and Applied Biosystems/MDS Sciex QStar. Interpretation of MS and MS/MS spectra was done using the program Mascot (Perkins *et al.*, 1999), with MS searches initially done with a maximum mass tolerance of ± 0.2 Da, a single trypsin missed cleavage, and no phosphorylation modification. MS/MS analysis was used to confirm all spot identifications. While MS/MS can be used to detect the phosphorylation of the extracted peptides, this methodology was not used during this analysis.

2.2.12 Microscopy

Phase contrast, DIC (differential interference contrast) and epifluorescent images of live amoebae were observed with an Olympus IX-70 inverted microscope equipped with 20x and 40x objective lenses and a 1.5x multiplier. In chemotaxis assays, a Narishige MN-151 joystick style micromanipulator (Narishige Instruments) was used for positioning of micropipet tips. Images were captured with a DAGE-100 CCD camera (Dage Corp) using a Scion LG-3 frame grabber on a Pentium PC running Scion Image 4.0 (Scion Corp). For streaming assays, phase contrast images of live amoebae were observed with an Olympus CK inverted microscope equipped with 4x, 10x and 20x objectives, captured with the DAGE-100 CCD camera (Dage Corp) using a Scion VG-5 frame grabber on a PowerPC Macintosh running Scion Image 1.62 (Scion Corp). For indirect immunofluorescence images, mounted slides were observed on an Zeiss Axioplan fluorescent microscope equipped with 40x, 60x and 100x objective lenses using a DVC camera (Diagnostic Instruments) and Northern Eclipse imaging software. Images were subsequently complied and edited using Scion Image and Adobe Photoshop 5.0.

2.2.13 Indirect immunofluorescence

For indirect immunofluorescence staining for DdCAD-1, cells were deposited on No.1 glass coverslips (VWR Scientific Inc.) and allowed to adhere for 10 min in HL5 media. Once adhered, the media was removed and the cells were gently washed with KK2 to remove the remaining media. Cells were fixed in 4% formaldehyde in KK2 for 15 min at room temperature.

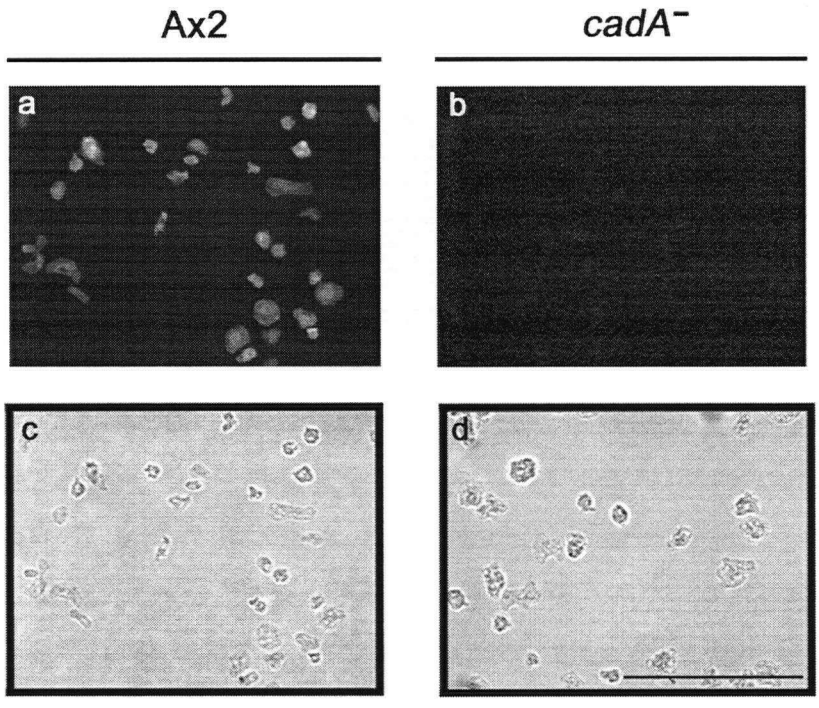

Figure 4. **Immunofluorescent staining of DdCAD-1 in Ax2 and *cadA* null cells.** Ax2 (a, c) and *cadA* null (b, d) fixed and permeablized with cold methanol before being immunostained by indirect immunofluorescence with anti-DdCAD-1 antibodies (a, b) as described in Materials and Methods. Corresponding DIC images are shown (c, d). Images were taken on an Olympus IX-70 inverted microscope. Bar: 100 μm.

In the cases where cells were permeablized, the previous solution was removed and cold methanol (-20°C) containing 1% formaldehyde was added for 5 min (Fukui *et al.*, 1987). Nonspecific binding was blocked with 1% (w/v) BSA in PBS for 10 min, before samples were incubated with DdCAD-1 antiserum (1:400 dilution in PBS containing 1% BSA) (Sesaki and Siu, 1996) for 1 hr. Samples were then washed three times in PBS containing 0.05% Tween 20 and then stained with FITC-conjugated goat anti-rabbit IgG (1:200) (Jackson Laboratories) for 1 hr. Samples were then washed three times in PBS containing 0.05% Tween 20 and the coverslips mounted in Prolong^{R} Antifade mounting media (Molecular probes) on Premium microscope slides (Fisher). Images were acquired using a Zeiss Axioplan fluorescent microscope equipped with 60x objective lenses using a DVC camera (Diagnostic Instruments) and Northern Eclipse imaging software. The specificity of DdCAD-1 antiserum (Sesaki and Siu, 1996) was confirmed by staining of *cadA* null strain (*Figure 4*).

2.2.14 Cell cohesion assays

Cell cohesion assays were performed using a modification (Wong *et al.*, 2002) of the original roller tube assay of Gerisch (Gerisch, 1980). Vegetative cells were centrifuged at 700 x g for 4 min, washed in KK2 and resuspended in KK2 at 2 x 10^7 cells/ml. Cells were starved in rotatory agitated suspension (175 rpm) at 22°C for 4 hrs, after which they were resuspended to a density of approximately 2.5 x 10^6 cells/ml. Cell aggregates were dispersed by vigorously vortexing for 15 sec. Aggregates were allowed to re-form while rotating on a platform shaker rotating at 180 rpm at room temperature. At indicated times, the number of non-aggregated cells, including singlets and doublets, were scored using a hemocytometer. The percentage of cell aggregation was calculated by subtracting the number of non-aggregating cells (singlets and doublets) from the total number of cells and dividing this number by the total number of cells. The requirement for divalent cations for cell cohesion was assayed in the presence of 10 mM EDTA (Wong *et al.*, 2002).

For the visual monitoring of cell cohesion, cells were allowed to adhere together in HL5 media alone or HL5 media supplemented with 10 mM EDTA or 50 μg/ml anti-DdCAD-1 antibodies. After the indicated times, cells were seeded on Nunc tissue culture dishes and images taken on an Olympus CK inverted microscope equipped with equipped with a DAGE-100 CCD camera (Dage Corp).

2.2.15 Chemotaxis and aggregation streaming assays

Micropipet chemotaxis assays were carried out on vegetative cells that were dispersed at a density of approximately 4 x 10^5cells/cm^2 in HL5 media on Nunc tissue culture dishes. The cells were then rinsed once and submerged in 20% HL5 (Palmieri *et al.*, 2000). At t=0, a micropipet (Eppendorf Femtotip II) filled with 25 mM folate was positioned in the field of view and cell movements monitored by time-lapse microscopy. To observe aggregation streaming, vegetative cells were seeded at approximately 5 x 10^5 cells/cm^2 in Nunc tissue culture dishes and allowed to adhered for 30 min. Cells were washed twice with Bonner's salts (10 NaCl, 10 mM KCl, 2 mM $CaCl_2$) and then submerged under Bonner's salts. Images were taken on an Olympus CK inverted microscope with the DAGE-100 CCD camera.

2.2.16 Assay of folate stimulation of ERK2 and PKB phosphorylation

For folate stimulation of ERK2/p70 phosphorylation the procedure used by Maeda and Firtel (1997) was utilized. Vegetative cells were washed twice in KK2 buffer, resuspended at approximately 5 x 10^6 cells/ml in KK2 and then agitated at 175 rpm at 22°C for 30 min. For folate stimulations to monitor PKB phosphorylation (Lim, 2002), the above step was excluded. Cells were then washed twice in KK2 buffer, resuspended in 1 ml of KK2 at a density of 1 x 10^8 cells/ml and vortexed gently. Cells were stimulated with folate to a final concentration of 50 nM. At the indicated times, 50 µl samples were lysed by mixing with 10 µl 6x Laemmli SDS-PAGE loading buffer (6x Laemmli SDS-PAGE is 350 mM Tris-Cl, pH 6.8, 10% SDS, 600 mM DTT, 0.012% w/v bromophenol blue, 30% glycerol, 12 mM NaF, 12 mM Na_3VO_4, 12 mM EDTA, and complete protease inhibitor cocktail (Roche)). Protein samples were fractionated by 1D electrophoresis and subjected to immunoblot analysis as described in Sections 2.2.8. The antibodies used were the Phospho-p44/42 MAP kinase polyclonal antibody (Cat# 9101) and the phosphothreonine polyclonal antibody (Cat# 9381). Equal loading of proteins was ensured through determining protein concentrations using a D_C Protein Assay and checking a duplicate gel with Coomassie G-250. Bound antibody was analyzed using GeneQuant Analysis software (Molecular Dynamics).

2.2.17 Protein translocation assays

Cells (1 x 10^7) were washed in KK2 buffer and then resuspended in 1 mL KK2 buffer supplemented with complete protease inhibitors (Roche), 1 mM NaF and 1 mM Na_3VO_4. Cell

suspensions were lysed by filtration through a 5.0 μm TMTP membrane and the lysates were collected in microcentrifuge tubes (Diamed). Samples were microfuged at 16,000 x g for 1 min, the sedimented pellet dissolved in 100 μl 1x Laemmli SDS-PAGE loading buffer (6x Laemmli SDS-PAGE is 350 mM Tris-Cl, pH 6.8, 10% SDS, 600 mM DTT, 0.012% w/v bromophenol blue, 30% glycerol, 12 mM NaF, 12 mM Na_3VO_4, 12 mM EDTA, and complete protease inhibitor cocktail (Roche)) and subjected to immunoblot analysis as described in Sections 2.2.8. A sample of non-lysed cells was also collected as a 'total protein' control and lysed directly in 1x Laemmli SDS-PAGE loading buffer.

2.2.18 Subcellular fractionation

For the separation of membranes by differential centrifugation (Bush *et al.*, 1994), 1 x 10^8 cells were stimulated with folate as described in section 2.2.16 for 8 min. Cells were then pelleted, resuspended in 0.25 M sucrose, 1.0 mM NaF, 1.0 mM Na_3VO_4, 1.0 mM EDTA and broken with a Dounce homogenizer. Under these conditions, 95% of the cells were broken as determined by phase-contrast light microscopy. The homogenate was then subject to differential centrifugation to generation a P1 (1000 x g for 5 min) and P2 (10,000 x g for 10 min) membrane fractions. The resulting pellet and supernatant fractions were subjected to SDS-polyacrylamide gel electrophoresis and immunoblot analysis as described in Section 2.2.8.

3 RESULTS

3.1 The effects of RasG protein levels on *discoidin* expression

3.1.1 Introduction

Preliminary experiments, conducted in collaboration with Meenal Khosla, and described in the Introduction to this thesis, had indicated that activated RasG inhibits *discoidin* expression. However, the interpretation of the inhibitory effects of RasG(G12T) on *discoidin* expression was complicated by the fact that the activated RasG protein was itself expressed from the *discoidin* promoter and therefore could repress its own production.

3.1.2 Accumulation of RasG(G12T) is accompanied by decreased *discoidin* mRNA levels

To independently demonstrate that the presence of RasG(G12T) suppressed expression from the *discoidin* promoter, transformants were isolated that expressed *rasG*(G12T) under the control of the ribonucleotide reductase (*rnrB*) promoter (Gaudet and Tsang, 1999). This promoter has been shown to respond to DNA-damaging agents (e.g. methyl methanesulfonate, 4-nitroquinoline 1-oxide and UV light) by increasing expression, making it useful for the inducible expression of endogenous genes (Gaudet *et al.*, 2001). *rnrB-rasG*(G12T) transformants rapidly induced the production of RasG(G12T) protein upon exposure to 10 mM methyl methanesulfonate (MMS) (*Figure 5A*) and a reduction of *discoidin* mRNA level was observed after two hrs of MMS treatment (*Figure 5B*). A similar repression of *discoidin* mRNA levels was observed at all the cell densities tested (8×10^5 to 4×10^6 cells/ml) (data not shown). When wild-type Ax-2 cells were treated with 10 mM MMS, there was no effect on RasG protein level (*Figure 5A*) or *discoidin* mRNA level (*Figure 5B*). The sensitivity of the *discoidin* promoter to the presence of RasG(G12T) was further revealed by decreasing the concentration of MMS to 5 mM. While the amount of RasG(G12T) protein that was reduced (*Figure 5A*), there was still an appreciable repression of *discoidin* mRNA levels (*Figure 5B*). These results showed that increased intracellular RasG(G12T) was associated with repressed *discoidin* mRNA levels.

3.1.3 Discoidin expression in *rasG* null cells

Since *discoidin* expression was repressed in the presence of elevated levels of RasG(G12T) in the cell, it was anticipated that it would be unaffected, or even enhanced, in *rasG*

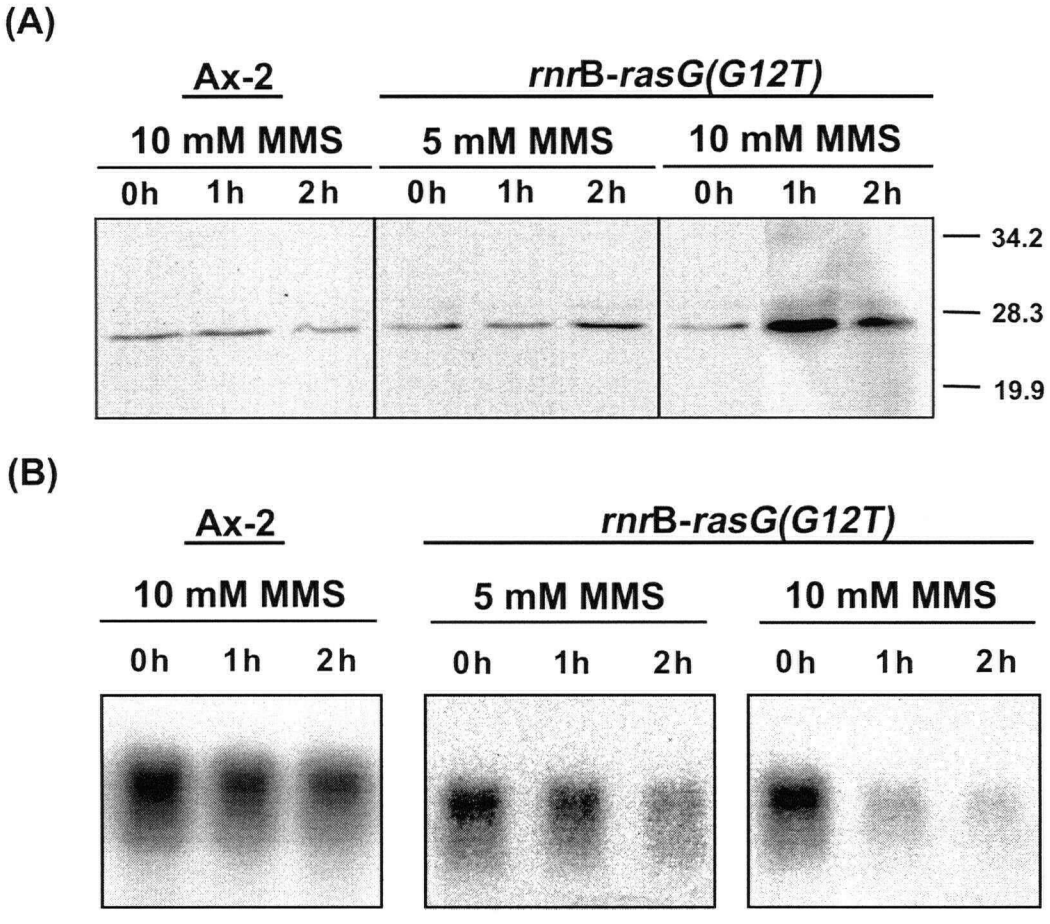

Figure 5. **Effect of RasG(G12T) expression from the *rnrB* promoter on *discoidin* mRNA levels.** Ax-2 and *rnrB-rasG(G12T)* transformed cells were grown in HL5 media to a cell density of approximately 1 x 10^6 cells/ml and then supplemented with methyl methanesulfonate (MMS) at the indicated concentration. (A) Aliquots were taken either immediately or 1 and 2 hrs after the addition of MMS and RasG protein levels were determined by immunoblot analysis as described under Materials and Methods. Molecular weight markers in kDa are shown. (B) The samples described in (A) were also assayed for discoidin mRNA levels by northern blot analysis.

null cells (Tuxworth *et al.*, 1997). In fact, the Discoidin level in *rasG* null cells was considerably lower than the level in the Ax2 parental line (*Figure 6A, lane 7 verses lane 1*), suggesting a requirement of RasG for high level *discoidin* expression. This finding raised the question as to whether the presence of RasG was necessary for any of the previously described aspects of *discoidin* promoter regulation (Blusch *et al.*, 1992; Burdine and Clarke, 1995; Gomer *et al.*, 1991; Wetterauer *et al.*, 1995).

It has been shown that Discoidin levels first increase and then decrease during the growth of Ax2 cells in axenic medium (Wetterauer *et al.*, 1995). The levels of Discoidin in *rasG* null cells were therefore monitored during axenic growth and compared to the levels in Ax2. The expected pattern of Discoidin expression in Ax2 was observed, with maximum levels of Discoidin occurring during late exponential phase at a cell density of 8.5 x 10^6 cells/ml (*Figure 6A, lanes 1-6*). A similar, but less pronounced pattern of discoidin expression was observed in the *rasG* null cells, with maximum levels of discoidin occurring during late exponential phase for these cells at a cell density of 2.6 x 10^6 cells/ml (*Figure 6A, lanes 7-12*). Since more pronounced differences between the two strains might have been masked by a low turnover of the Discoidin protein, *discoidin* mRNA levels were also monitored. This analysis emphasized the similarities rather than the differences in *discoidin* expression between the two strains (*Figure 6B*). Despite the fact that the axenic growth characteristics of the *rasG* null cells are quite different from those of Ax2 (i.e. *rasG* null cells growing to lower cells densities in shake suspension) (Tuxworth *et al.*, 1997), the overall expression of *discoidin* in the two strains in response to axenic growth was remarkably similar. These results suggested that the presence of RasG was not necessary for the axenic growth dependent regulation of *discoidin* expression, but that RasG did impact *discoidin* mRNA translation or protein stability (*Figure 6A verses 6B*).

To determine if folate repressed *discoidin* expression in the absence of RasG, cells were grown in the presence and absence of folate and Discoidin protein levels determined (*Figure 7*). Growth in axenic medium supplemented with 1mM folate for 24 hrs resulted in a decline in Discoidin protein levels in both control Ax2 cells and *rasG* null cells, indicative of a repression of *discoidin* promoter activity in response to folate (Blusch *et al.*, 1992). These results demonstrated that RasG was not necessary for folate repression of *discoidin* expression.

When wild-type Ax2 cells are grown in suspension with bacteria, discoidin expression is suppressed until the bacteria are consumed and the amoebae reach stationary phase (Rathi et

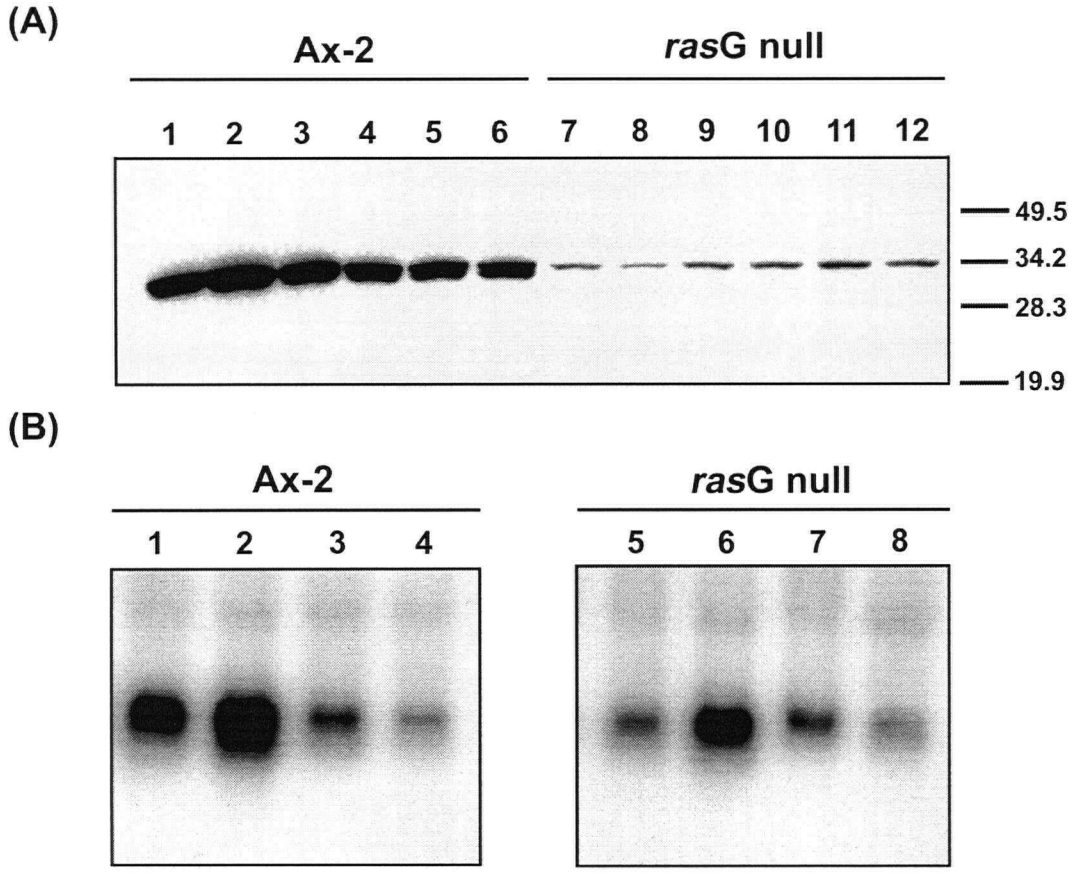

Figure 6. **Discoidin expression in *rasG* null cells during axenic growth.** Ax-2 and *rasG* null cells were grown in rotatory agitated suspension in HL5 media and aliquots were taken at various times during growth. Under these conditions *rasG* null cells grew with a generation time of approximately 30 hrs and only reached a cell density of 2 x 10^6 cells/ml in stationary phase. (A) Discoidin protein levels were determined by immunoblot analysis during growth at the following cell densities (cells/ml): for Ax-2, 1 x 10^6 (lane 1), 4.2 x 10^6 (lane 2), 8.5 x 10^6 (lane 3), 1.2 x 10^7 (lane 4), 1.8 x 10^7 (lane 5), 2.2 x 10^7 (lane 6); for *rasG* null, 1.2 x 10^6 (lane 7), 1.4 x 10^6 (lane 8), 1.9 x 10^6 (lane 9), 2.3 x 10^6 (lane 10), 2.6 x 10^6 (lane 11), 2.8 x 10^6 (lane 12). Molecular weight markers in kDa are shown. (B) Samples taken at the following cell densities (cells/ml): for Ax-2, 4.2 x 10^6 (lane 1), 8.5 x 10^6 (lane 2), 1.2 x 10^7 (lane 3), 2.2 x 10^6 (lane 4); for the *rasG* null, 1.4 x 10^6 (lane 5) 1.9 x 10^6 (lane 6), 2.3 x 10^6 (lane 7), 2.8 x 10^6 (lane 8) were also assayed for discoidin mRNA levels by northern blot analysis. Equal loading of RNA confirmed by EtBr staining as described in Material and Methods. Figure Credit: Done in collaboration with M. Khosla.

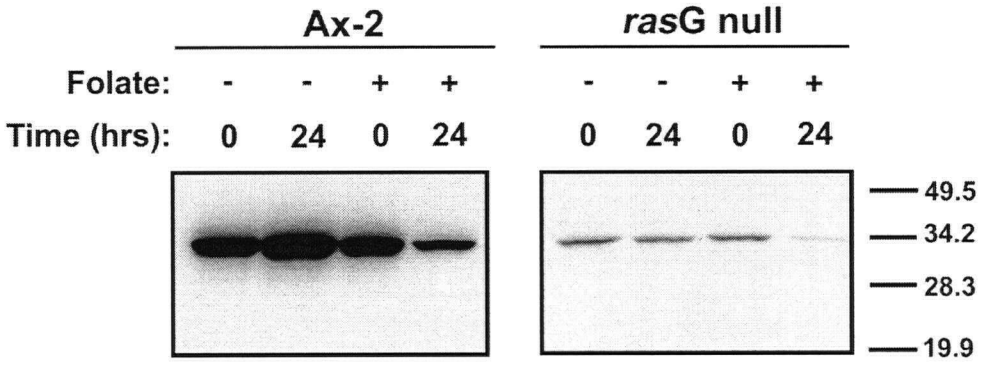

Figure 7. **Folate-repression of discoidin protein levels in Ax2 and *rasG* null cells.** Ax-2 and *rasG* null cells were grown in HL5 media to a density between 1-2 x 10^6 cells/ml, washed and then resuspended in fresh HL5 media in the presence (+) or absence (-) of 1 mM folate for 24 hrs. Aliquots were taken at the indicated times and discoidin levels were determined by immunoblot analysis as described in Materials and Methods. Molecular weight markers in kDa are shown. Figure Credit: Done in collaboration with M. Khosla.

al.,1991; Rathi and Clarke, 1992). The induction of discoidin expression during this growth period has been attributed to the removal of the inhibitory effects of the bacteria and to increasing levels of PSF in the medium (Burdine and Clarke, 1995). In order to determine if RasG was necessary for this induction, Discoidin expression in Ax2 and *rasG* null cells grown in suspension with bacteria was compared (Figure 8). In both strains, Discoidin levels increased when cells had consumed all the bacteria and entered stationary phase (Figure 8), indicating that RasG was not necessary for the inhibition by bacteria and for PSF induction.

Discoidin expression is also induced during early development and this induction has been attributed to CMF stimulation (Gomer et al., 1991). To determine if RasG was necessary for this induction, *rasG* null cells were washed free of media and plated on agar after growth in suspension with bacteria. The *rasG* null cells displayed a delay in Discoidin expression relative to that observed for Ax2 (Figure 9). This result was similar to the result described above for the induction of Discoidin during growth on bacteria. The delay in Discoidin expression corresponded to the delay in the aggregation of the *rasG* null cells (see section 3.3.6), indicating that the presence of RasG was not required for the induction of Discoidin expression normally observed as cells aggregate. Nevertheless, this result indicated that RasG might modulate the induction of Discoidin expression observed during the first six hrs of development.

3.1.4 Summary

The expression of activated RasG(G12T) from the *rnrB* promoter was shown to repress *discoidin* expression. Despite this repression, RasG was found to be required for high *discoidin* expression, since *discoidin* expression was low in *rasG* null cells. However, RasG was not involved in the regulation of *discoidin* expression by folate, CMF, PSF, bacteria and growth in axenic media, all signals shown previously to regulate *discoidin* expression. It should be noted here that although the expression of RasG(G12T) from the discoidin promoter in *pVEII-rasG*(G12T) cells has been shown to reduce Discoidin protein levels due to protein turnover (Secko *et al.*, 2001), using the induction times shown in Figure 5, expression of RasG(G12T) from the *rnrB* promoter did not reduce Discoidin protein levels (D. Secko, *unpublished observations*). This difference may be due to difference in the time frame of inducible expression, since *pVEII-rasG*(G12T) cells are typically induced for 48-72 hrs while *rnrB-rasG*(G12T) cells were induced for 2 hrs (Secko *et al.*, 2001).

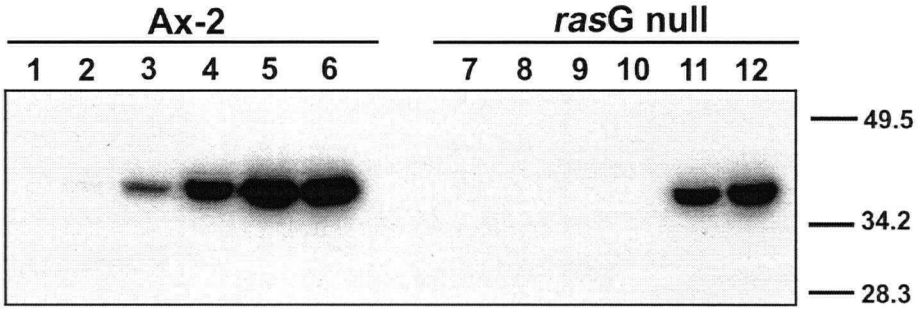

Figure 8. **Discoidin expression in *rasG* null cells during growth on bacteria.** Ax-2 and *rasG* null cells were grown in a suspension of *Klebsiella aerogenes* as described in Materials and Methods. Cells that had been previously grown in a bacterial suspension for seven-eight generations were inoculated at a density of 5 x 10^4 cells/ml into a fresh bacterial suspension and discoidin protein levels were monitored during growth at the following cell densities (cells/ml): for Ax-2, 1.6 x 10^6 (lane 1), 3.5 x 10^6 (lane 2), 7 x 10^6 (lane 3), 8.6 x 10^6 (lane 4), 1.1 x 10^7 (lane 5), 1.7 x 10^7 (lane 6); for the *rasG* null, 1.2 x 10^6 (lane 7), 3.8 x 10^6 (lane 8), 5.3 x 10^6 (lane 9), 7.6 x 10^6 (lane 10), 8.1 x 10^6 (lane 11), 8.4 x 10^6 (lane 12).

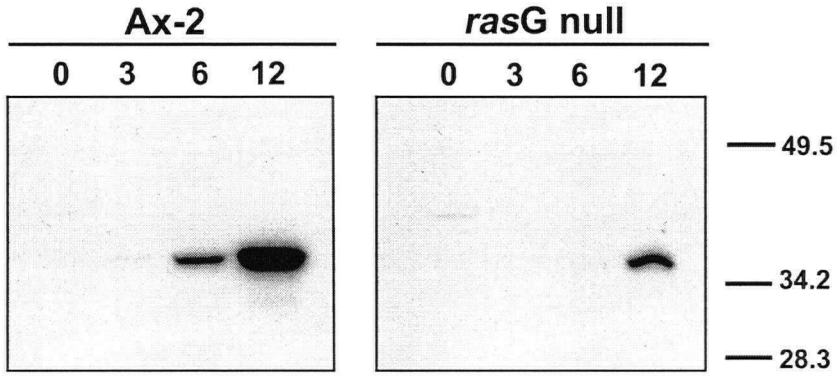

Figure 9. **Discoidin expression during the development of *rasG* null cells.** Cells were set up to develop on non-nutrient agar buffered with KK2 after growth in a bacterial suspension to a density of approximately 3 x 10^6 cells/ml. Protein samples were taken at the indicated times (in hrs) after plating and discoidin protein levels determined. Molecular weight markers in kDa are shown.

3.2 Use of an inducible RasG(G12T) expression system to identify *Dictyostelium* phosphoproteins altered by the expression of RasG(G12T)

3.2.1 Introduction

The discovery that RasG regulated *discoidin* expression revealed an inherent problem with the use of the *discoidin* promoter to express RasG, and thus the need for an alternative expression system. The studies with the *rnrB* promoter, outlined in the previous section (3.1), indicated that the effects of RasG(G12T) on *discoidin* expression were rapid and raised the possibility that this might be a useful system for determining downstream effectors involved in RasG signaling. However, although the *rnrB* promoter was a useful alternative expression system, it had two shortcomings for additional studies: the need to use DNA damaging agents for induction and the stability of expression. Although the former can be overcome through the use of short induction times (*Figure 5*), the induction agent does cause cell death over extended exposure times (Gaudet *et al.*, 2001). More troublesome was the observation that RasG(G12T) induction from the *rnrB* promoter became non-responsive to MMS after the strains had been grown for several passages, ultimately requiring re-transformation and the selection of new transformants (D. Secko, *unpublished observations*).

3.2.2 Expression of RasG(G12T) from the tetracycline promoter, an alternative expression system

Given the constraints of the *rnrB* promoter system, an alternative *Dictyostelium* expression system based on the adaptation of the widely used tetracycline (*tet*) promoter (Blaauw *et al.*, 2000) was tested. To monitor the effectiveness of the tetracycline repressible promoter system the levels of RasG protein in wild-type Ax2 cells containing an empty vector (Ax2::MB) and in cells containing RasG(G12T) under control of the *tet* promoter (Ax2::MB-*rasG*(G12T)) were measured. Levels of *discoidin* mRNA were also determined. When Ax2::MB and Ax2::MB-*rasG*(G12T) cells were grown in the presence of 5 μg/ml tetracycline the expression of RasG protein in these cells was similar (*Figure 10A*). Comparison of the levels of *discoidin* mRNA in the Ax2::MB and Ax2::MB-*rasG*(G12T) cells revealed the *discoidin* mRNA levels to be slightly repressed Ax2::MB-*rasG*(G12T) cells (*Figure 10A*). This suggested that repression of the *tet* promoter in the presence of 5 μg/ml tetracycline was not complete and that potentially

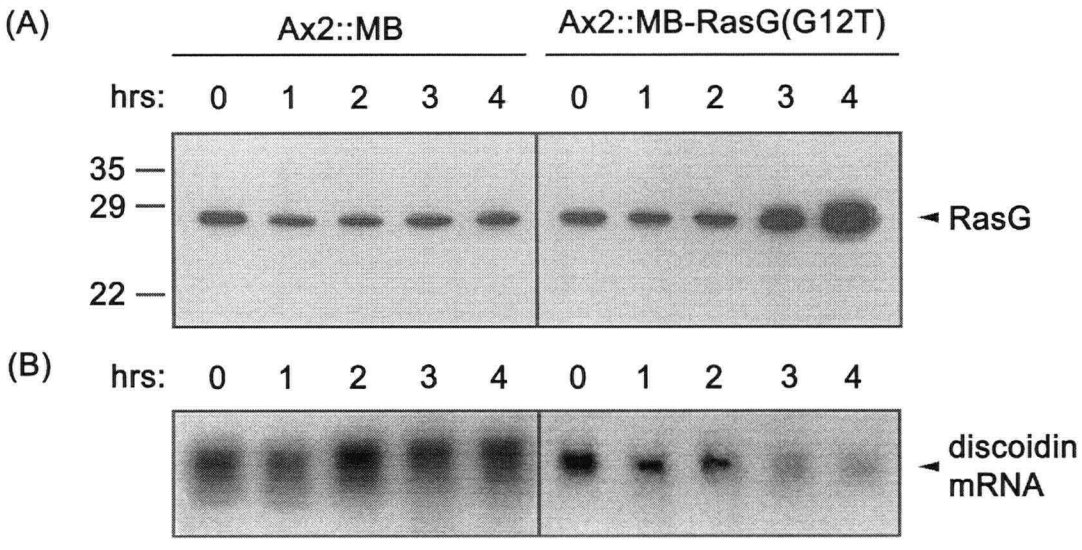

Figure 10. **Induction of RasG(G12T) protein levels from the *tet* promoter and its effect on discoidin mRNA levels.** (A) Transcription from the *tet* repressible promoter in Ax2::MB and Ax2::MB-*rasG*(G12T) cells was induced by washing two times with HL5 to remove tetracycline. Washed cells were resuspended in HL5 and allowed to grow for 4 hrs, during which aliquots were taken at the times indicated and RasG levels determined by immunoblot analysis. Molecular weight markers in kDa are shown. (B) The cell samples taken in (A) were also used for RNA isolation and subsequently assayed for *discoidin* mRNA levels by Northern blot analysis.

undetectable levels of RasG(G12T) were being expressed in the presence of tetracycline. Increases in the levels of RasG were clearly observable in the Ax2::MB-*rasG*(G12T) cells as early as three hrs after the removal of tetracycline (*Figure 10A*). This increase was sufficient to induce a repression of *discoidin* gene expression (*Figure 10B*). These results revealed that tetracycline repressible promoter system was an effective alternative for the expression of RasG(G12T) and that under these conditions signaling was occurring from RasG to *discoidin* gene expression.

3.2.3 Detection of protein phosphorylation changes upon the expression of activated RasG

The availability of a system for the regulated expression of activated RasG provided an opportunity to further define the molecular components of the RasG signaling pathway. Ras activation in other organisms has been shown to activate phosphorylation cascades, in which proteins are sequentially phosphorylated as signals are transmitted through the cell (Hunter, 2000; Campbell *et al.*, 1998). It was, therefore, hypothesized that the rapid expression of RasG would result in changes in the phosphorylation of proteins that are putative RasG signaling pathway components and/or targets.

To determine if differences in protein phosphorylation could be detected, cells that were either expressing or not expressing activated RasG were induced for three hrs and lysed by the addition of lysis buffer (see Materials and Methods). Ten μg of protein was fractioned by SDS-PAGE and then transferred to a PDVF membrane. Immunoblot analysis using monoclonal phosphotyrosine or polyclonal phosphothreonine antibodies allowed the detection of a subset of vegetative phosphoproteins (*Figure 11*). Several proteins exhibited reproducible changes in protein phosphorylation in cells expressing *rasG*(G12T) relative to cells containing the empty vector (*Figure 11*).

3.2.4 Separation of RasG-responsive phosphoproteins by 2D gel electrophoresis

To determine the identity of the vegetative proteins exhibiting altered phosphorylation, proteins were first separated by 2D gel electrophoresis, using a pI range of 3-10. These gels were blotted to PVDF membranes and phosphorylated proteins detected once again using monoclonal phosphotyrosine or polyclonal phosphothreonine antibodies (*Figure 12*). The increased resolution afforded by this method allowed the detection of over 70 phosphothreonine proteins.

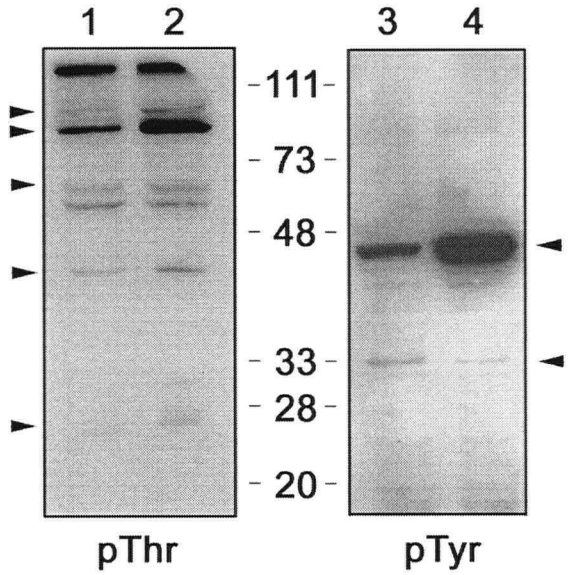

Figure 11. **Effect of RasG(G12T) expression from the *tet* promoter on the phosphorylation of vegetative proteins.** Ax2::MB (lanes 1 and 3) and Ax2::MB-*rasG*(G12T) (lanes 2 and 4) cells were sampled three hrs after removal of tetracycline and fractionated by 1D gel electrophoresis. Immunoblots were assayed for phosphothreonine (lanes 1 and 2) or phosphotyrosine (lanes 3 and 4) containing proteins by using phosphothreonine and phosphotyrosine specific antibodies. Changes in the vegetative phosphorylation pattern caused by RasG(G12T) induction are indicated (closed arrows).

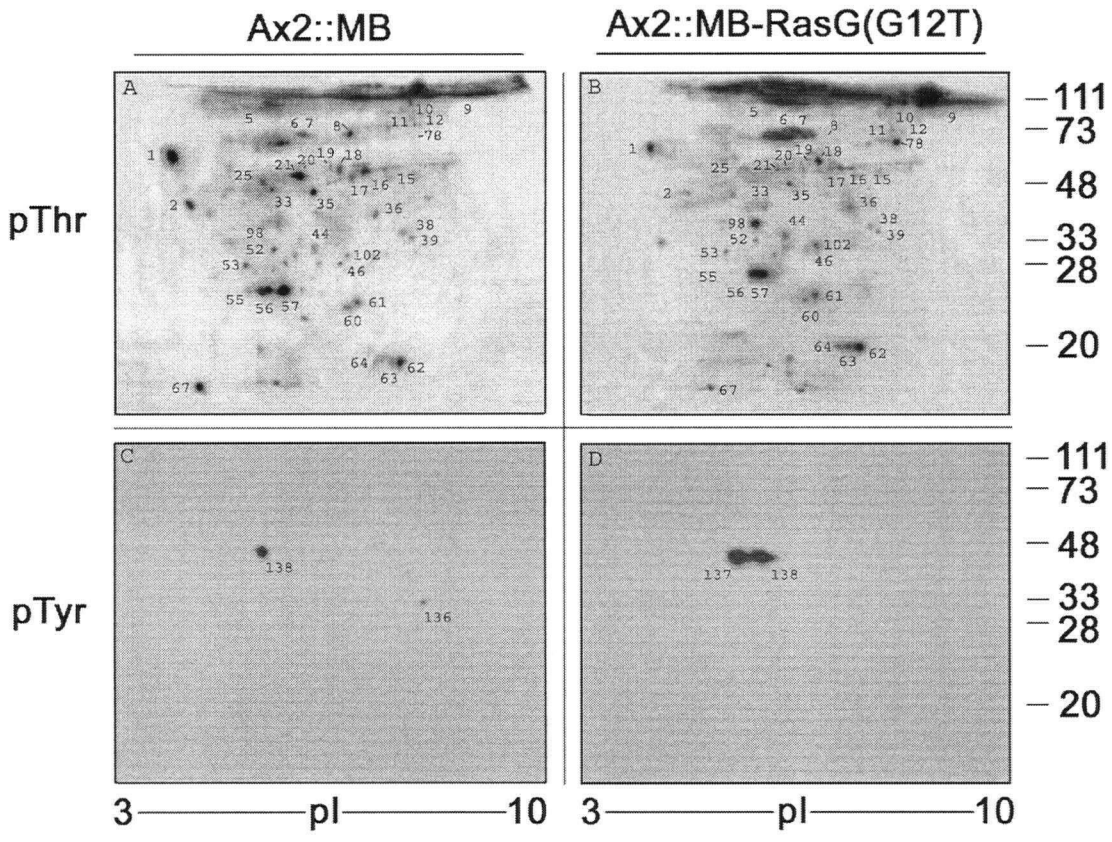

Figure 12. **Immunoblots of vegetative phosphoproteins separated by 2D gel electrophoresis.** Total protein from Ax2::MB (A, C) and Ax2::MB-*rasG*(G12T) (B, D) cells three hrs after removal of tetracycline was fractionated by 2D electrophoresis and blotted. Membranes were probed with either anti-phosphothreonine (A, C) or anti-phosphotyrosine (B, D) antibodies. Every spot was systematically numbered, irrespective of its detection on other gels and then cross-referenced between gels. The blots shown are representative of three independent experiments and molecular weight (kDa) and pI ranges indicated. For simplicity, only a subset of the detected spots are labeled.

This is likely to be a minimum estimate of phosphothreonine containing proteins present in vegetative cells, since, for example, s5 and s9 were smeared spots that probably contain several poorly resolved proteins. Consistent with this interpretation, it has been observed previously that high molecular mass components are difficult to resolve (Gorg *et al.*, 2000). Only three phosphotyrosine containing proteins were detected (*Figure 12*), suggesting that the method was not sufficiently sensitive to detect most species. The predominant phosphotyrosine protein detected in 1D SDS-PAGE gels (*Figure 11*) was resolved into two spots, s137 and s138 (*Figure 12*), both of which showed an increase in tyrosine phosphorylation in the Ax2::MB-*rasG*(G12T) cells.

The phosphoproteins could be subdivided into three categories: those exhibiting unchanged intensity, those exhibiting altered intensity, and those exhibiting apparent pI shifts, as assessed by alterations in position, and examples of each category are shown in Figure 13. The majority of phosphoproteins detected fell into the first category, those not showing any significant change in response to RasG(G12T) induction, e.g. s60 and s61 (*Figure 13A*). Of the proteins in the second category, some showed a detectable level of phosphorylation in uninduced cells and were then further phosphorylated or dephosphorylated in response to activated RasG; for example, proteins s20 and s35 were present in uninduced cells, but exhibited a marked reduction in phosphorylation in response to RasG(G12T) expression (*Figure 13B*). For some proteins in this category, phosphorylation increased from or decreased to undetectable levels in response to the activation of RasG. For example, protein s98 was not detectably phosphorylated in uninduced cells but was significantly phosphorylated in response to activated RasG (*Figure 13C*). A few proteins fell into the third category as being phosphorylated in both strains, but also exhibiting an apparent shift in pI in response to activated RasG, e.g. s138 (*Figure 13D*), although identification of both spots will be essential to confirm that a pI shift has occurred. It should be noted that s138 was also a category 2 protein, since the spot increased appreciably in intensity in the induced cells.

Nineteen phosphoproteins (3 phosphotyrosine and 16 phosphothreonine), shown in Figure 12, displayed an appreciable and reproducible alteration in phosphorylation level and were considered for further study. Some of the changes in phosphorylation were very large (e.g. the increased phosphorylation of s137), while some were more modest (e.g. the increased

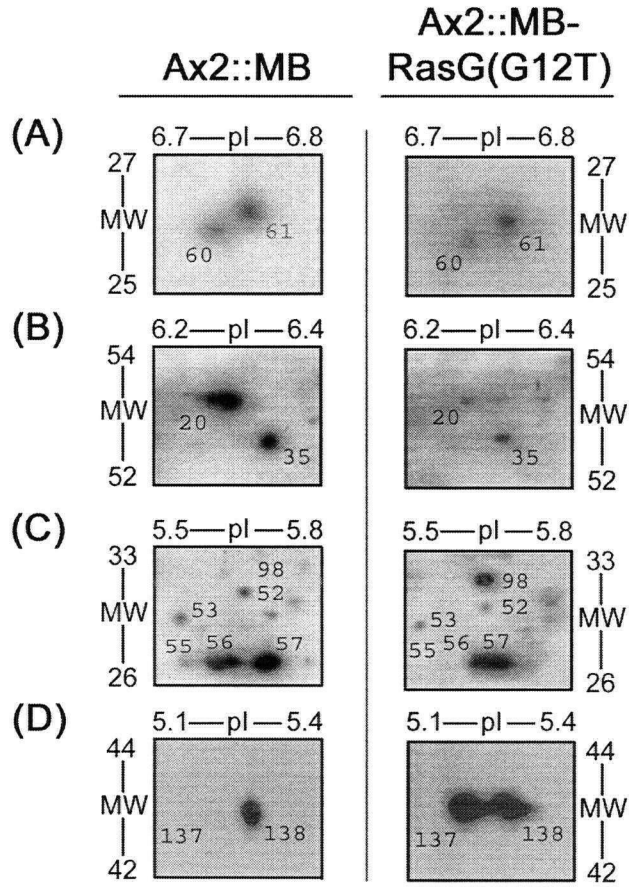

Figure 13. **Representative changes in phosphorylation between the Ax2::MB and Ax2::MB-*rasG*(G12T) strains.** Selected phosphoproteins are shown as image expanded blots. Molecular weight (kDa) and pI ranges are shown. (A) Proteins whose phosphorylation was unchanged by RasG(G12T) induction. (B and C) Proteins whose phosphorylation was altered (D) A phosphoprotein showing a possible shift in pI.

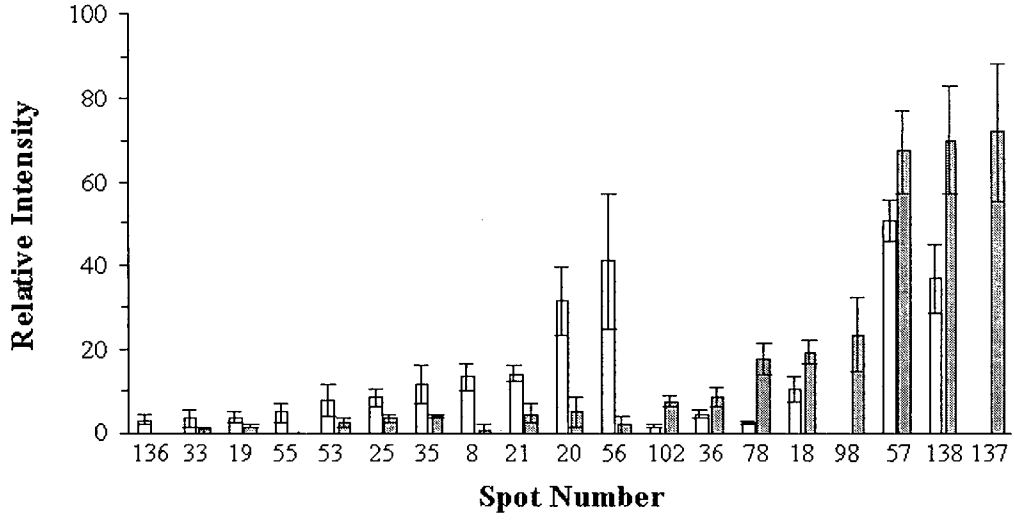

Figure 14. **Quantification of protein phosphorylation levels between the Ax2::MB and Ax2::*rasG*(G12T) strains.** 2D immunostained spots detected with anti-phosphothreonine or anti-phosphotyrosine antibodies (*Figure 10*) were quantified, their intensities normalized to an unchanged 2D reference spot on each gel. In addition, standard markers on each gel were used to check this normalization. The relative intensity of a subset of spots is indicated. Values plotted are the means and standard deviations for three experiments. Only proteins that showed a reproducible alteration in the three independent experiments are shown. Ax2::MB, *white bars*; Ax2::MB-*rasG*(G12T), *gray bars*.

phosphorylation of s18 and the decreased phosphorylation of s19) (*Figure 14*). Since these proteins represented only those most easily detected, there is clearly a complex pattern of protein phosphorylation or dephosphorylation in response to activated RasG. One component that did not exhibit an appreciable change (s57) was included in the analysis, since it appeared to be a major phosphorylated species.

3.2.5 Identification of putative RasG-responsive phosphoproteins

Of the nineteen phosphoproteins displaying changes in phosphorylation, only thirteen were clearly resolved by 2D electrophoresis into individual proteins and these were chosen for identification by mass spectrometry. The degree of resolution of these proteins was determined by matching the immunoblots to a corresponding brilliant blue G-colloidal or silver stained gel (*Figure 15*) as described under Materials and Methods. This allowed an estimation of the amount of a protein of interest and provided a measure of the reproducibility of the separation of neighboring proteins. Although the silver stained immunoblots contained a lower spot density than the stained gel, their overlay with the original immunoblot proved useful for determining the location of the proteins. For each of these thirteen proteins, the corresponding brilliant blue G-colloidal or silver stained spots did not noticeably change in staining intensity upon induction of activated RasG (*Figure 15*), indicating that the changes in phosphorylation were not due to differences in protein levels. As was found with *rnrB-rasG*(G12T) cells (Section 3.1.4), expression of RasG(G12T) from the *tet* promoter under the time frame utilized did not affect Discoidin protein levels.

These 13 proteins were excised from brilliant blue G-colloidal or silver stained gels, in-gel digested with trypsin (Wilm *et al.*, 1996) and the peptides extracted from these digests were used for peptide mass fingerprint analysis. Proteins present in low abundance, as revealed by weak silver stain intensity, were pooled from up to five individual gels to obtain adequate material for identification. Mass spectral identifications were accomplished by both peptide mass fingerprinting and MS/MS analysis (Graves and Haystead, 2002). Matching the obtained mass data against the *Dictyostelium* database (http://dictybase.org/index.html) allowed an identification of all 13 spots (*Table 1*). When selected peptides from each sample were subsequently subjected to MS/MS analysis to generate peptide sequence data, the results

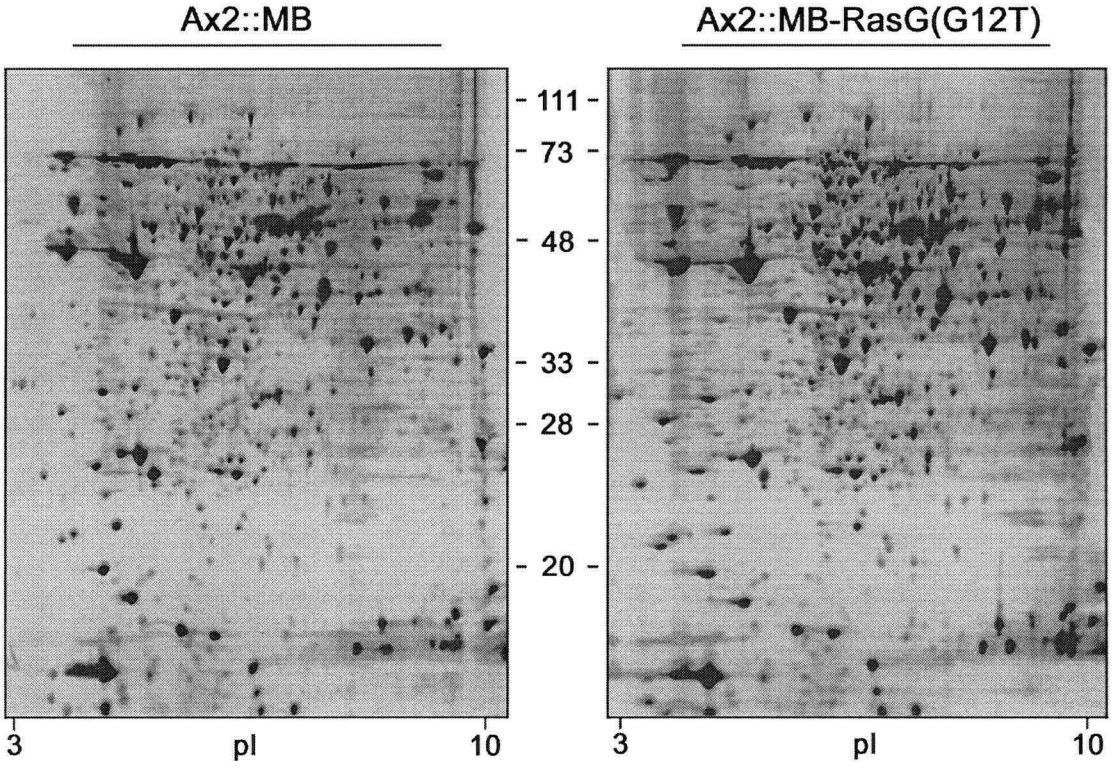

Figure 15. **Brilliant blue G-colloidal stained 2D gels of vegetative Ax2::MB and Ax2::MB-*rasG*(G12T) lysates.** A representative example of the 2D separation of acetone-precipitated vegetative cell lysates is shown for the strains Ax2::MB and Ax2::MB-*rasG*(G12T). Molecular weight markers (kDa) and pI ranges are indicated.

Table 1: A list of Ras-responsive phosphoproteins identified in this study

Known/ Predicted Function	Spot Number	Identified Protein	Mass (Da)	pI	% Sequence[a]	Genbank Accession Number
Signaling Proteins	8	RasGEF-R	70959	7.23	28	AAN46870
	20	Protein Kinase B	51315	6.42	22	AAA76692
	102	Phosphatidylinositol transfer protein 1	31365	5.84	23	AAF74409
	21	Putative cell division protein FtsZA	56854	5.42	29	AAG37880
Adhesion/ Cytoskeletal	55	Calcium-dependent cell adhesion moleclue-1	24139	5.40	88	P54657
	56	Calcium-dependent cell adhesion moleclue-1	24139	5.40	73	P54657
	57	Calcium-dependent cell adhesion moleclue-1	24139	5.40	55	P54657
	137	Actin	41803	5.23	37	ATDO
	138	Actin	41803	5.23	30	ATDO
Translation/ Metabolism	18	Similar to seryl-tRNA synthetase, cytoplasmic	52058	6.13	46	AC117072
	19	Putative UDP-glucose:glycoprotein glucosyltransferase precursor	192908	5.85	20	AAM08766
	98	Pyruvate dehydrogenase E1 component beta subunit	39217	5.69	40	AAO52409
Unknown	78	Hypothetical protein	67328	9.58	14	AAO52604

[a] % sequence equals the percetage of a protein sequence matched by peptide mass fingerprinting (Graves and Haystead, 2002)

confirmed the database identification. In two cases, the same protein was identified in more than one spot, e.g. s55, s56 and s57 (Calcium-dependent cell adhesion moleclue-1 or DdCAD-1), and s137 and s138 (Actin), suggesting that these proteins were phosphorylated on more than one site. Therefore, the thirteen identified spots totaled ten different proteins.

Of the phosphoproteins identified as being RasG-responsive, several were signaling molecules, including PKB and a RasGEF, proteins that have been shown to be involved in Ras signaling pathways in other cells, as well as Phosphatidylinositol Transfer Protein 1 (PITP1) and FtsZA. The remaining proteins were: a cell adhesion protein (DdCAD-1) and the cytoskeletal protein, actin; two proteins involved in metabolism (a pyruvate dehydrogenase and UDP-glucose:glycoprotein glucosyltransferase); a seryl-tRNA synthetase, and a protein of unknown function. Five of the proteins showed an increase in phosphorylation in response to RasG(G12T) expression; Actin [s137, s138], Pyruvate Dehydrogenase [s98], Seryl-tRNA Synthetase [s18], PITP1 [s102], and the unknown protein [s78]. Four proteins showed a decrease in phosphorylation in response to RasG(G12T) expression; RasGEF-R [s8], PKB [s20], FtsZA [s21], and UDP-glucose:glycoprotein glucosyltransferase [s19]. One protein, DdCAD1 showed a complex pattern of phosphorylation changes, indicating multiply phosphorylated forms of the protein. These forms exhibited either an appreciable decrease (s55 and s56) or a slight increase (s57) in phosphorylation response to RasG(G12T) expression. These alterations in phosphorylation did not correlate with predicted function, as both increases and decreases in phosphorylation appeared in each functional category (compare Table 1 with Figure 14). Furthermore, these proteins are not expected to all be components of a single RasG pathway, since RasG has been suggested to regulate multiple signaling pathways (Zhang et al., 1999) and mammalian Ras proteins interact with multiple effectors to regulate several signaling pathways (Shields et al., 2000).

3.2.6 Total protein level of a subset of RasG-responsive phosphoproteins does not change upon RasG(G12T) expression

The detection of phosphorylation differences in the identified RasG-responsive phosphoproteins (*Table 1*) could be interpreted in two ways: (i) as changes in activity of kinases or phosphatases in the cell that result in altered phosphorylation or (ii) changes in the total

protein level of these targets. As mentioned in the previous section, the brilliant blue G-colloidal or silver staining intensity between the Ax2::MB and Ax2::MB-*rasG*(G12T) strains did not significantly change upon induction (*Figure 15*), suggesting that the alterations in phosphorylation observed were not the result of changes in protein levels. To further confirm this, Ax2::MB and Ax2::MB-*rasG*(G12T) cells were sampled after three hrs of induction and lysed directly in SDS-PAGE lysis buffer. Ten μg of protein were then loaded onto a 1D SDS-PAGE gel, subjected to electrophoresis and transferred to a PDVF membrane. Immunoblot analysis was carried out to detect the total protein levels of three of the RasG-responsive phosphoproteins identified in Table 1, namely Actin, PKB, and DdCAD-1 (*Figure 16*). As expected, the levels of RasG protein increased in the Ax2::MB-*rasG*(G12T) cells upon removal of tetracycline, but in contrast, the levels of Actin, PKB and DdCAD-1 all remained constant. Additionally, the level of RasC, a protein that was not expected to be affected by RasG(G12T) induction, provided an additional control (*Figure 16*). These results confirmed that for a subset of the identified RasG-responsive proteins the levels of total protein did not change, further suggesting that the observed changes were due to differences in phosphorylation.

3.2.7 Confirmation of the identities of RasGEF-R and DdCAD-1

The gene encoding RasGEF-R was initially identified by the Insall laboratory as a cDNA clone, SSD492, whose predicted product showed strong homology to the *Dictyostelium* RasGEF-A (Aimless) and to other putative RasGEF proteins (Wilkins et al., 2001). The Insall laboratory subsequently went on to create three independent isolates that were null for RasGEF-R protein. The availability of these strains allowed confirmation that RasGEF-R was indeed one of the phosphothreonine proteins. Total protein samples taken from the *gefR* null strain, along with a random integrant control (IR26), were subjected to 2D immunoblot analysis. The s8 immuno-spot identified as RasGEF-R was found in the random integrant strain as before, but was not observed in the *gefR* null strain (Figure 17). The corresponding silver stained protein spot that had been used for mass spectrometric identification of s8 was also absent (Figure 17). Together these results support the conclusion that s8 is in fact RasGEF-R (Secko et al., 2004).

A strain null for DdCAD-1 has also been created (Wong *et al.*, 2002) and the availability of this strain allowed a similar spot identity confirmation. Total protein samples taken from the

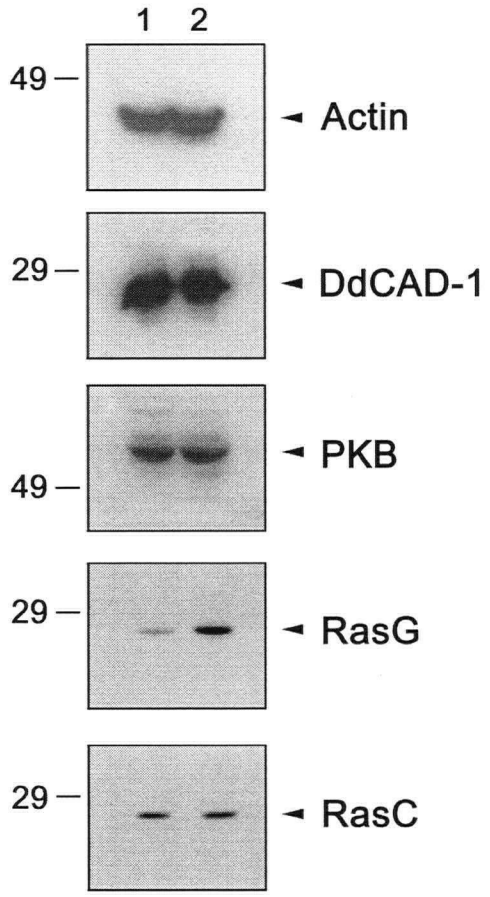

Figure 16. **Total protein levels of three putative RasG-responsive phosphoproteins in a RasG(G12T) expressing and vector control strain.** Total protein from Ax2::MB (1) and Ax2::MB-*rasG*(G12T) (2) cells three hrs after removal of tetracycline was fractionated by 1D electrophoresis. Total protein levels of Actin, DdCAD-1, PKB, RasG and RasC were detected by immunoblotting with specific antibodies to each protein as described in Materials and Methods. Molecular weight markers (kDa) are indicated.

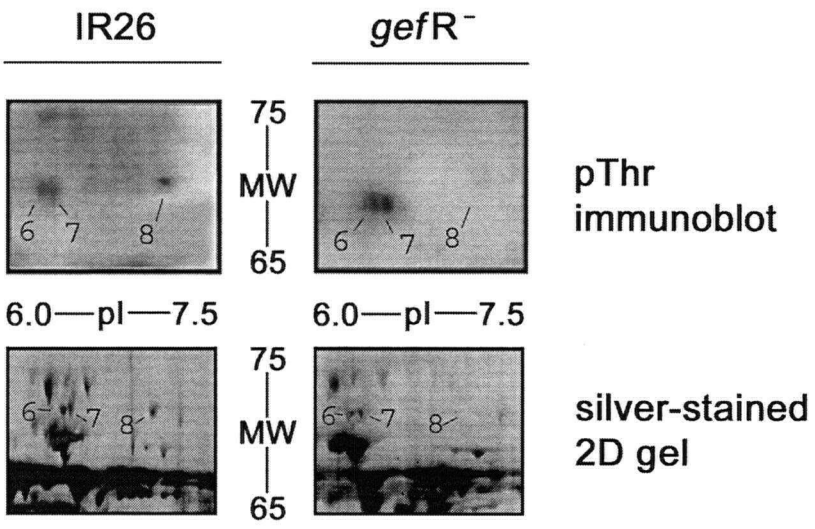

Figure 17. **Examination of the *gefR*⁻ and parental control strains for the presence of RasGEF-R phosphoprotein.** Total protein from a *gefR*⁻ and parental control strain (IR26) was fractionated by 2D electrophoresis. Blotted membranes were probed with anti-phosphothreonine antibody to detect phosphoproteins. The section of the 2D immunoblot and a corresponding silver-stained 2D gel known to contain the s8 immunospot, identified as RasGEF-R, is shown along with two additional spots (s6, s7) for reference. Molecular weight (kDa) markers and pI ranges are indicated.

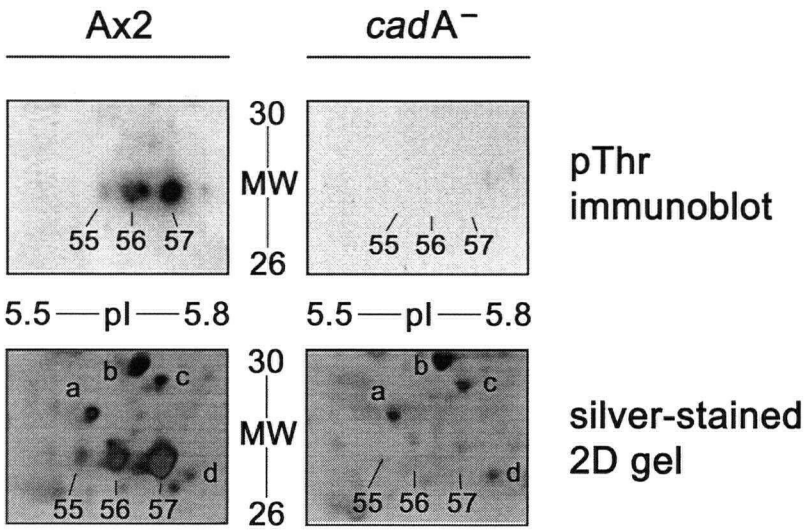

Figure 18. **Examination of the *cadA*⁻ and Ax2 strains for the presence of DdCAD-1 phosphoprotein.** Total protein from *cadA*⁻ and Ax2 strains was fractionated by 2D electrophoresis and blotted membranes were probed with anti-phosphothreonine antibody to detect phosphoproteins. The section of the 2D immunoblots and silver-stained 2D gels known to contain the s55, s56, and s57 immunospots, identified as DdCAD-1, are shown. Additional silver-stained spots (a, b, c, d) are labeled for reference. Molecular weight (kDa) markers and pI ranges are indicated.

cadA null strain (*cadA*$^-$), along with a control Ax2 strain, were subjected to 2D immunoblot analysis. The s55, s56, and s57 immuno-spots identified as DdCAD-1 were all found in the Ax2 strain as before, but not observed in the *cadA* null strain (*Figure 18*). The corresponding silver stained protein spots that had been used for mass spectrometric identification of s55, s56, and s57 were also absent (*Figure 18*). Together these results suggest that s55, s56, and s57 are in fact DdCAD-1. For clarity these phosphoproteins have therefore been re-named DdCAD-1a (s57), DdCAD-1b (s56) and DdCAD-1c (s55).

3.2.8 Summary

Rapid RasG(G12T) expression from the inducible tetracycline promoter was found to alter the phosphorylation of a sub-set of vegetative phosphoproteins. Thirteen of these phosphoproteins were recovered from 2D gels, in-gel digested with trypsin, and identified by mass spectrometry. Since some of these components represented the same protein in different phosphorylation states a total of ten putative RasG-regulated signaling targets were identified by this analysis. Total protein levels for a subset of these identified proteins were found not to change upon Ras(G12T) induction, indicating that the observed phosphorylation changes were not due to changes in protein synthesis of protein degradation, and suggesting the existence of as-yet-unidentified RasG regulated kinases and/or phosphatases during vegetative growth. Two of these phosphoproteins, RasGEF-R and DdCAD-1, were shown to be absent in their respective null strains. Although, it cannot be ruled out that the loss of RasGEF-R and DdCAD-1 affects the expression or phosphorylation of these phosphoproteins, resulting in their absence in each respective null strain, the data tentatively identified the spots s55, s56, and s57, as DdCAD-1 and the spot s8 as RasGEF-R.

3.3 Activated RasG and cell-to-cell adhesion in *Dictyostelium*

3.3.1 Introduction

The identification of DdCAD-1, a known developmental adhesion molecule in *Dictyostelium* (Coates *et al.*, 2001), as a RasG-responsive phosphoprotein (*Figure 18*) raised the question as to whether this phosphorylation in any way affects cell adhesion.

3.3.2 Expression of RasG(G12T) during vegetative growth is accompanied by cell clumping

Vegetative *Dictyostelium* cells are normally not cohesive when grown in shake suspension on HL5 media, but upon starvation and the initiation of development cells start to adhere to each other and DdCAD-1 is involved in this initial adhesion (Coates *et al.*, 2001). When Ax2::MB and Ax2::MB-*rasG*(G12T) cells were grown in shake suspension in the presence of 5 μg/ml tetracycline they grew as individual cells and were not cohesive (*Figure 19*). In contrast, when Ax2::MB-*rasG*(G12T) cells were grown in the absence of tetracycline to allow the induction of RasG(G12T) expression, some cells formed clumps, whereas, Ax2::MB cells grown in the absence of tetracycline did not clump (*Figure 19*), indicating that the induction of cell-to-cell adhesion was due to the increased levels of RasG(G12T) and not the removal of tetracycline. DdCAD-1 is expressed during vegetative growth in axenic media (*Figure 16*; Coates *et al.*, 2001), although it is not normally involved in mediating cell-to-cell adhesion until the on-set of early development (Sesaki and Sui, 1996). The finding that RasG(G12T) expression caused cell cohesion during growth raised the possibility that the activation of RasG signaling was prematurely inducing cell adhesion through the dephosphorylation of DdCAD-1.

3.3.3 RasG(G12T)-induced vegetative cell clumping can be blocked with DdCAD-1 inhibitors

To test whether the RasG(G12T)-induced cell clumping was mediated by DdCAD-1 two properties of DdCAD-1-mediated adhesion were examined. First, DdCAD-1 adhesion requires Ca^{2+} and is thus sensitive to calcium chelators like EDTA (Wong *et al.*, 1996) and second, antibodies specific to DdCAD-1 have been shown to block cell-to-cell adhesion

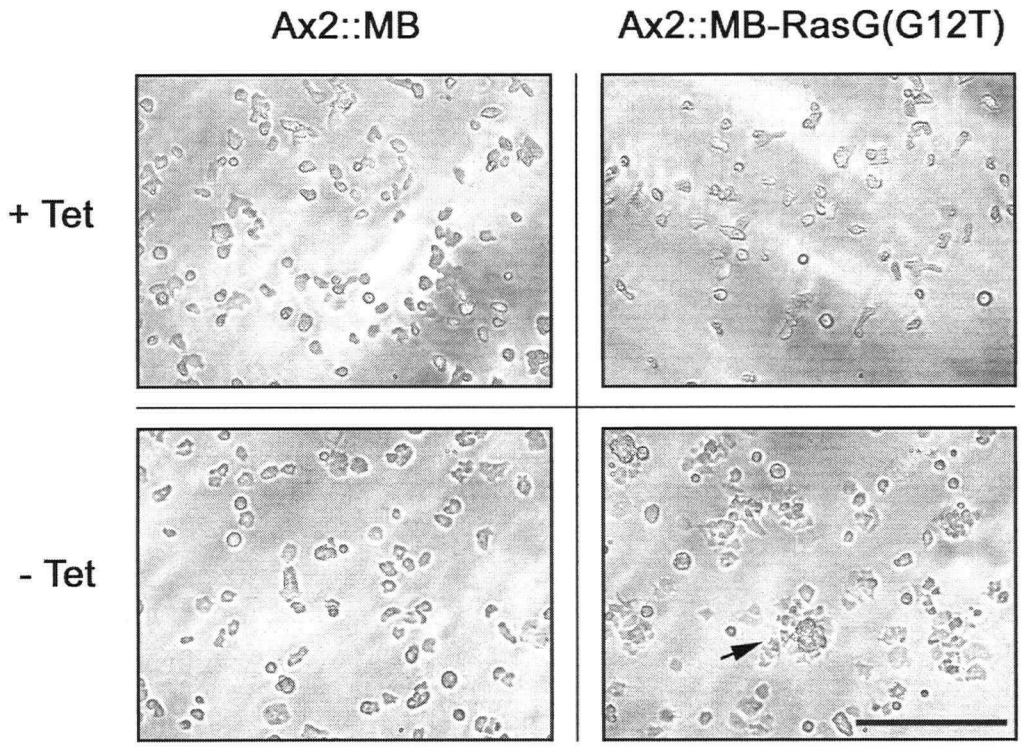

Figure 19. **Induction of cell-to-cell adhesion during vegetative growth in a RasG(G12T) expressing strain.** Ax2::MB and Ax2::MB-*rasG*(G12T) cells, grown in HL5 media in the presence of 5 μg/ml tetracycline (+ Tet) or absence of tetracycline (-Tet) for three hrs, were photographed on an Olympus CK inverted microscope. The arrow indicates an example of the cell-to-cell adhesion observed in Ax2::MB-*rasG*(G12T) cell cultures washed free of tetracycline. Bar: 100 μm.

mediated through this molecule (Brar *et al.*, 1993). Ax2::MB and Ax2::MB-*rasG*(G12T) cells were grown in the absence of tetracycline for three hrs to allow the induction of RasG(G12T) in the presence of either 10 mM EDTA or 50 μg/ml anti-DdCAD-1 antibodies. Control cells incubated in the absence of EDTA or anti-DdCAD-1 antibodies formed clumps as before (*Figure 20*). The addition of either EDTA or antibodies specific for DdCAD-1 to the media prevented Ax2::MB-*rasG*(G12T) cells from adhering (*Figure 20*), consistent with the idea that the observed vegetative cell-to-cell adhesion induced by RasG(G12T) expression is mediated by DdCAD-1.

3.3.4 DdCAD-1 localizes to the cell surface upon the expression of RasG(G12T)

During vegetative growth in axenic media, DdCAD-1 is localized in the cytoplasm and the absence of DdCAD-1 at the cell surface may explain why vegetative cells are not adhesive (Sesaki and Sui, 1996; Sesaki *et al.*, 1997). However, during development, as cells become more cohesive, some DdCAD-1 becomes localized at the cell surface (Sesaki and Sui, 1996; Sesaki *et al.*, 1997). The observation that cells expressing RasG(G12T) tend to be adhesive during vegetative growth raised the possibility that DdCAD-1 was re-localized to the surface upon the expression of activated RasG.

Indirect immunofluorescence microscopy using anti-DdCAD-1 antibodies (Sesaki and Siu, 1996) was undertaken to determine the localization of DdCAD-1 in induced Ax2::MB and Ax2::MB-*rasG*(G12T) vegetative cells (*Figure 21*). In vegetative Ax2::MB cells that had been permeablized with cold methanol (Fukui *et al.*, 1987) a diffuse cytoplasmic localization of DdCAD-1 was observed (*Figure 21a*), that was similar to the previously reported result (Sesaki and Sui, 1996). In contrast, permeablized vegetative Ax2::MB-*rasG*(G12T) cells additionally contained intensely stained rings of DdCAD-1, that were clearly observable in individual cells (*Figure 21b*), although somewhat masked in cell clumps due to the increased background staining (*Figure 21c*).

To restrict the staining to DdCAD-1 localized at the cell surface, non-permeablized cells were subjected to indirect immunofluorescence microscopy with the anti-DdCAD-1 antibodies. Under these conditions, vegetative Ax2::MB cells were largely unstained (*Figure 21d*), consistent with DdCAD-1 being localized predominately in the cytoplasm in these cells. In contrast the DdCAD-1 ring structures were once again observed in the vegetative Ax2::MB-

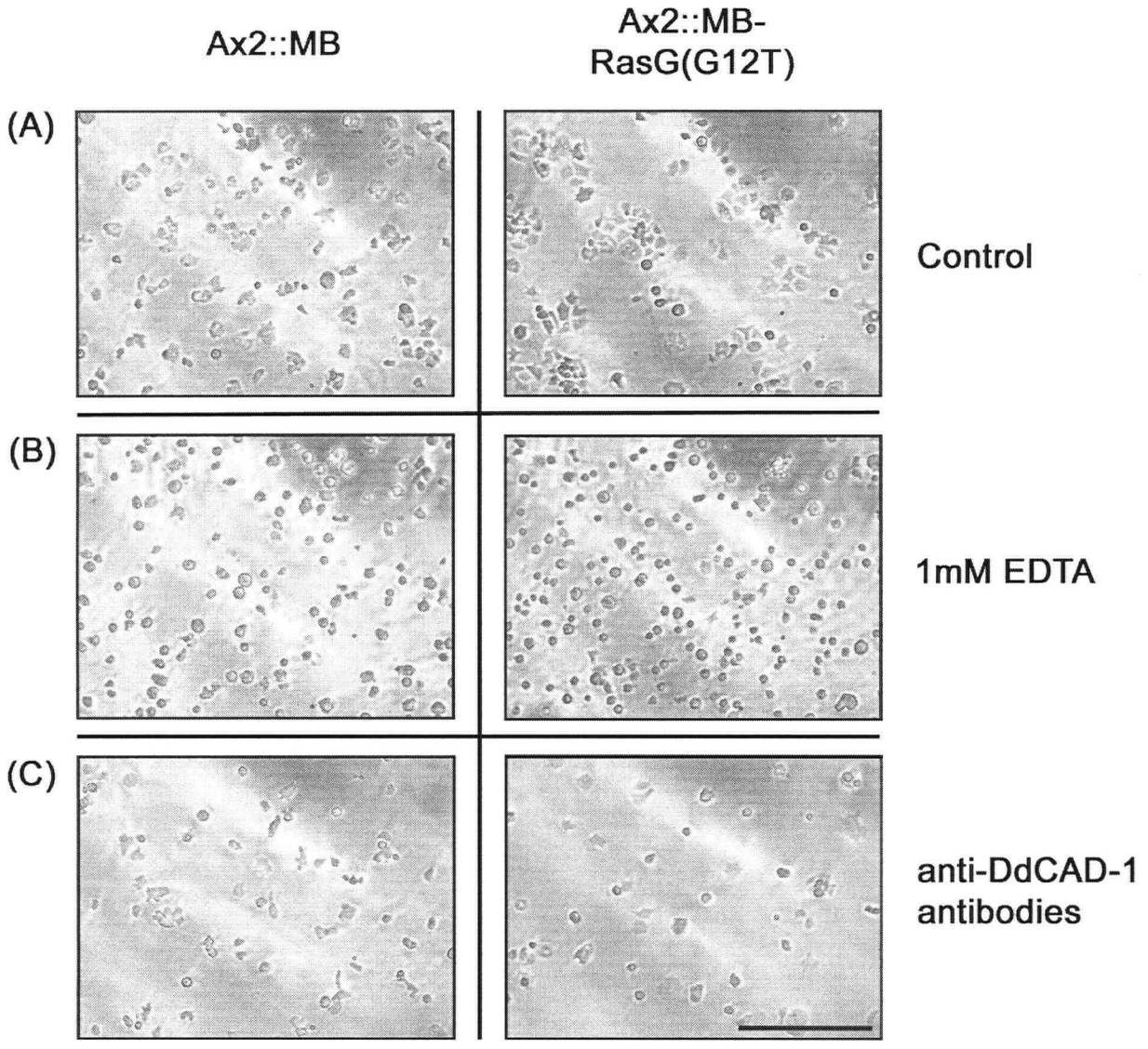

Figure 20. **Disruption of RasG(G12T) mediated cell-to-cell adhesion with inhibitors of DdCAD-1 adhesion.** Ax2::MB and Ax2::MB-*rasG*(G12T) cells were washed and incubated for three hrs in tetracycline-free media with either no additions (A), 1 mM EDTA (B), or 50 μg/ml anti-DdCAD-1 antibodies (C). Cells were photographed on an Olympus CK inverted microscope. Bar: 100 μm.

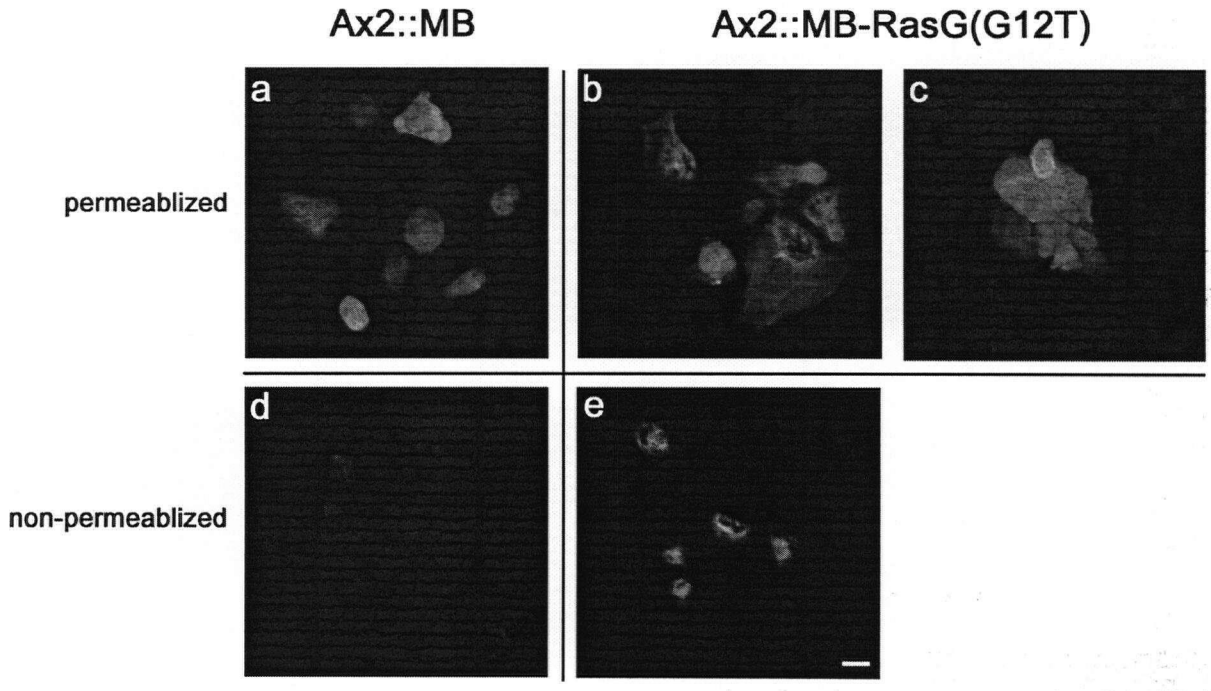

Figure 21. **Immunofluorescent localization of DdCAD-**1. Ax2::MB (a, d) and Ax2::MB-*rasG*(G12T) (b, c, e) cells were grown in the absence of tetracycline for three hrs. Cells were then fixed and either permeablized with cold methanol (a, b, c) or not permeablized (d, e), before being immunostained by indirect immunofluorescence with anti-DdCAD-1 antibodies as described in Materials and Methods. Images were taken on a Zeiss Axioplan Fluorescent Microscope. Bar: 5 μm.

rasG(G12T) cells (*Figure 21e)*, strongly suggesting that DdCAD-1 was localized to the cell surface of these cells. This observation revealed that the activation of RasG resulted in the re-localization of DdCAD-1 and offers an explanation as to why the vegetative Ax2::MB-*rasG*(G12T) cells tended to be more cell-to-cell adhesive than the control cells.

3.3.5 Cell adhesion during early developmental is enhanced in RasG(G12T) expressing cells

DdCAD-1 mediated adhesion has been proposed as the major adhesion process present soon after the on-set of starvation (Coates *et al.*, 2001), with other adhesion systems (e.g. gp80 and gp150) induced several hrs later (Desbarats *et al.*, 1994). Gerisch's original analysis of this process made use of a rolling tube cohesion assay to show the ability of early developing *Dictyostelium* cells to adhere to one another (Gerisch, 1968). This cell cohesion assay was later adapted by Sui and colleagues to assess the ability of strains to adhere via DdCAD-1 contacts sites during early development (Lam *et al.*, 1981; Wong *et al.*, 2002).

This standard cell cohesion assay was preformed on Ax2::MB-*rasG*(G12T) and Ax2::MB cells that had been washed free of tetracycline and starved for 4 hrs (*Figure 22*), a time when only EDTA-sensitive DdCAD-1 dependent cell adhesion is occurring (Wong *et al.*, 2002). The cells were dissociated by vigorous vortexing so that cells were not in aggregates at time zero and then allowed to re-associate. Some re-association of the Ax2::MB cells was detected 20 minutes after their dissociation (*Figure 22*). However, the re-association of induced Ax2::MB-*rasG*(G12T) cells was much more rapid, with significant adhesion occurring within 5 minutes after the cells had been vortexed (*Figure 22*). The addition of 10 mM EDTA during the assay completely prevented re-association of both sets of cells, indicating that the observed re-association was in fact due to EDTA-sensitive adhesion. These results indicated that cells expressing RasG(G12T) were not only more cohesive during vegetative growth but also exhibited an enhanced ability to adhere to each other during early development.

3.3.6 DdCAD-1 phosphorylation decreases during *Dictyostelium* development

Since there was a decrease in DdCAD-1 phosphorylation in cells expressing activated RasG, the forgoing results suggested that there was an inverse relationship between DdCAD-1 phosphorylation and DdCAD-1 mediated cell adhesion. Since wild-type cells became more

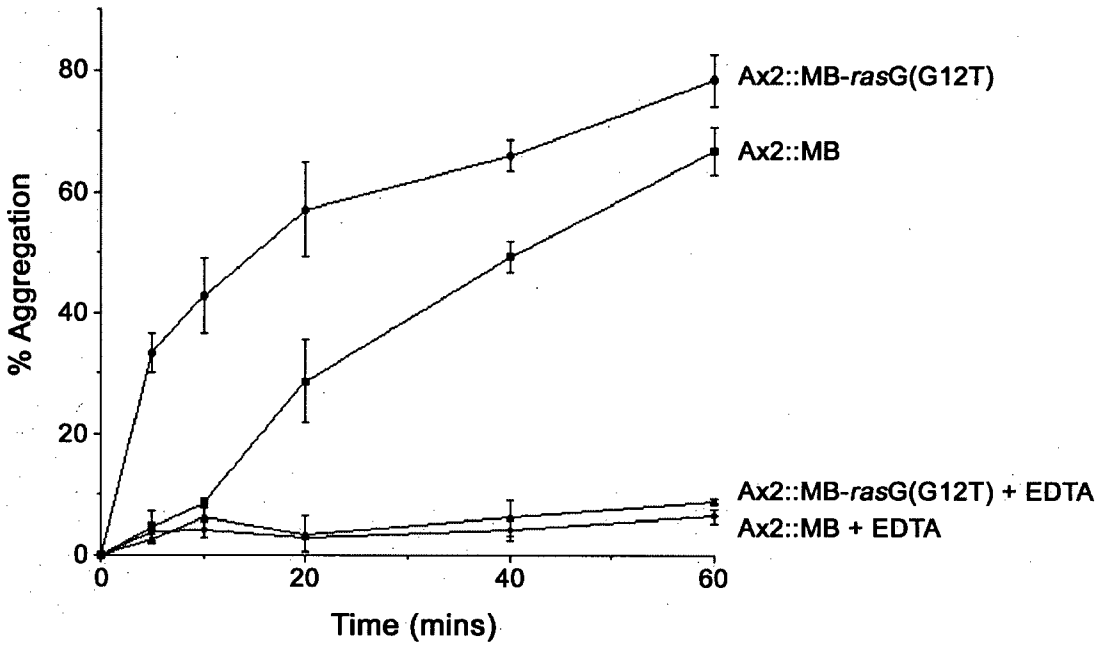

Figure 22. **Cell-to-cell cohesion in developing Ax2::MB and Ax2::MB-*rasG*(G12T) cells.** Ax2::MB and Ax2::MB-*rasG*(G12T) cells were washed free of tetracycline and starved for four hrs in KK2 in shake suspension. Cells were subsequently disassociated by vortexing and cell re-association monitored over time with or without the addition of 10 mM EDTA. Cells are not in aggregates at time zero and the percentage of cell re-association was calculated by scoring non-aggregated cells with a hemocytometer (% Aggregation = [total number of cells – non-aggregating cells] / total number of cells). Data represents mean of three independent experiments ± standard deviations. (Ax2::MB [■], Ax2::MB + EDTA [♦], Ax2::MB-*rasG*(G12T) [●], Ax2::MB-*rasG*(G12T) + EDTA [▲]).

adhesive through DdCAD-1 contact sites as development proceeds (Sesaki and Sui, 1996; Sesaki *et al.*, 1997), it was important to determine whether DdCAD-1 phosphorylation decreased during development. Because of the technical difficulties involved in processing multiple samples for comparison by 2D electrophoresis, this analysis was performed using 1D electrophoresis.

Ax2::MB cells washed free of tetracycline and starved had relatively constant levels of phosphorylated DdCAD-1 during the first 4 hrs of development, after which the levels of phosphorylated DdCAD-1 decreased (*Figure 23*). In contrast, Ax2::MB-*rasG*(G12T) cells had a level of phosphorylated DdCAD-1 throughout the starvation period that was similar to that for the Ax2::MB cells that had been starved for 8 hrs (*Figure 23*). Both sets of cells had similar levels of total DdCAD-1 throughout the starvation period (*Figure 23*), indicating that the observed phosphorylation changes were not due to changes in protein level. *cadA* null cells were included to control for other phosphothreonine proteins that might co-migrate with DdCAD-1 during the 1D electrophoretic procedure. In the *cadA* null samples a low intensity band that increased during development migrated in the same position as DdCAD-1 (*Figure 23*). The gels shown in Figure 23A were therefore quantitated by densitometry, so that the contribution of the non-DdCAD-1 phosphorylation to the phosphoprotein signal could be subtracted. This analysis suggested that the decrease in DdCAD-1 phosphorylation for the Ax2::MB was somewhat greater than the uncorrected data showed (*Figure 23B*) and that a slight decrease in DdCAD-1 phosphorylation in the Ax2::MB-*rasG*(G12T) cells may have occurred during the course of the 8 hr starvation (*Figure 23B*). Although not quantited by densitometry, a similar decreasing trend in DdCAD-1 phosphorylation was also observed for an independent repeat of this experiment.

3.3.7 A correlation between the decrease in DdCAD-1 phosphorylation and the cellular localization of DdCAD-1

DdCAD-1 is known to move from the cytoplasm to the cell surface as development proceeds (Sesaki and Sui, 1996) and it was of interest to determine in this movement correlated with the observed decrease in DdCAD-1 phosphorylation. To investigate this Ax2::MB and Ax2::MB-*rasG*(G12T) cells were stained for DdCAD-1 at 8 hrs after the onset of starvation (*Figure 24*). As Sesaki and Sui (1996) had reported, DdCAD-1 was diffusely localized to the cytoplasm at the onset of development in Ax2::MB cells, and after 8 hrs of starvation was more localized to the cell periphery, which correlated with the large decrease in DdCAD-1

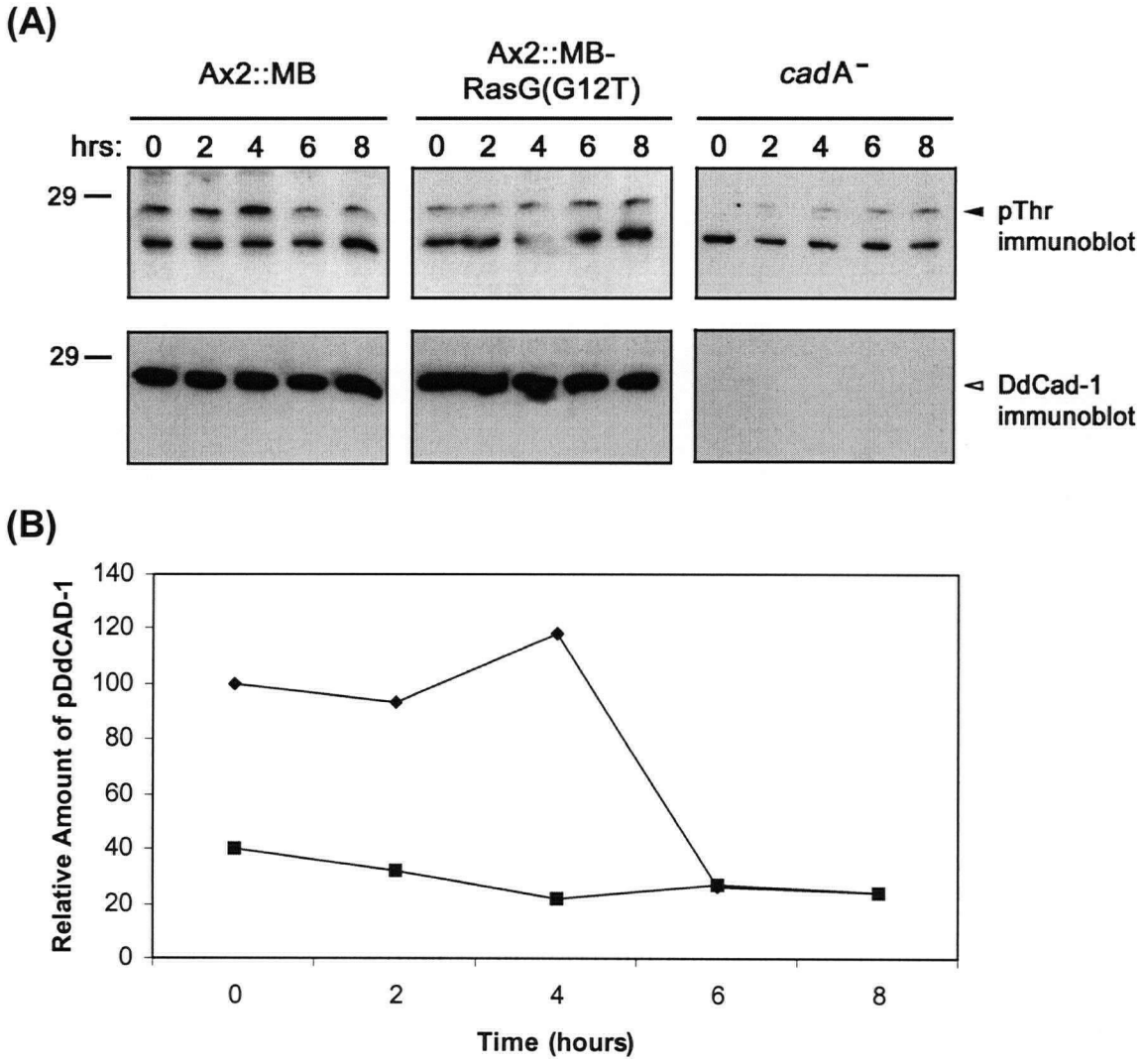

Figure 23. **Levels of DdCAD-1 phosphorylation during development.** Ax2::MB, Ax2::MB-*rasG*(G12T) and *cadA*⁻ cells were starved in KK2 in shake suspension in the absence of tetracycline. (A) At the indicated times, protein samples were fractionated by 1D electrophoresis and immunoblots probed with anti-phosphothreonine antibodies to detect phosphorylated DdCAD-1 (closed arrow). Blots were then stripped of bound antibody and re-probed with anti-DdCAD-1 antibodies to detect total DdCAD-1 levels (open arrow). Molecular weight (kDa) markers are indicated. (B) The immunoblots probed with anti-phosphothreonine antibodies shown in (A) were quantified by densitometric analysis. The values observed for *cadA*⁻ cells were subtracted from the phosphorylated DdCAD-1 for Ax2::MB (♦) and Ax2::MB-*rasG*(G12T) (■) cells and normalized relative to amount of phosphorylated DdCAD-1 in Ax2::MB cells at 0 hrs.

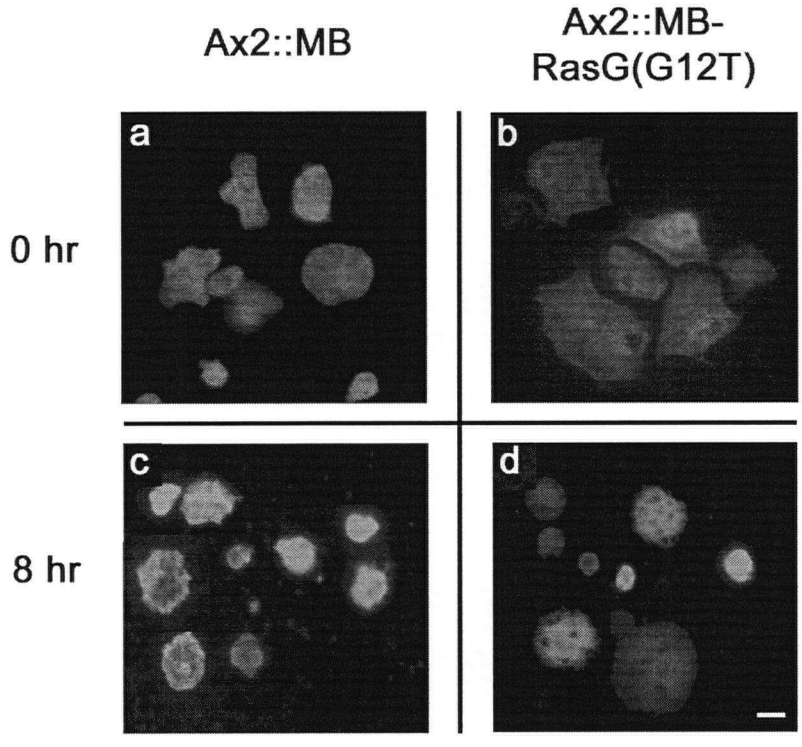

Figure 24. **Comparison of DdCAD-1 localization during development in Ax2::MB and Ax2::MB-*rasG*(G12T) cells.** Ax2::MB (a, c) and Ax2::MB-*rasG*(G12T) (b, d) cells were washed free of tetracycline and starved in KK2 in shake suspension for the indicated times. They were then fixed and immunostained by indirect immunofluorescence with anti-DdCAD-1 antibodies as described in Materials and Methods. Images were taken on a Zeiss Axioplan Fluorescent Microscope. Bar: 5 μm.

phosphorylation (*Figure 21*). In Ax2::MB-*rasG*(G12T) cells expressing RasG(G12T), the DdCAD-1 rings structures present at the onset of starvation became replaced with more general membrane staining after 8 hrs of starvation (*Figure 24*), also correlating with the smaller decrease in DdCAD-1 phosphorylation (*Figure 23*).

3.3.8 *rasG* null cells are defective in streaming during aggregation

DdCAD-1 has been implicated in mediating side-to-side contact between cells during aggregation (Coates *et al.*, 2001) and the above findings suggest that RasG may partly regulate this function. Since RasG(G12T) expressing cells do not develop (Khosla *et al.*, 1996) and therefore do not form aggregation streams in which side-to-side contacts can be monitored, the effects of RasG(G12T) on aggregation stream formation could not be monitored. However, *rasG* null cells do develop (Tuxworth *et al.*, 1997) and I was therefore able to assess aggregation stream formation by these cells. Since cells expressing RasG(G12T) show increased cohesion (see Section 3.3.5), it was hypothesized that *rasG* null cells would show defective side-to-side contacts indicative of a reciprocal decrease in cell cohesion during early development.

Cellular streaming was observed in cell monolayers washed free of nutrient media and submerged under a non-nutrient solution (Bonner's salts). Ax2 cells began to form aggregation streams after 8 hrs under these conditions and by 12 hrs had begun to form aggregation centers (*Figure 25*). *rasG* nulls cells did not begin to form aggregation streams until 12 hrs (*Figure 25*). This result was consistent with the approximately 4 hr delay observed in the initiation of developmental Discoidin expression discussed previously (*Figure 9*). At 14 hrs, *rasG* null cells had begun to form aggregation centers, but these were more disorganized than in the wild type and multiple aggregation centers were evident (*Figure 25A, bottom panel, 14hr*). For comparison, *cadA* null cells were included in this analysis (*Figure 25A, middle panel*). *cadA* null cells also formed cellular streams that were less organized than those of the wild type and multiple small aggregation centers, a phenotype similar to that for the *rasG* null cells. In addition, the aggregation of *cadA* null cells was delayed by approximately 2 hours (*Figure 25A, middle panel*).

These results indicated that *rasG* null cells are defective in developmental streaming, providing further evidence that RasG might be important in the regulation of side-to-side contacts during aggregation (Sesaki and Siu, 1996) by regulating DdCAD-1 phosphorylation. In

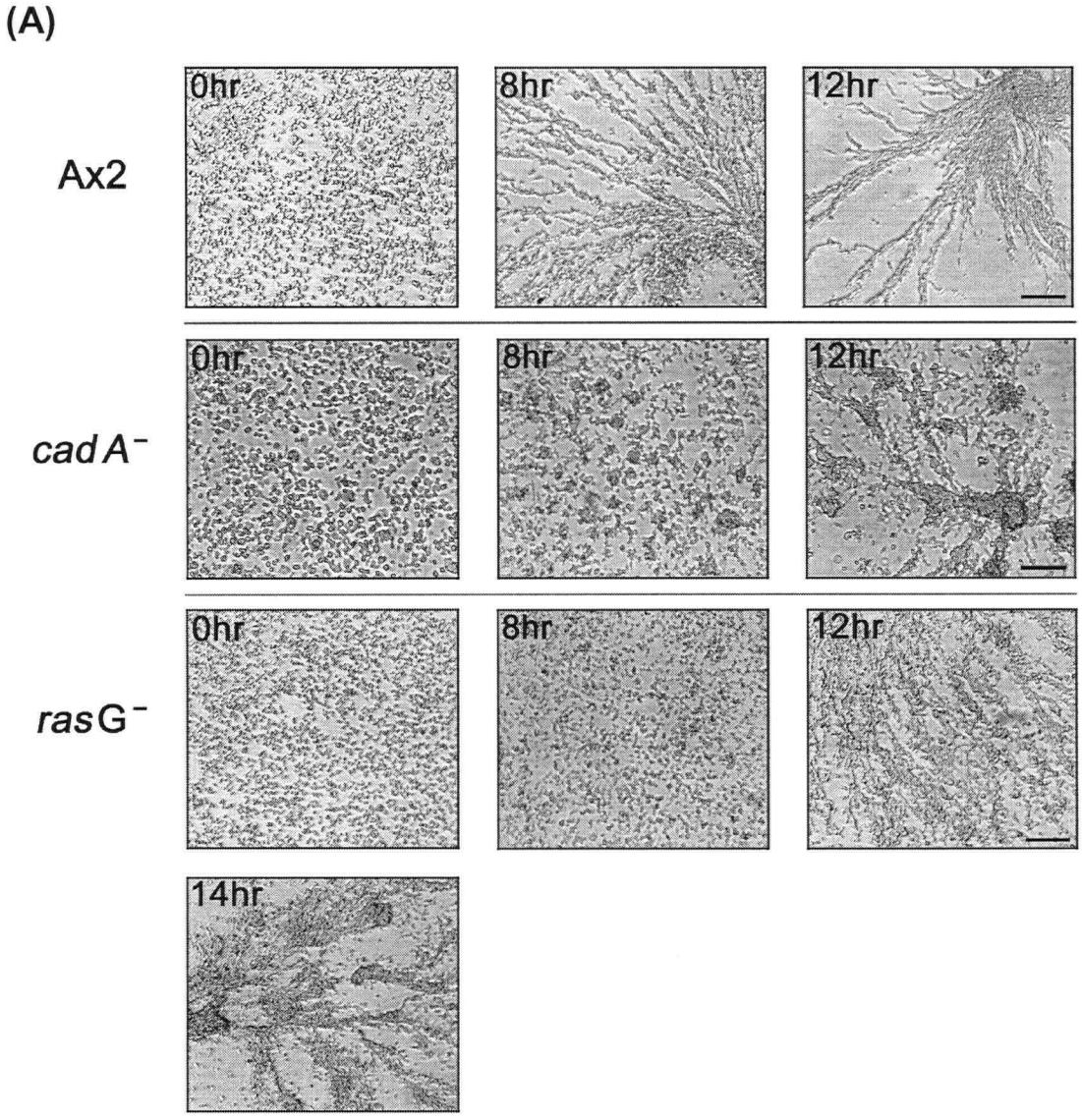

Figure 25.

(B)

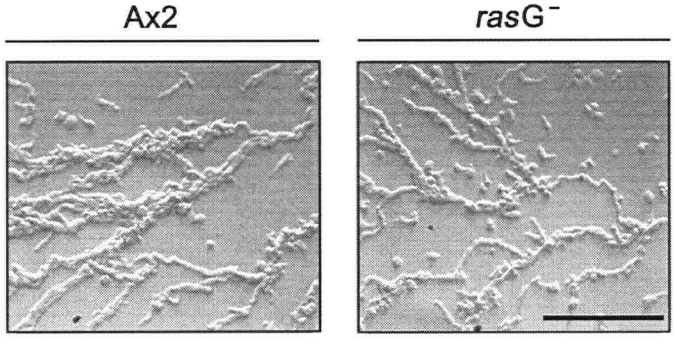

Figure 25. **Cellular streaming in Ax2, *rasG* null and *cadA* null cells.** Cells were seeded as monolayers at a density of 5 x 10^5 cells/cm^5 in Nunc tissue culture dishes and submerged under Bonner's salts solution. (A) Images were photographed at the indicated time (hrs) after the initiation of starvation. Bar: 100 μm. (B) Aggregation streams corresponding to 8 hrs for Ax2 and 12 hrs for the *rasG* null were also photographed at higher magnification. Cells were photographed on an Olympus CK inverted microscope. Bar: 50 μm.

addition, these results revealed a role for RasG in regulating developmental timing during early development.

3.3.9 RasG is required for high levels of DdCAD-1 expression

Since *rasG* nulls cells were defective in developmental streaming, a process known to involve DdCAD-1 mediated adhesion, and RasG(G12T) expressing cells exhibited increased developmental adhesion and decreased DdCAD-1 phosphorylation, it was anticipated that the DdCAD-1 phosphorylation would be increased in *rasG* null cells. The level of DdCAD-1 phosphorylation was therefore measured in vegetative *rasG* null cells as compared to a vegetative Ax2 control strain (*Figure 26*).

Total protein samples, taken from the *rasG* null strain (*rasG*$^-$) and the control Ax2 strain, were subjected to 2D immunoblot analysis. All three DdCAD-1 phosphoproteins were found in the Ax2 strain as before, but surprisingly there was greatly reduced phosphorylation of all three DdCAD-1 species in the *rasG* null strain (*Figure 26A*). However, the total amount of DdCAD-1 was greatly decreased in *rasG* null cells in comparison to Ax2 control cells (*Figure 26B*), despite the fact that Discoidin protein levels do not change in response to the short term activation of RasG. These results suggest that the decrease in DdCAD-1 phosphorylation was due to decreased DdCAD-1 expression levels and indicate that RasG is an important regulator of DdCAD-1 expression during vegetative growth in axenic media. Furthermore, the results suggested that the similarity between the streaming defects in the *rasG* and *cadA* null strains could have been due to the reduction in the DdCAD-1 level in *rasG* null cells, in addition to an alteration in DdCAD-1 phosphorylation.

3.3.10 Summary

Cells expressing RasG(G12T) were found to have increased cohesive properties that were mediated by DdCAD-1. These enhanced cohesive properties correlated with a decrease in DdCAD-1 phosphorylation and increased cell surface localization of DdCAD-1. DdCAD-1 phosphorylation decreased during development, at time when DdCAD-1 mediated adhesion increased, consistent with an inverse relationship between DdCAD-1 phosphorylation and DdCAD-1 mediated cell adhesion. *rasG* null cells were defective in the formation of developmental streams and expressed greatly reduced levels of DdCAD-1.

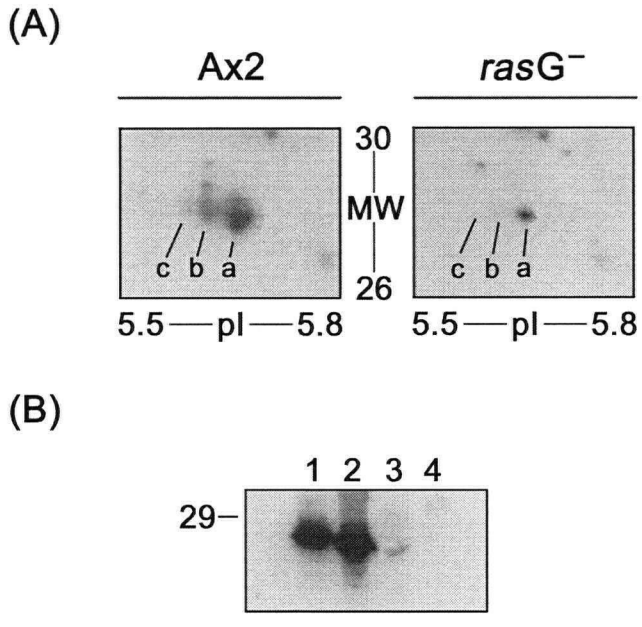

Figure 26. **Levels of total and phosphorylated DdCAD-1 in a *rasG* null and Ax2 control cells.** (A) Total protein from a *rasG*⁻ and Ax2 was fractionated by 2D electrophoresis. Blotted membranes were probed with anti-phosphothreonine antibody to detect phosphoproteins. The section of the 2D immunoblot blot known to contain DdCAD-1 is shown (a = DdCAD-1a, b = DdCAD-1b, c = DdCAD-1c a). (B) Total protein from induced Ax2::MB (lane 1), induced Ax2::MB-*rasG*(G12T) (lane 2), *rasG*⁻ (lane 3) and the *cad*A⁻ (lane 4) cells were fractionated by 1D electrophoresis and blotted with a DdCAD-1 specific antibody. Molecular weight (kDa) markers and pI ranges are indicated.

3.4 Effect of RasG(G12T) on *Dictyostelium* PKB phosphorylation

3.4.1 Introduction

The finding of a decrease in the level of phosphorylated PKB in response to the expression of RasG(G12T) (*Figure 27; Table 1*) was of considerable interest, since it has been reported that RasG binds to PI3K (Lee *et al.*, 1999) and PI3K is required for the receptor-mediated activation of PKB (Meili *et al.*, 1999), indicating a potential link between RasG and PKB. The activation and phosphorylation of PKB has previously only been studied in developing cells (Meili *et al.*, 1999; Lim *et al.*, 2001). In this study, PKB was identified as a vegetative phosphoprotein that was affected by the expression of RasG(G12T) (*Figure 27; Table 1*). A function of PKB in aggregating cells is the generation of cell polarity and chemotaxis to cAMP (Meili *et al.*, 1999), and PKB phosphorylation during aggregation occurs in response to stimulation by the chemoattractant cAMP (Lim *et al*, 2001). This raised the question as to whether PKB was involved in the generation of cell polarity and chemotaxis in vegetative cells and as a test of this hypothesis the stimulation of PKB phosphorylation in response to vegetative chemoattractant folate (Blusch and Nellen, 1994) was investigated.

3.4.2 Enhancement of folate-induced phosphorylation of *Dictyostelium* PKB in cells expressing RasG(G12T)

To investigate the relationship between activated RasG and PKB phosphorylation during vegetative growth, the effect of folate stimulation on the phosphorylation of PKB in Ax2::MB and Ax2::MB-*rasG*(G12T) cells was determined. Cells were grown in media free of tetracycline for three hrs before being harvested and washed free of HL5 media. Cells were then resuspended in KK2 buffer and stimulated by the addition of 50 μM folate. Since the activation and phosphorylation of PKB in response to cAMP shows complex kinetics (Meili *et al.*, 1999; Lim *et al.*, 2001), it was possible that PKB phosphorylation in response to folate might be equally complex. In addition, the phosphorlyation of PKB has been previously monitored by 1D gel electrophoresis of total proteins samples (Lim *et al.*, 2001) and a myc-tagged version of PKB has been immunoprecipated and shown to react against the phospho-threonine antibody used in this thesis (Lim, 2002). Since 1D gel electrophoresis allows the comparison of multiple samples, it was therefore used to analyze the affect of folate stimulation on the levels of phosphorlyated PKB.

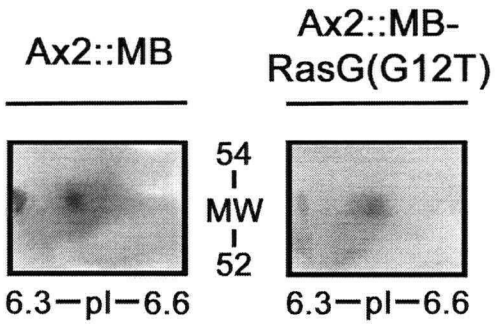

Figure 27. **Representative phosphorylation change in vegetative PKB between Ax2::MB and Ax2::MB-*rasG*(G12T) cells.** The phosphoprotein spot identified as PKB (*Table 1*) is shown in the center of the image expanded 2D immunoblots. Molecular weight (kDA) and pI ranges are indicated.

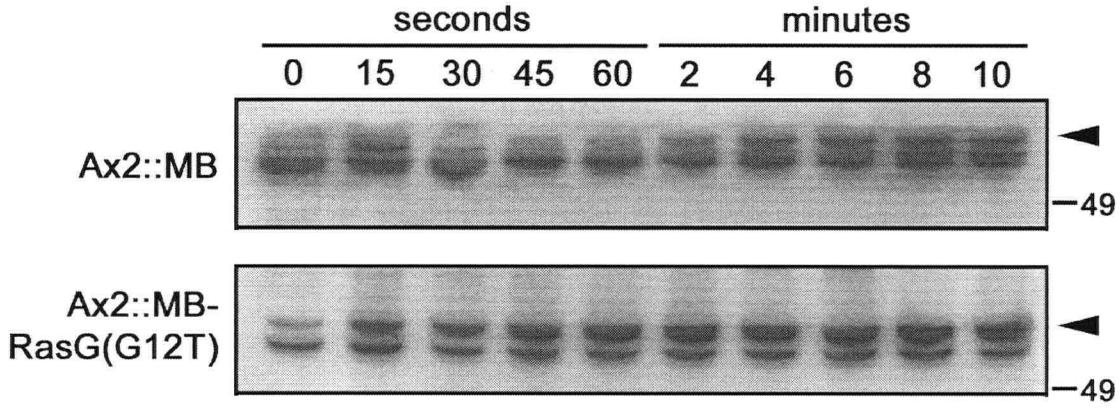

Figure 28. **Folate induced stimulation of PKB phosphorylation.** Ax2::MB and Ax2::MB-*rasG*(G12T) cells were grown in the absence of tetracycline in HL5 media for three hrs and then resuspended in KK2 at ~ 5 x 10^7 cells/ml and stimulated with 50 μM folate. At the indicated times (in minutes), 50 μl aliquots of cells were lysed and protein samples fractionated by 1D electrophoresis. Blots were probed with the anti-phosphothreonine antibody as described under Materials and Methods. A representative gel from three independent experiments is shown. Phosphorylated PKB (arrow) and molecular weight markers (kDa) are indicated.

An increase in the level of phosphorylated PKB was detected within 15 seconds of the addition of folate in Ax2::MB cells stimulated with 50 μM folate (*Figure 28*). The level of phosphorylated PKB then decreased. A second increase in the fraction of phosphorylated PKB was also detected. 2 minutes after the addition of folate, and by 6 minutes the level of phosphorylated PKB had reached that observed in the initial peak at 15 seconds. Thus, folate induced a bimodal PKB phosphorylation pattern (*Figure 28*). Cells expressing activated RasG exhibited increased levels of PKB phosphorylation relative to Ax2::MB cells upon exposure to folate (*Figure 28*). The bimodal pattern of PKB phosphorylation observed in Ax2::MB cells was not as evident in Ax2::MB-*rasG*(G12T) cells (*Figure 28*). Instead, the levels PKB phosphorylation remained high in Ax2::MB-*rasG*(G12T) cells through the time course of the experiment, suggesting that the presence of RasG(G12T) disrupted the bimodal pattern of activation. These results reveal for the first time that the chemoattractant folate stimulates the phosphorylation of vegetative PKB and that this phosphorylation is affected by levels of RasG(G12T).

Prior to folate stimulation the levels of phosphorylated PKB in the Ax2::MB-*rasG*(G12T) cells was higher than the Ax2::MB cells (compare zero time points in Figure 28), suggesting a higher basal level of phosphorylated PKB in the presence of RasG(G12T). This result is opposite to that obtained in the 2D analysis, where phosphorylated PKB is decreased in the Ax2::MB-*rasG*(G12T) cells prior to folate stimulation (*Figure 27*). This discrepancy in the steady state level of phosphorylated PKB in the activated RasG strain relative to the control strain is potentially due to removal of membrane protein in the 2D analysis, since membranes were pelleted after cell disruption (see Materials and Methods). The 1D analysis in Figure 25 therefore might detect phosphorylated PKB present in both the cytosol and the membrane.

3.4.3 Cells expressing RasG(G12T) have more PKB in their membrane fractions

Rapid translocation to the *Dictyostelium* plasma membrane upon receptor stimulation with cAMP has been observed for PH-domain containing proteins, including PKB, CRAC and PhdA (Parent *et al.*, 1998; Meili *et al.*, 1999; Moniakis *et al.*, 2001; Funamoto *et al.*, 2001). Since RasG(G12T) expression stimulates PKB phosphorylation in response to folate, it was possible that it also stimulated its translocation to the plasma membrane. To test this hypothesis, Ax2::MB and Ax2::*rasG*(G12T) cells, grown for 3 hrs in the absence of tetracycline, were lysed

by filtration through a 5.0 μm pore membrane and the lysate centrifuged to separate cell membranes from cytosol (Parent *et al.*, 1998; Lim, 2002). The pellet fraction, along with an un-fractionated lysate sample, was then subjected to immunoblot analysis using a PKB-specific antibody to determine the PKB protein level in the membrane (*Figure 29*). Although the total PKB levels were virtually identical between the two strains (*Figure 29*), the pelleted membrane fraction from Ax2::*rasG*(G12T) cells contained more PKB than Ax2::MB cells (*Figure 29*). As a control, the immunoblots were also probed for Actin using an actin-specific antibody and the actin levels were found to be the same for the membrane fractions of the two strains (*Figure 29*). Although the increase in PKB in the membrane fraction of Ax2::*rasG*(G12T) cells was only slight, three independent repeats of this experiment gave similar results, with the relative amount of PKB found in the membrane fraction of Ax2::MB cells being 24 ± 4.5, while in Ax2::*rasG*(G12T) cells it was found to be 37 ± 3.5 (*mean ± sd; n = 3*) (*Figure 29B*). A student's *t*-test of these differences revealed these changes to be statistically significant (*t = 3.95, p = 0.05*). If the phosphorylated PKB was primarily membrane bound in RasG(G12T) expressing cells, it would have been lost in Figure 27, thus explaining the differences in basal levels of phosphorylated PKB detected in 1D and 2D immunoblot analysis (*Figures 27 and 28*).

3.4.4 Cell polarity in RasG(G12T) expressing cells

The increased levels of membrane bound PKB in RasG(G12T) expressing cells might influence the ability of a cell to generate cell polarity in a chemoattractant gradient, since PKB has been shown to localize to the leading membrane edge of a chemotaxing cell (Meili *et al.*, 1999). PKB translocation has been implicated in generating cell polarity towards a chemotactic signal (Firtel and Chung, 2000). Thus it would be predictive that loss of polarity would inhibit chemotaxis. The ability of RasG(G12T) expressing cells to chemotax to a chemoattractant-filled micropipet (Firtel and Chung, 2000) was therefore determined using time lapse microscopy. When a micropipet containing 25 mM folate was immersed in buffer containing Ax2::MB cells, the movement of cells toward the tip was detectable after 20 minutes (*Figure 30*) and these cells were polarized towards the micropipet (*Figure 30*). In contrast, the RasG(G12T) expressing cells were less chemotactic to folate (*Figure 30*) and exhibited little or no cell polarity. The reduced chemotaxis and cell polarity could be consequences of a RasG(G12T)-mediated increase in membrane bound PKB, since this elevated level might interfer with the specific localization of

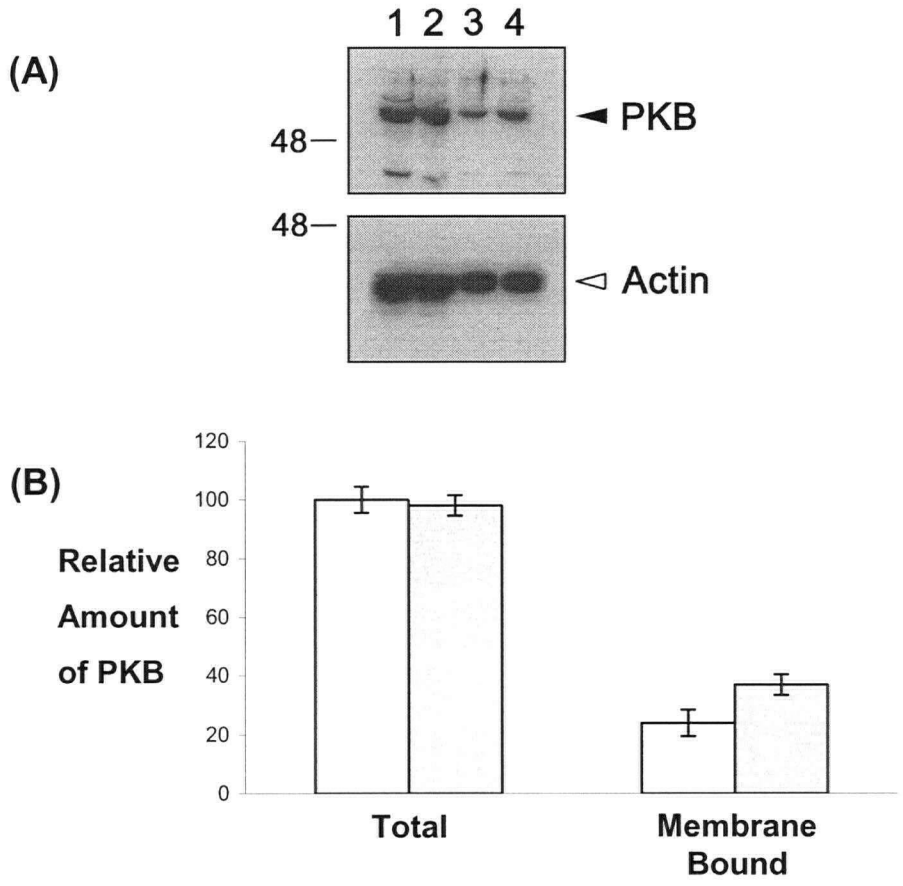

Figure 29. **PKB membrane localization in response to RasG(G12T) expression.** Ax2::MB (lanes 1 and 3) and Ax2::MB-*rasG*(G12T) (lanes 2 and 4) cells were grown in tetracycline-free media for three hrs. A portion of these cells were lysed by filtration through a 5.0 μm pore membrane and centrifuged at 16,000 x g to provide a membrane pellet fraction. The membrane fraction was resuspended in SDS lysis buffer and a non-fractionated total protein sample was prepared by direct resuspension of cells in SDS lysis buffer. (A) Total protein (lanes 1 and 2) and membrane-only (lanes 3 and 4) samples were fractionated by 1D electrophoresis and the blots were probed with PKB-specific (closed arrow) or Actin-specific (open arrow) antibodies. A representative gel from three independent experiments is shown. Molecular weight markers (kDa) are indicated. (B) The immunoblots from three independent experiments ± standard deviations were quantified by densitometric analysis as described under Material and Methods. The values normalized relative to the level of total PKB observed in Ax2::MB cells, arbitrarily set to a value of 100%.(Ax2::MB, white; Ax2::MB-*rasG*(G12T), dotted).

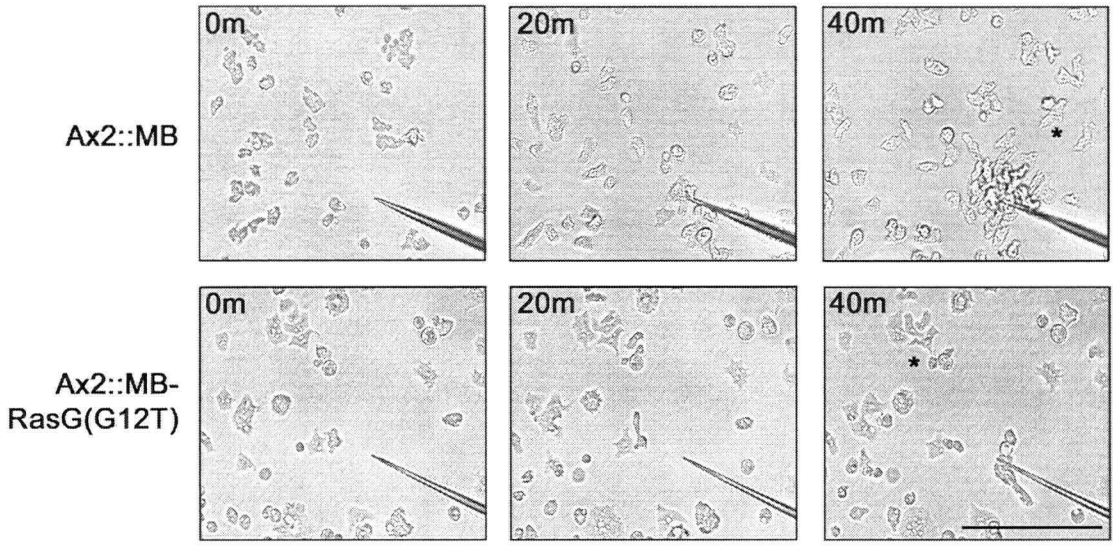

Figure 30. **Chemotaxis of Ax2::MB and Ax2::MB-*ras*G(G12T) cells in a spatial folate gradient.** Cells washed free of tetracycline and induced in HL5 media for three hrs were seeded at ~ 4 x 10^5 cells/cm^2 in Nunc dishes. After 30 minutes, the media was replaced with 20% HL5 and a micropipet filled with 25 mM folate inserted into the culture. Cell movements were monitored by time-lapse microscopy over 40 minutes. The star (*) indicates an example of cell polarity towards the spatial folate gradient. Images were taken on an Olympus IX-70 inverted microscope. Bar: 100 μm.

PKB at the leading edge of a chemotactically-stimulated cell, preventing adequate directional sensing (Firtel and Chung, 2000). In addition, the bimodal kinetics of PKB phosphorylation in response to folate for the Ax2::MB cells was largely abolished in the Ax2::MB-*rasG*(G12T) cells expressing RasG(G12T) and this might adversely affect cell polarity.

3.4.5 Summary

RasG was found to regulate both the basal and folate-induced level of PKB phosphorylation, and cells expressing RasG(G12T) contained slightly more membrane bound PKB. In addition, the bimodal kinetics of PKB phosphorylation in response to folate was abolished in Ax2::MB-*rasG*(G12T) cells expressing RasG(G12T). RasG(G12T) cells were less polarized and exhibited less efficient chemotaxis in a spatial folate gradient. Since PKB localization is required for efficient chemotaxis (Meili *et al.*, 1999), these results suggested that RasG may influence chemotaxis through its effect on PKB.

3.5 Identification of a protein phosphorylation in response to chemoattractant and its modulation by RasG

3.5.1 Introduction

During the course of studies on the phosphorylation of ERK2 in response to cAMP in *rasC* null cells, the phosphorylation of a second protein of 70 kDa (p70), which peaked at 8 minutes after the addition of cAMP, was detected in wild type cells (C. J. Lim, *unpublished observations*). p70 was also phosphorylated in response to folate, also peaking at 8 minutes in wild type cells (*Figure 31*). This stimulation was considerably enhanced in the Ax2::MB-*rasG*(G12T) cells and reduced in *rasG* null cells stimulated with folate (*Figure 31*). It was unlikely that p70 was a complex containing phosphorylated ERK2, since the kinetics of ERK2 phosphorylation were quite different to those for p70. Since RasG clearly modulated the phosphorylation of p70 (*Figure 31*), I attempted to identity this novel chemoattractant modulated protein.

3.5.2 Use of narrow-range 2D gel electrophoresis for the resolution of p70

To identify the p70 phosphoprotein, 2D electrophoretic fractionation in combination with immunoblot detection was used as described in Section 3.2. Ax2::MB-*rasG*(G12T) cells were stimulated with folate for 4 minutes, which corresponds to the maximum level of p70 phosphorylation in these cells (*Figure 31*), lysed and proteins separated by 2D gel electrophoresis, using a pI range of 3-10. This gel was blotted to a PVDF membrane and p70 was detected using the phosophospecific MAPK antibody (*Figure 32A*). Part of the sample was lysed directly in SDS lysis buffer and fractionated during the 2nd electrophoretic fractionation to provide a direct molecular weight comparison for the 2D fractionated sample. Two major phosphoprotein spots were detected, one of which was phosphorylated ERK2 and the other the p70 phosphoprotein running at an approximate pI of 5.4 (*Figure 32A*). The degree of resolution of the p70 phosphoprotein was determined by matching this immunoblot to its corresponding brilliant blue G-colloidal stained gel (*Figure 32B*) as described under Materials and Methods. Unfortunately, the p70 component was not well resolved from other proteins (*Figure 32B*), making the recovery of uncontaminated p70 impossible.

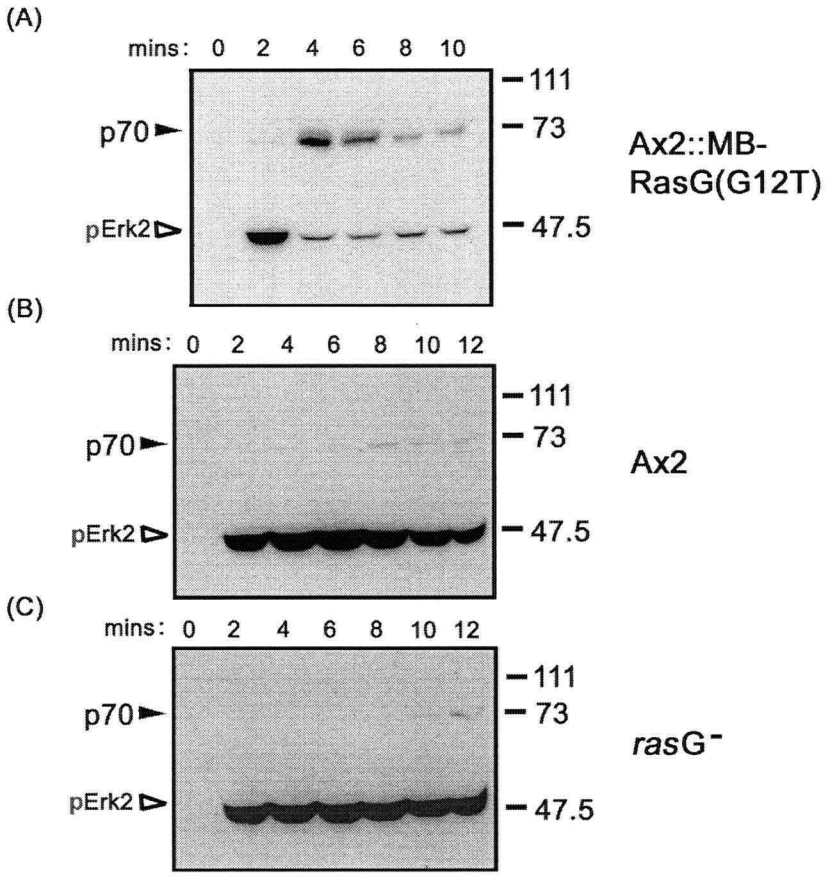

Figure 31. **Detection of a novel 70 kDa protein phosphorylated in response to folate.** Induced Ax2::MB-*rasG*(G12T) (A), Ax2 (B) and *rasG* null (C) cells were washed free of HL5 media, resuspended in KK2 at a density of 5 x 10^6 cells/ml and starved for 30 minutes. Cells were then washed in KK2 and resuspended at ~ 5 x 10^7 cells/ml and stimulated with 50 μM folate. At the indicated times (in minutes), 50 μl aliquots of cells were lysed and fractionated by 1D electrophoresis. Blots were probed with a phosophospecific MAPK antibody. A novel 70 kDa phosphoprotein termed p70 (closed arrow), phosphorylated ERK2 (open arrow), and molecular weight markers (kDa) are indicated.

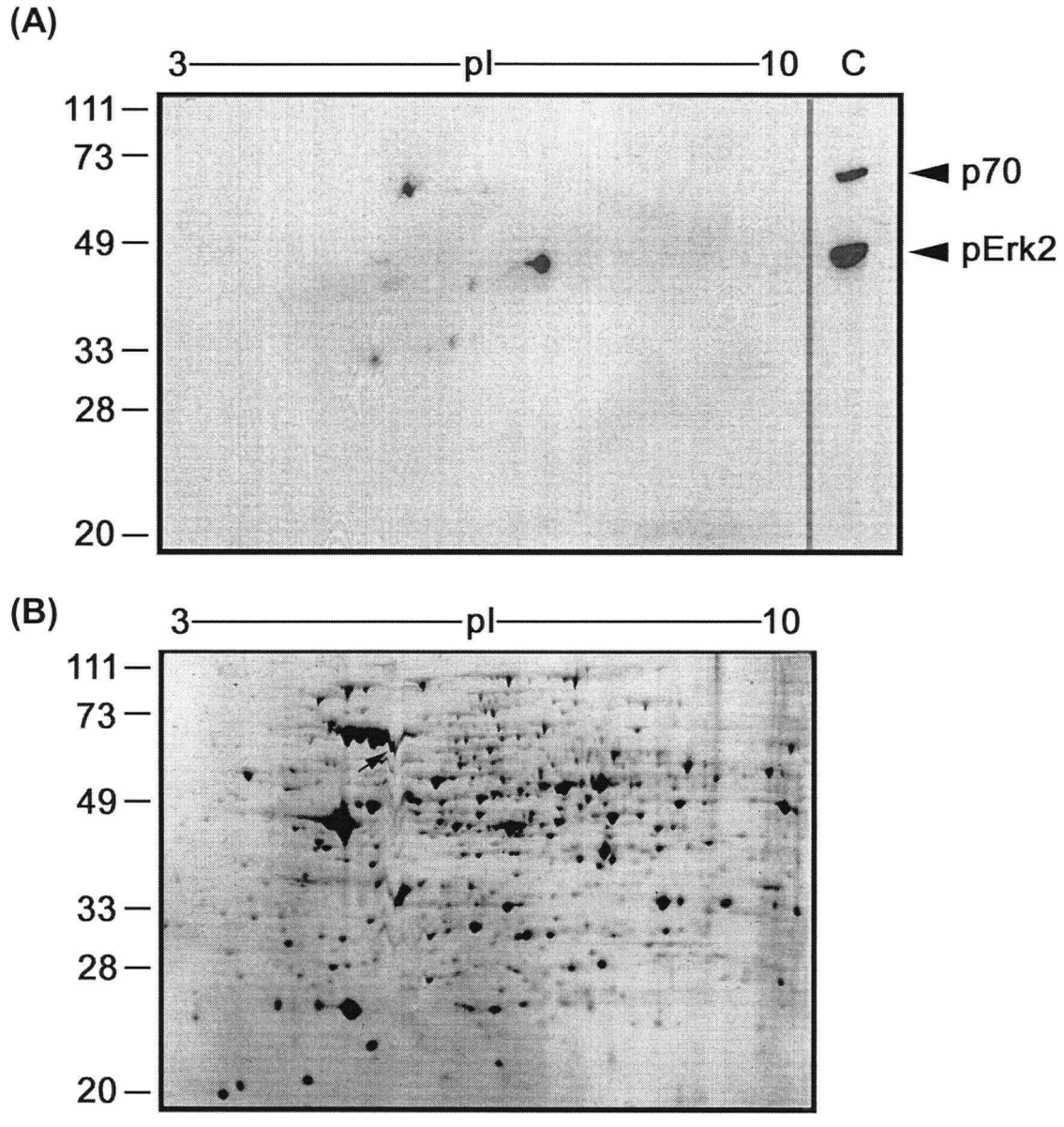

Figure 32. **Fractionation of the folate-stimulated phosphoprotein p70 by 2D gel electrophoresis.** Ax2::MB-*ras*G(G12T) cells, grown in the absence of tetracycline in HL5 media for three hrs, were resuspended in KK2 at a density of 5 x 10^6 cells/ml and starved for 30 minutes. Cells were then washed and resuspended in KK2 at ~ 5 x 10^7 cells/ml and stimulated with 50 μM folate. After 4 minutes, cell aliquots (250 μg) were fractioned by 2D gel electrophoresis as described under Materials and Methods. (A) An immunoblot probed with phosophospecific MAPK antibody. A 50 μM folate-stimulated protein sample (20 μg) lysed directly in SDS sample buffer was included in the 2nd dimension (C). (B) A corresponding brilliant blue G-colloidal stained gel. The position of p70, molecular weight markers (kDa), and pI ranges are indicated.

The p70 phosphoprotein was fractionated by narrowing the pI range of the isoelectric focusing from 3-10 to 5-6, a range encompassing the observed pI of 5.4 for the p70 phosphoprotein (*Figure 32A*). Immunoblot analysis of these narrow-range 2D gels matched the p70 phosphoprotein spot to a single resolved protein spot (*Figure 33*). This spot was excised from the brilliant blue G-colloidal stained gel, in-gel digested with trypsin (Wilm *et al.*, 1996) and the extracted peptides were used for peptide mass fingerprint analysis. Matching the obtained mass data against the *Dictyostelium* database (http://dictybase.org/index.html) resulted in the identification of a leucine-rich repeat protein A (LrrA) (*Table 2*). When selected peptides from this sample were subsequently subjected to MS/MS analysis to generate peptide sequence data, 3 peptides sequences corresponded to portions the LrrA sequence (*Table 2*), confirming the identification.

Table 2: A list of proteins identified as putative p70 candidates

Identified Protein	Known/ Predicted Function	Mass (Da)	pI	% Sequence	Peptides Matched by MS/MS Analysis	Genbank Accession Number
LrrA	Ras Binding Protein	59807	5.4	18	LTIDNIPSEIGK GTESIIQWLK VSGLGIQQDNEK	AAK71315
VatA	vacuolar H+-ATPase A subunit	68671	5.4	23	LPCNYPLLTGQR VGHNQLVGEIIR	AAB50981

3.5.3 LrrA is a predicted Ras-binding protein, but is not p70

The *Dictyostelium lrr*A gene sequence has been placed in GenBank (accession # AF388909), but as yet, nothing has been published reporting its characterization. Therefore, database homology searches were preformed to provide clues to *lrr*A gene function. NCBI blast searches (http://www.ncbi.nlm.nih.gov/BLAST/) revealed LrrA to be homologous to the protein SUR-8, a Ras-binding protein that positively regulates MAPK pathways in *Caenorhabditis elegans* and mammalian cells (Sieburth *et al.*, 1998; Li *et al.*, 2000). The 29% overall identity LrrA shared with *C. elegans* SUR-8 (*Figure 34A*) was primarily due to 19 leucine-rich repeats

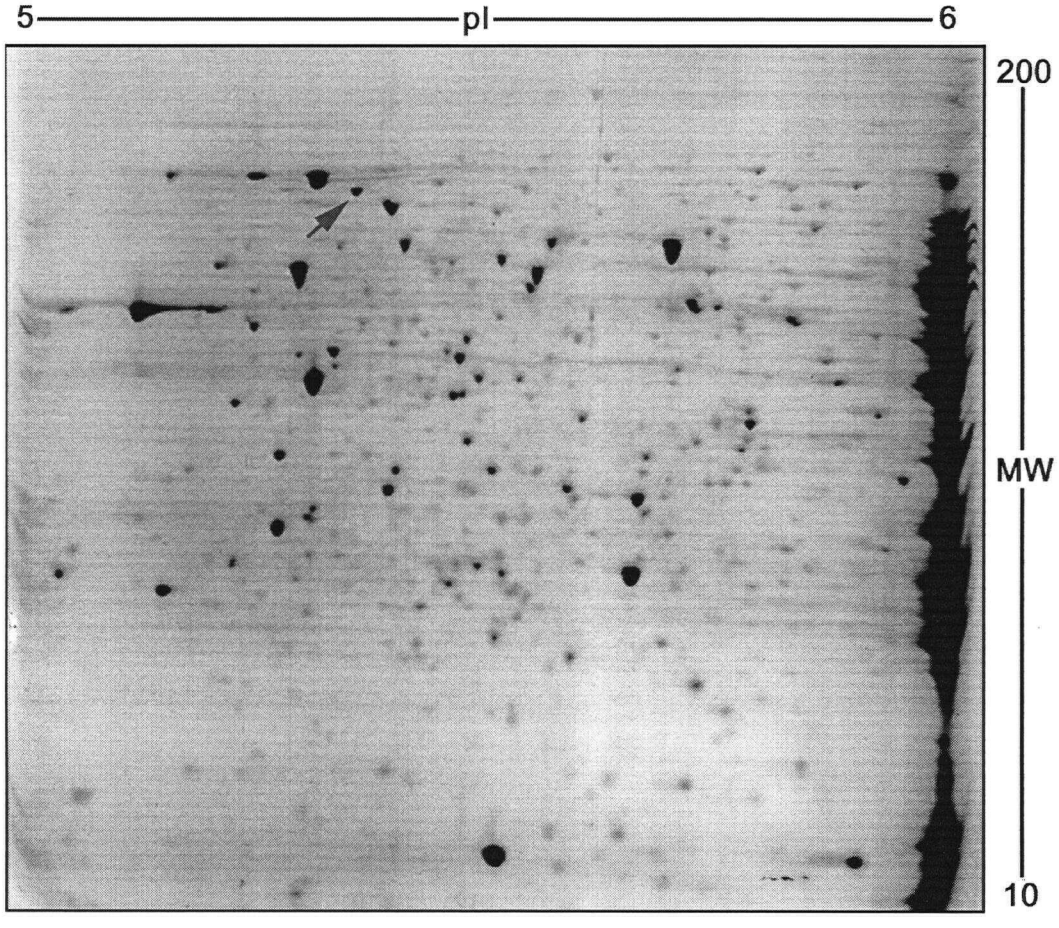

Figure 33. **Fractionation of the folate-stimulated phosphoprotein p70 on a narrow-pI range 2D gel.** Ax2::MB-*ras*G(G12T) cells, grown in the absence of tetracycline in HL5 media for three hrs, were resuspended in KK2 at a density of 5 x 10^6 cells/ml and starved for 30 mins. Cells were then washed and resuspended in KK2 at ~ 5 x 10^7 cells/ml and stimulated with 50 μM folate. After 4 mins, cell aliquots were fractioned by 2D gel electrophoresis using a narrow range pI of 5-6. The resulting gel was brilliant blue G-colloidal stained and the p70 phosphoprotein was localized as described under Materials and Methods. The arrow indicates the position of p70. Molecular weight markers (kDa) and the pI range are shown.

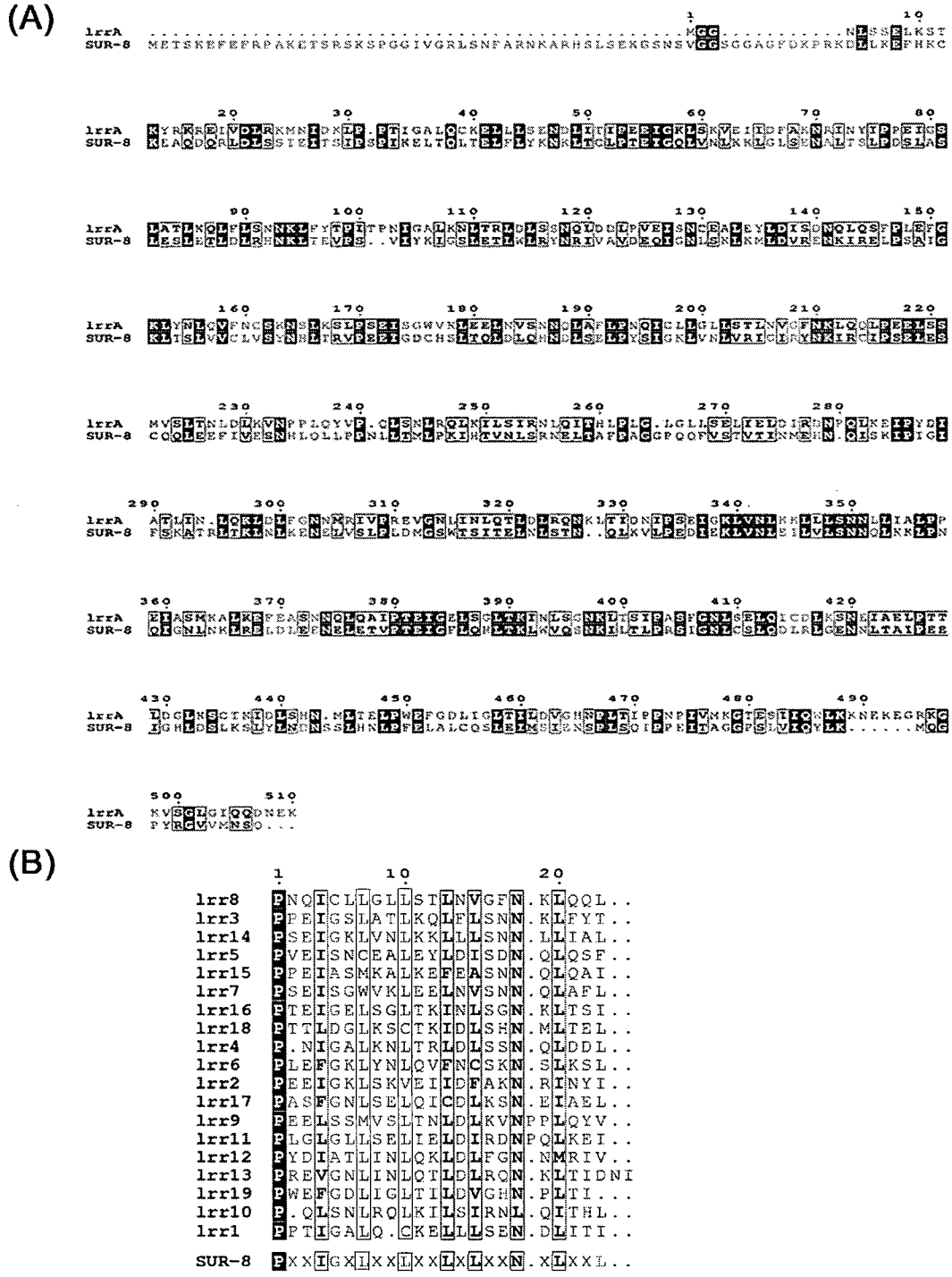

Figure 34. **Sequence alignment of *Dictyostelium* LrrA and *C. elegans* SUR-8.** (A) Alignment of *C. elegans* SUR-8 and *Dictyostelium* LrrA, regions of significant similarity are boxed. (B) Alignments of the 19 leucine-rich repeat regions (lrr) of LrrA. Consensus sequence of SUR-8 lrr's is shown for reference.

(LRRs) found in both proteins and other SUR-8 family members (*Figure 34B*) (Kobe and Kajava, 2001).

To confirm the identity of LrrA as the p70 phosphoprotein, a c-Myc epitope tag was added to the C-terminus of LrrA and this construct was inserted behind an inducible tetracycline promoter. Ax2 cells were transformed with this expression vector and a clone expressing $LrrA^{MYC}$ (Ax2::MB-$LrrA^{MYC}$) was isolated. This strain was then stimulated with 50 μM folate for 8 minutes, after which cells were lysed in a non-ionic detergent supplemented with phosphatase inhibitors. If LrrA was identical to p70 it would be expected that immunoprecipitated $LrrA^{MYC}$ would react with the phosphospecific MAPK antibody in immunoblots. To test this, a monoclonal c-Myc epitope tag antibody was added to the samples to form immunocomplexes with the $LrrA^{MYC}$, which were then immunoprecipitated by binding to Protein-A agarose beads. The immunoprecipitated complexes were then solubilized in SDS, separated by SDS-PAGE, blotted onto PDVF membranes, and the membranes immunoblotted with both the c-Myc epitope antibody and phosphospecific MAPK antibody (*Figure 35*). The addition of c-Myc epitope antibody to the above experiments permitted immunoprecipitation of $LrrA^{MYC}$ in both stimulated (folate) and mock-stimulated (KK2) cells, but the presence of p70 was not detected in stimulated c-Myc immunoprecipitated samples (*Figure 35*). Total protein samples from stimulated and mock-stimulated cells, which were directly lysed in SDS lysis buffer, revealed p70 to be phosphorylated in stimulated cells before immunoprecipitation (*Figure 35*). These data indicated that immunoprecipitated $LrrA^{MYC}$ did not react with the phosphospecific MAPK antibody.

It was subsequently learned that Dr. Wen-Tsan Chang from National Cheng Kung University Medical College had created an *lrrA* null strain. This strain was obtained from Dr. Chang to determine if folate-stimulated p70 phosphorylation could still be detected in the absence of LrrA. Protein samples taken from *lrrA* null cells after stimulation with 50 μM folate were used for immunoblot analysis with the phosphospecific MAPK antibody (*Figure 36*). p70 phosphorylation was still detectable in this strain, confirming that LrrA was not p70.

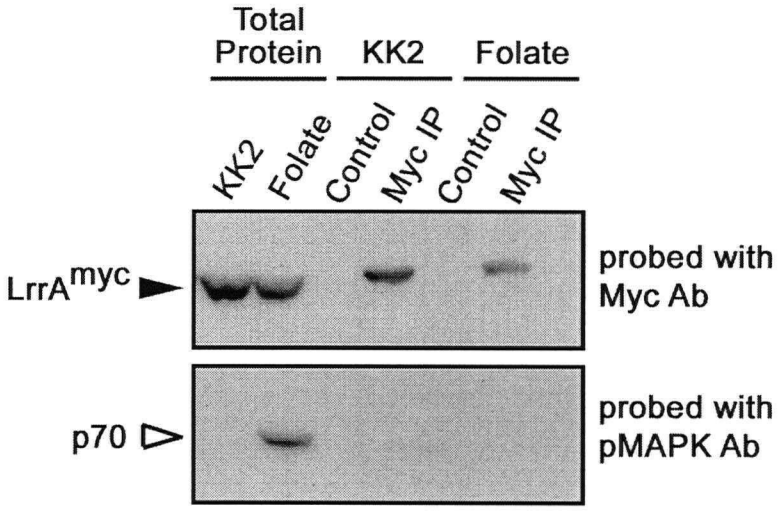

Figure 35. **A test for the reaction of LrrA with the phosphospecific MAPK antibody used to detect p70 phosphorylation.** Ax2::MB-LrrA^{MYC} cells induced to express LrrA^{MYC} were resuspended in KK2 at a density of 5 x 10^6 cells/ml and starved for 30 mins. Cells were then washed and resuspended in KK2 at ~ 5 x 10^7 cells/ml and either mock-stimulated (KK2) or stimulated (50 μM folate) for 8 mins. After which, cell aliquots were lysed in either 6x SDS lysis buffer (Total Protein) or a non-ionic detergent supplemented with phosphatase inhibitors (KK2 and Folate). LrrA^{MYC} was immunoprecipitated with the addition of a monoclonal c-Myc antibody (Myc IP) and samples used for 1D immunoblot analysis (lanes 4 and 6). In addition, a mock immunoprecipitation was preformed by adding KK2 to a set of non-ionic detergent lysed samples (Control).

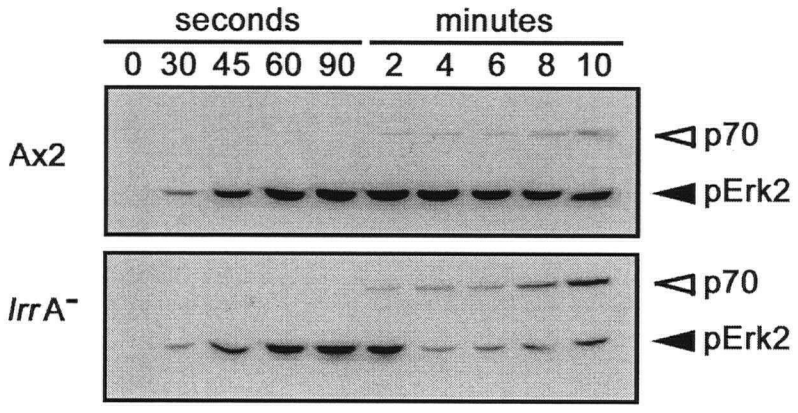

Figure 36. **Detection of p70 in folate-stimulated *lrrA* nulls cells.** Ax2 and *lrrA* null cells were resuspended in KK2 at a density of 5 x 10^6 cells/ml and starved for 30 minutes. Cells were then washed and resuspended in KK2 at ~ 5 x 10^7 cells/ml and stimulated with 50 μM folate. After the indicated times, cell aliquots were lysed directly in 6x SDS Lysis Buffer. Protein samples were then used for 1D immunoblot analysis with a phosphospecific MAPK antibody. Phosphorylated p70 (open arrow), phosphorylated ERK2 (closed arrow), and molecular weight markers (kDa) are indicated.

3.5.4 Isolation of a protein from the *lrrA* null that co-migrates with LrrA in wild type cells

These results suggested that LrrA was a more abundant component that co-migrated with the p70 phosphoprotein, i.e. p70 and LrrA were not resolved by 2D electrophoresis and p70 was not present in high enough quantities to be identified by MS analysis. The *lrrA* null strain was therefore subjected to narrow-range 2D electrophoresis as described in section 3.5.3. This analysis revealed the presence of a protein localized in the same position as LrrA in the Ax2::MB-*rasG*(G12T) cells (*Figure 37*), indicating these proteins co-fractionated on a 2D gel. Consistent with the idea that LrrA obscured the identification of this component during MS analysis, the protein in the *lrrA* null strained weakly with silver reagent, whereas LrrA was easily detected by brilliant blue G-colloidal staining (compare Figure 37A to Figure 37B). To determine the identity of the p70 protein from the *lrrA* null cells, the spot was excised and pooled from 5 silver stained gels to allow adequate material for identification. Pooled spots were in-gel digested with trypsin (Wilm *et al.*, 1996) and the peptides extracted from this digest were used for peptide mass fingerprint analysis and MS/MS analysis as before. The protein was identified as vacuolar H(+)-ATPase subunit A (VatA) (*Table 2*), a component of the vacuolar ATPase complex of *Dictyostelium* (Fok *et al.*, 1993; Finbow and Harrison, 1997).

3.5.5 Attempts at confirming that p70 is VatA

The contractile vacuole network, of which the vacuolar H(+)-ATPase complex is a major component, has been extensively studied in *Dictyostelium* (Heuser *et al.*, 1993; Fok *et al.*, 1993; Clarke *et al.*, 2002; Liu *et al.*, 2002). Since the vacuolar H(+)-ATPase subunits are also major components, VatA would be expected to be present in larger amounts than LrrA, rather than the opposite (*Figure 37*). This is probably also explained by the removal of the membrane fraction prior to the analysis, since VatA is a tightly bound membrane protein.

The creation of *vatA* null strain has been repeatedly attempted without success in Dr. Margaret Clarke's Laboratory at the Oklahoma Medical Research Foundation, leading to the conclusion that VatA is essential for *Dictyostelium* viability (M. Clarke, *personal communication*). Dr. Clarke provided an antibody that recognizes VatA in immunoblots, and I attempted to use this antibody to immune precipitate VatA to determine if the precipitated protein was phosphorylated in response to folate stimulation. However, the antibody did not

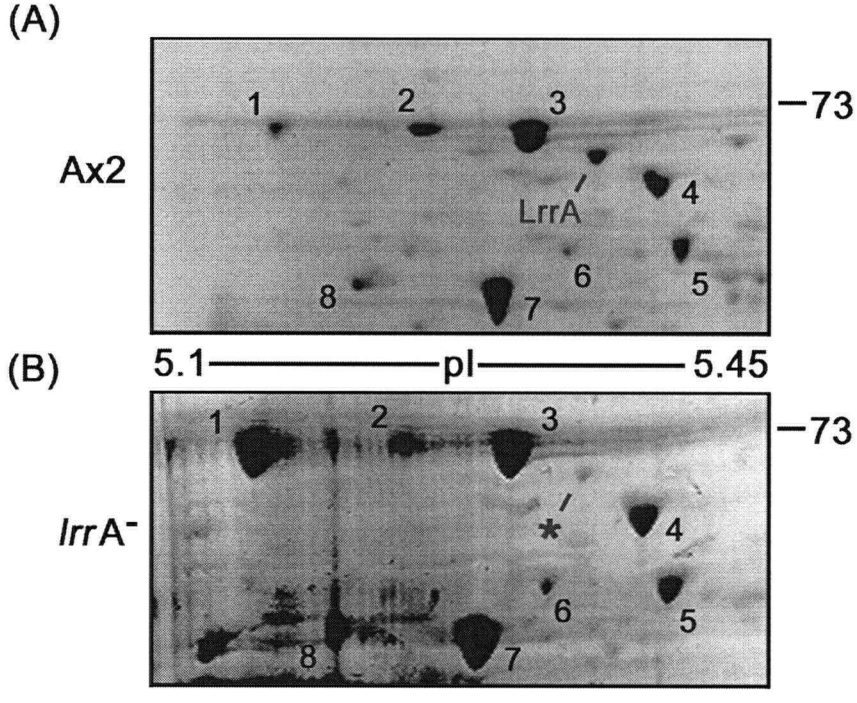

***Figure 37.* 2D gel analysis of an *lrrA* null strain for the presence of p70.** Ax2 and *lrrA* null cells were resuspended in KK2 at a density of 5 x 10^6 cells/ml and starved for 30 mins. Cells were then washed and resuspended in KK2 at ~ 5 x 10^7 cells/ml and stimulated with 50 μM folate. After 8 mins, cell aliquots were fractioned by 2D gel electrophoresis with a narrow range pI of 5-6. (A) The Ax2 lysates were stained with brilliant blue G-colloidal. (B) The *lrrA* null lysates were silver stained. The location of the LrrA protein and a protein spot localizing to the same location as LrrA (star) in the *lrr*A null in shown. Molecular weight markers (kDa) and pI ranges are indicated.

immunoprecipitate VatA. Since studies with a *vatA* null strain were not feasible and the VatA antibody did not immunoprecipitate VatA, attempts were made to overexpress tagged versions of VatA to confirm that this protein was in fact p70.

Repeated attempts to express c-Myc tagged VatA fusion proteins (on both the C- and N-terminal ends of VatA) were unsuccessful; no transformants expressing the fusion proteins were obtained even when an inducible promoter was utilized. A strain overexpressing wild-type VatA (*vatA-oe*) was therefore employed to determine if VatA overexpression would lead to enhanced p70 phosphorylation. This strain grew very slowly and after a few passages would no longer overexpress VatA. Nevertheless, it was possible to obtain sufficient cells that expressed 2-3 times the normal level of VatA so that the effect of increased VatA levels on p70 phosphorylation could be determined (see Figure 38). *vatA-oe* and Ax2 control cells were stimulated with 50 μM folate and samples taken at various time points after stimulation were used for immunoblot analysis (*Figure 38*). In Ax2 control cells, p70 phosphorylation was first detectable at 2 minutes after stimulation, whereas in *vatA-oe* cells this phosphorylation was detectable after 30 seconds (*Figure 38*). However, although p70 phosphorylation was detectable earlier in the *vatA-oe* strain, the increased levels of VatA in the cell did not lead to an increase in the levels of phosphorylated p70 as had been hoped. This experiment provides some evidence that p70 is VatA, in that folate-stimulated p70 phosphorylation occurred earlier in the *vatA-oe* cells, but there was no correlation between the levels of phosphorylated p70 and the amount of VatA.

An alternative approach to try to link p70 and VatA relied on the enrichment of the vacuolar H(+)-ATPase complex in the membrane fraction of *Dictyostelium* cells (Fok *et al.*, 1993; Nolta *et al.*, 1993; Nolta *et al.*, 1994). Ax2 cells stimulated with 50 μM folate for 8 minutes to maximally phosphorylate p70 were pelleted and resuspended in buffered 0.25 M sucrose (Bush *et al.*, 1994). These cells were broken with a Dounce homogenizer and the percentage of broken cells determined by phase-contrast light microscopy (under these conditions, greater than 95% of the cells were broken). Homogenized samples were subjected to differential centrifugation to generate pellet and supernatant fractions, and these fractions were subsequently used for immunoblot analysis with the VatA-specific and phosphospecific MAPK antibodies (*Figure 39*). VatA and p70 were similarly enriched in the pelleted fractions (P1 and P2), a result consistent with the idea that VatA is p70.

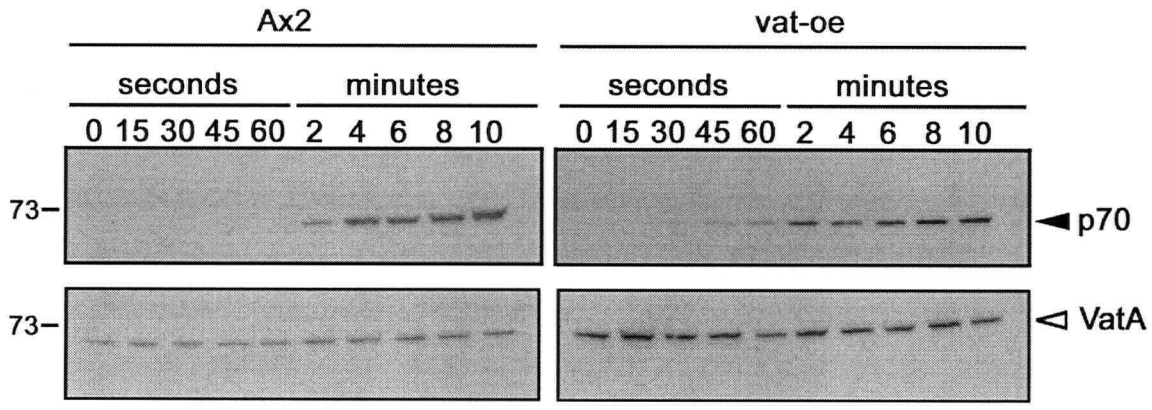

Figure 38. **VatA overexpression changes the phosphorylation of p70.** Ax2 and *vatA-oe* (B) cells were washed free of HL5 media, resuspended in KK2 at ~ 5 x 10^7 cells/ml and stimulated with 50 μM folate. At the indicated times, 50 μl aliquots of cells were lysed, fractionated by 1D electrophoresis and blots probed with both a phosphospecific MAPK antibody to detect phosphorylated p70 (closed arrow) and a VatA-specific antibody to determined VatA levels (open arrow). Molecular weight markers (kDa) are indicated.

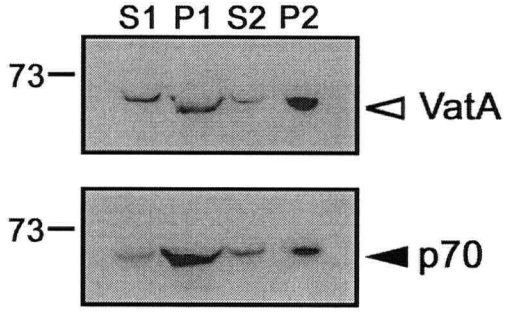

Figure 39. **Subcellular fractionation of VatA and p70.** Ax2 cells were stimulated with 50 μM folate for 8 mins, pelleted and resuspended in buffered 0.25 M sucrose. These cells were broken with a Dounce homogenizer and homogenized samples were subjected to differential centrifugation to generate pellet and supernatant fractions (S1 = supernatant fraction 1000 g for 5 mins, P1 = pellet fraction 1000 g for 5 mins, S2 = supernatant fraction 10,000 g for 10 mins, P2 = pellet fraction 10,000 g for 10 mins). These fractions were used for immunoblot analysis with the VatA-specific (open arrow) and phosphospecific MAPK (closed arrow) antibodies. Molecular weight marker (kDa) is indicated.

3.5.6 Summary

A 70 kDa protein (p70) that was phosphorylated in response to chemoattractant stimulation was detected. Since RasG modified p70 phosphorylation it was thus targeted for identification. 2D immunoblot analysis followed by mass spectrometry identified two previously studied proteins, LrrA and VatA, which co-localized with p70. Myc tagged LrrA was not phosphorylated in response to folate, suggesting that p70 was not LrrA and this was confirmed by the continued phosphorylation of p70 in an *lrrA* null strain. Eliminating or confirming p70 as VatA was less definitive. Overexpression of VatA resulted in changes in p70 phosphorylation and VatA and p70 co-localized upon cellular fractionation, consistent with the idea the p70 is VatA. However definitive proof of this identification is still lacking. Although outside the scope and time frame of this body of work, further experiments involving the creation of a new antibody for the immunoprecipitation of VatA or analysis of the VatA phosphorylation sites via mass spectrometry (Shou *et al.*, 2002) should provide more direct evidence.

4 DISCUSSION

4.1 Inducible expression of activated RasG and its effects on *discoidin* expression

In the fifteen years since the *Dictyostelium rasG* gene was discovered (Robbins *et al.*, 1989), a number of studies have shown that RasG regulates growth, early development and cytoskeletal functions (Khosla *et al.*, 1996; Tuxworth *et al.*, 1997; Zhang *et al.*, 1999; Khosla *et al.*, 2000; Jaffer *et al.*, 2001), but these studies have not yielded a molecular understanding of the signaling pathways involved. Attempts to identify RasG signaling components, using co-immunoprecipitation and affinity chromatography or restriction enzyme mediated integration to produce genetic suppressors of *rasG* mutant strains, have proved unsuccessful (M. Khosla and G. Weeks, *personal communication*). The observation that *discoidin* gene expression changed in response to the synthesis of an activated form of RasG provided an alternative experimental approach, which was used to search for signaling proteins that changed their phosphorylation state during this response (*Figures 10 and 11*). In total, 10 putative RasG-regulated components were identified by this method. In addition, the modulation of a chemoattractant-induced phosphorylation by RasG(G12T) was demonstrated. This work provides new molecular insights into how RasG functions.

The identification of putative RasG signaling targets depended on the inducible expression of RasG(G12T) and two inducible expression systems were analyzed. Prior to the late 1990's only one inducible expression system was available for *Dictyostelium* expression, the folate-repressible *discoidin* I? promoter (Blusch *et al.*, 1992) and this system was exploited to express *rasG*(G12T) in Ax2 cells (Khosla *et al.*, 1996). Although this system proved to be useful for earlier studies (Liu *et al.*, 1992; Khosla *et al.*, 1996; Zhang *et al.*, 1999; Jaffer *et al.*, 2001), there was an appreciable basal level of expression in the presence of folate, induction in the absence of folate was slow, expression fluctuated during exponential growth and there were inhibitory effects of RasG(G12T) on expression (Secko *et al.*, 2001).

The *rnrB* promoter was tested as an alternative, since exogenous agents induced *rnrB* expression (Gaudet *et al.*, 1999). However, strains expressing RasG(G12T) under the control of the *rnrB* promoter became un-responsive to the mutagenic stimulus after several passages of growth in HL5 media (see Section 3.2.2). Most of the studies reported in this thesis made use of

a third inducible expression system based on a tetracycline-repressible *tet* promoter (Blaauw *et al.*, 2000), which did not suffer from the disadvantages displayed by the other two experimental systems.

Induction of RasG(G12T) synthesis from the *rnrB* and *tet* promoters was accompanied by repression of *discoidin* mRNA levels (*Figure 5 and 10*). In addition, RasG, while not essential for *discoidin* expression, was necessary for high levels of expression (*Figure 6*). RasG regulation functioned independently of a number of factors (PSF, CMF, folate) and growth conditions (bacteria and axenic media) that are known to regulate *discoidin* expression (Blusch *et al.*, 1992; Burdine and Clarke, 1995; Gomer *et al.*, 1991; Wetterauer *et al.*, 1995). However, in all these experiments, Discoidin levels were considerably lower in the *rasG* null cells than in the wild type cells (*Figures 6-9*), suggesting that loss of RasG signaling affects some regulator of *discoidin* expression. Although RasG(G12T) overexpression has been previously shown to reduce the final cell density observed during growth (Khosla *et al.*, 1996), to cause changes in cell shape (Zhang *et al.*, 1999) and to prevent aggregation when nutrients are removed (Khosla *et al.*, 1996), there is no evidence that any of these effects are directly related to the effect on *discoidin* gene expression.

Thus, the data presented in this thesis indicated that RasG had two effects on *discoidin* expression; it was required to maintain high Discoidin levels but, when present in an activated form at high concentrations, *discoidin* gene expression was repressed. It is possible, however, that RasG(G12T) acted as a dominant negative form of the protein rather than as an activated form, and thereby inhibited signaling pathways that it does not normally regulate. For example, such a dominant negative effect of the RasG(G12T) protein could function through the sequestration of effector proteins, either through increased binding of RasG effectors or alternatively the binding of the effectors of *Dictyostelium* Ras proteins other than RasG. However this possibility is unlikely, given the fact that the effects of RasG(G12T) on cell shape and the initiation of aggregation (Khosla *et al.*, 1996; Zhang *et al.*, 1999) are quite different to the phenotypes of the *rasG* null strain (Tuxworth *et al.*, 1997). For example, *rasG* null cells do not exhibit the flattened characteristics of *pVEII-rasG*(G12T) transformants and *rasG* null cells are capable of initiating development (Tuxworth *et al.*, 1997). Furthermore, while *rasG* null cells and *pVEII-rasG*(G12T) transformants both exhibit impaired growth, the nature of the growth inhibition is quite different in the two strains (Khosla *et al.*, 1996; Tuxworth *et al.*, 1997).

Nevertheless, it will be important to consider possible alternative approaches for investigating the activation of the RasG pathway to resolve this issue in the future, for example, through the overexpression of wild-type RasG and RasG(G12T) in the *rasG* null strain or the use of activating stimuli upstream of RasG (Kae *et al.*, 2004).

Three other *Dictyostelium* proteins have been shown to modulate *discoidin* expression: Ga2, PKA and Dd-STATb (Blusch *et al.*, 1995; Primpke *et al.*, 2000; Zhukovskaya *et al.*, 2004). Ga2 null cells are reduced in their induction of *discoidin* expression at the onset of starvation after growth on bacteria (Blusch *et al.*, 1995). Cells disrupted in the PKA catalytic subunit (PKA-C) express reduced levels of Discoidin during growth in axenic media, but are still able to induce Discoidin expression in response to PSF and CMF (Primpke *et al.*, 2000). *Dd-STATb* null cells express higher levels of *discoidin* mRNA than wild type cells (Zhukovskaya *et al.*, 2004). It is not uncommon in eukaryotes to have multiple pathways acting on a gene, so RasG, Ga2, PKA and Dd-STATb could be in independent pathways. But if the proteins were linked, epistasis experiments should be able to demonstrate such a linkage.

4.2 Combining RasG activation and functional proteomics to uncover novel phosphoproteins

Proteomic techniques provide powerful approaches to study biological problems that were intractable a mere decade ago. A prime example is the recent undertaking to understand biological systems as a whole, i.e. "systems biology", which relies heavily on proteomics, computational biology and genomics (Hood, 2003). Overall the goal of using proteomics has been to better understand biological problems by looking at global changes in cellular proteins (Graves and Haystead, 2002).

The study of signal transduction has benefited from the application of proteomic techniques to specific problems and this is well illustrated by the study of growth-promoting signals in mammalian cells. For example, the effect of the mitogen fibroblast growth factor 2 (FGF2) on MCF7 human mammary epithelial cells was analyzed by 2D gel electrophoresis and mass spectrometry (Vercoutter-Edouart *et al.*, 2001). This study monitored changes in protein expression upon FGF2 stimulation, finding four proteins that were up-regulated after 12 hrs, including heat shock protein 90 (HSP90), HSP70, proliferating cell nuclear antigen (PCNA), and the transcriptionally controlled tumor protein (TCTP) (Vercoutter-Edouart *et al.*, 2001). In

another study, the MEK1 inhibitor PD98059 was used to inhibit the ERK1/2 pathway in human breast epithelial cells to 10-25% (Seddighzadeh *et al.*, 2000). This 2D electrophoretic analysis detected alterations in the expression of seven proteins upon PD98059 treatment, such as annexin V, HSP80 and cytokeratin 8 (Seddighzadeh *et al.*, 2000). In a similar approach, 12-phorbol 13-myristate acetate (PMA) activation of MAPK in human erytholeukemia K562 cells was combined with selective activation and inhibition of the upstream MAPK components MKK1/2 (Lewis *et al.*, 2000). This analysis detected 25 putative targets of the MKK1/2-MAPK pathway in PMA-treated cells, of which only five had been previously characterized.

The above approaches are useful for studying global protein expression changes in response to various signals, but signal transduction cascades also involve more rapid changes in protein phosphorylation (Hunter, 2000). Therefore, over the last six years, proteomics techniques have been developed to monitor changes in protein phosphorylation in an effort to examine the "phosphoproteome" (Graves and Haystead, 2002). One approach involves the use of 2D immunoblotting with phospho-specific antibodies and mass spectrometry (e.g. Godovac-Zimmermann *et al.*, 1999; Soskic *et al.*, 1999; Yanagida *et al.*, 2000; Yuan and Desiderio, 2003). One notable early example was the identification of proteins that responded to platelet-derived growth factor (PDGF) stimulation of mouse fibroblasts (Soskic *et al.*, 1999). A number of the identified proteins had previously been reported to be involved in the PDGF signaling pathway (for example, ERK1, Akt and Src), but several novel components were also reported (for example, FGR and PTP-2) (Soskic *et al.*, 1999). Immunoprecipitation with phosphotyrosine antibodies, which allows the enrichment of tyrosine phosphorylated proteins before electrophoretic fractionation has also been used (Graves and Haystead, 2002). This approach led to the identification of the tyrosine phosphorylation of Vav-2 in response to EGF stimulation (Pandey *et al.*, 2000) and to the identification of phosphotyrosine proteins involved in colony-stimulating factor-1 stimulation of macrophages (Yeung *et al.*, 1998). Immunoprecipitation has been less successfully applied to the study of phosphothreonine- and phosphoserine-containing proteins due to a lack of phosphoserine and phosphothreonine antibodies capable of immunoprecipitating a wide selection of phosphoproteins (Graves and Haystead, 2002). Other techniques that have been described for the proteomic investigation of protein phosphorylation include: the conversion of phosphoserine residues to biotinylated residues followed by avidin affinity chromatography (Oda *et al.*, 2001), multi-step conversion of phosphoamino acids in

protein digests into free sulfhydryl groups and the capture of the derivatized peptides (Zhou *et al.*, 2001), and the use of immobilized metal affinity chromatography (IMAC) based on the affinity of negatively charged phosphate groups for positively charged metal ions (e.g. Fe^{3+} or Ga^{3+}) (Ficarro *et al.*, 2002). However, these last three techniques have yet to be extensively applied to the study of signaling pathways.

In the studies described in this thesis, a functional proteomic approach involving 2D immunoblotting with phosphospecific antibodies and mass spectrometry (Soskic *et al.*, 1999) was used to identify proteins that are potentially involved in RasG signaling. With this approach, it was possible to identify thirteen well-separated vegetative proteins that underwent changes in phosphorylation upon the expression of RasG(G12T), considerably more proteins than are generally identified by more traditional methods, such as immunoprecipitation or yeast-two hybrid analysis. These putative changes in phosphorylation appeared to respond to RasG(G12T) expression, since Ax2::MB and Ax2::MB-*rasG*(G12T) cells were grown in the presence of tetracycline, conditions in which RasG(G12T) is not noticeably expressed, extracts from these two cells showed similar patterns of protein phosphorylation (D. Secko, *unpublished observations*). Two of the identified proteins, namely actin and PKB, had been shown previously to be phosphorylated (Jungbluth *et al.*, 1995; Meili *et al.*, 1999), but this is the first report of a change in their phosphorylation state in response to the expression of RasG(G12T). The identification of actin and PKB underlines the potential usefulness of this approach for the detection of downstream signaling components. Since RasG(G12T) expression is known to have multiple effects on the cell that involve more than one downstream signaling pathway (Zhang *et al.*, 1999), it's not surprising that these RasG-responsive phosphoproteins were quite diverse in their predicted function (*Table 1 and 2*). In addition, these phosphoproteins are not necessarily RasG signaling components and some of the phosphorylations may be end products of a signaling pathway. Of these phosphoproteins, RasGEF-R and DdCAD-1 were found to be absent in their respective null strains (*Figure 17 and 18*). Similar validation will ultimately be necessary for each of the other proteins, since the possibility cannot be ruled out that each of the identified phosphorylated proteins co-migrates with a more abundant protein species that was not phosphorylated. This potential problem is well exemplified by the attempt at the identification of p70 in Section 3.5. In addition, it will be important to begin to validate the threonine and tyrosine phosphorylation of these proteins, for example, through the analysis of phosphorylation sites via

mass spectrometry (Shou *et al.*, 2002), phosphoamino acid analysis, or the immunoprecipation of tagged versions of these proteins.

4.3 The role of *Dictyostelium* kinases and phosphatases

The ultimate goal for identifying phosphoproteins responsive to Ras(G12T) (*Table 1*) would be to use them to find kinases and phosphatases responsible for the changes in phosphorylation. A number of kinases and phosphatases have been identified in *Dictyostelium* and it is therefore pertinent to discuss the function of a few of the better-characterized examples that could be regulated by RasG.

Two extracellular signal-regulated kinases (ERKs), also called mitogen-activated protein kinases (MAPKs), have been identified in *Dictyostelium*. ERK1 was the first to be identified and expression of antisense ERK1 mRNA using the *discoidin* promoter originally suggested that it was essential for vegetative growth (Gaskins *et al.*, 1994). Subsequently, *erk1* null cells were created. These cells were viable but showed defects in chemotaxis and development (Sobko *et al.*, 2002). ERK1 reacts with phosphotyrosine antibodies (Gaskins *et al.*, 1994), suggesting it may be regulated in a manner similar to mammalian ERK proteins, which require phosphorylation on threonine/tyrosine residues for activity, although this has yet to be confirmed (Pearson *et al.*, 2001). The second ERK to be identified, ERK2, is required for aggregation, since *erk2* null cells do not activate adenylyl cyclase upon receiving a pulse of cAMP and activation of adenylyl cyclase is necessary for aggregation (Segall *et al.*, 1995). *erk2* null cells also chemotax poorly to both cAMP and folate, possibly due to defects in polarization (Wang *et al.*, 1998). Based on these phenotypes it is not surprising that ERK2 is phosphorylated and activated in response to both cAMP (Maeda *et al.*, 1996; Kosaka and Pears, 1997) and folate (Maeda *et al.*, 1997; Kosaka and Pears, 1997). ERK2 kinase activity peaks approximately one minute after stimulation and has been correlated with ERK2 phosphorylation (Kosaka *et al.*, 1998).

In mammalian cells, ERK proteins are components of MAPK cascades, which include upstream MAP/ERK kinases (MEKs) and MEK kinases (MEKKs) (Pearson *et al.*, 2001). Two such proteins have been identified in *Dictyostelium*: DdMEK-1 and MEKKa. Disruption of DdMEK-1 results in cells that produce small aggregates and chemotax inefficiently, but in these cells ERK2 is still activated to wild-type levels, indicating that DdMEK1 is in a different pathway than ERK2 (Ma *et al.*, 1997). Although, it has been suggested that DdMEK-1 may lie in

a pathway leading to ERK1, since the developmental phenotypes of *erk1* and *mek-1* null cells are similar and the overexpression of constitutively active DdMEK-1 in *erk1* null cells does not alter the *erk1* phenotype (Sobko *et al.*, 2002). Alternatively, MEKKa may be in a pathway separate from ERK1 and ERK2 that is involved in regulating cell-type patterning and morphogenesis (Chung *et al.*, 1998). Since ERK2, MEK1 and MEKKa cells all have different developmental phenotypes, it would appear that there are at least three MAPK cascades functioning in *Dictyostelium,* at least during development, but the other components of these cascades have yet to be determined.

The most extensively studied *Dictyostelium* kinase is PKA, which is essential for aggregation, but which also functions during other stages of the life cycle (Loomis, 1998; Primpke *et al.*, 2000). It is composed of a single catalytic subunit (PKA-C) associated with a single regulatory subunit (PKA-R), as opposed to two of each subunit as seen in many other organisms (Burki *et al.*, 1991; Mann *et al.*, 1992; Simon *et al.*, 1992). Disruption of PKA-C prevents aggregation (Mann *et al.*, 1992), which has been linked to the loss of preaggregative gene expression (Schulkes and Schaap, 1995). PKA activity is determined by the level of intracellular cAMP, which is regulated by the rate of cAMP synthesis by adenylyl cyclases (Saran *et al.*, 2002) and cAMP degradation by RegA (Shaulsky *et al.*, 1998; Thomason *et al.*, 1998). RegA is part of a two-component system that has been linked to the control of terminal differentiation (Thomason *et al.*, 1999). A pathway involving RegA, ERK2, PKA and potentially RasG has been postulated (Lim *et al.*, 2003). This hypothetical pathway is based on the observation that the disruption of RegA in cells lacking ERK2 restores the ability of these cells to aggregate. This finding suggests that ERK2 inhibits the phosphodiesterase activity of RegA (Shaulsky *et al.*, 1998), leading to the accumulation of cAMP and the activation of PKA (Loomis, 1998). In cells expressing RasG(G12T), there is a reduction in the phosphorylation of ERK2, which could result in insufficient cAMP accumulation and thus decreased PKA activity. The loss of PKA activity could explain the inability of cells expressing RasG(G12T) to aggregate (Khosla *et al.*, 1996). In the above model, ERK2 influences PKA activity, but PKA can also influence ERK2 activity. For example, as discussed in more detail below, the addition of cAMP to wild type cells results in the activation of ERK2, and *pka* null cells show lower more extended levels of ERK2 activation in response to cAMP and PKA overexpression increases ERK2 activation in response to cAMP (Aubry *et al.*, 1997). In addition, expression of the PKA catalytic

subunit in *erk2* null cells rescues their aggregation-deficient phenotype, indicating that PKA expression can bypass some functions of ERK2 (Aubry *et al.*, 1997). Although these results suggest a cAMP-regulated pathway that involves PKA and ERK2, the direct phosphorylation of either PKA or ERK2 by other components or each other has yet to be demonstrated. The expression of PKA subunits in *rasG* mutant strains should help evaluate the role of RasG in the above model.

PKB is rapidly phosphorylated and activated upon the reception of a cAMP signal at the cell surface (Meili *et al.*, 1999; Lim *et al.*, 2001). Concurrent with its activation, PKB translocates to the plasma membrane and is localized to the leading edge. The localization of PKB at the leading edge suggests that PKB is important for regulating directional sensing during chemotaxis and, in fact, *pkbA* null cells lack cell polarity and also move slower in a chemotactic gradient (Meili *et al.*, 1999). In addition, aggregation is delayed in *pkbA* null cells, and these cells form few aggregation centers and can not aggregate at low cell density (Meili *et al.*, 1999). A role for RasG signal transduction in this process is suggested because RasG(G12T) expression affected both the phosphorylation of PKB and levels of membrane bound PKB (discussed in Section 4.8). PAKa, a member of the Ste/PAK protein kinase family, has been shown to be an *in vitro* substrate of PKB, being phosphorylated on Thr579. This phosphorylation has been suggested to be required for both PAKa activity and subcellular localization (Chung *et al.*, 2001). Members of the Ste/PAK protein kinase family are regulated by the binding of Rac family members to their CRIB domain (Bokoch *et al.*, 2003). The CRIB domain of PAKa can interact with *Dictyostelium* Rac1-GTP in a yeast two-hybrid assay, but it has yet to be shown directly that any *Dictyostelium* Rac regulates PAKa (Chung and Firtel, 1999). PAKa is believed to function through effects on myosin II, since *paka* null cells chemotax poorly and are defective in the assembly of myosin II into the cytoskeleton (Chung and Firtel, 1999). A PKB-related protein, PKBR-1, has also been partially characterized in *Dictyostelium*. This protein is atypical in that it contains no PH domain and is instead constitutively membrane localized (Meili *et al.*, 2000). PKBR-1 is also activated in response to cAMP through a PI3-kinase independent pathway.

Several proteins identified in this thesis were dephosphorylated in response to the expression of RasG(G12T), thus raising the possibility that RasG(G12T) expression activated a phosphatase. Three protein-tyrosine phosphatases (PTP1-3) have been described in *Dictyostelium,* the mutation of which changes the global wild type pattern of tyrosine

phosphorylation (Howard *et al.*, 1992; Howard *et al.*, 1994; Gamper *et al.*, 1996). Spalten, a serine/threonine phosphatase of the PPC2 family, has been shown to be required for cell-type differentiation (Aubry and Firtel, 1998). In addition, the recent identification a *Dictyostelium* phosphatase and tensin homologue (PTEN) homolog and the creation of a *pten* null strain have linked this PtdIns(3,4,5)P_3/PtdIns(3,4)P_2 degrading enzyme to the regulation of cell polarity and chemotaxis (Iijima and Devreotes, 2002). To date, none of these phosphatases have been linked to RasG signaling, but as mentioned above, a necessary next step is to identify both the phosphatases, and kinases, that RasG activates.

4.4 Actin phosphorylation and RasG regulation of the cytoskeleton

As mentioned previously, several lines of evidence have pointed to a role for RasG in regulating the actin cytoskeleton and, in particular, F-actin distribution (Tuxworth *et al.*, 1997; Zhang *et al.*, 1999). In mammalian cells, Ras proteins have been implicated in the regulation of the actin cytoskeleton through the activation of Rac (Burridge and Wennerberg, 2004). This activation leads to the activation of PAK and WAVE and subsequently LIM kinases and the Arp2/3 complex respectively. Rac activation is crucial in mammalian cells for the generation of actin-rich lamellipodial protrusions (Burridge and Wennerberg, 2004). In *Dictyostelium*, 15 homologs of mammalian Rac proteins have been identified and the functions of several of these proteins have been investigated by gene disruption and overexpression studies (Rivero *et al.*, 2001). For example, RacE has been implicated in organization of the cortical cytoskeleton since *racE* null cells are unable to grow in suspension due to cytokinesis defects (Larochelle *et al.*, 1996). The function of the Rac1A, B and C isoforms have also been investigated through the expression of constitutively active and dominant negative forms of these proteins, and the results of these studies link these proteins to the regulation of F-actin (Palmieri *et al.*, 2000). Two PAKs, PAKa and MIHCK, have been studied in *Dictyostelium* (Lee *et al.*, 1998; Chung and Firtel, 1999), and recently an Arp2/3 complex has been cloned (Insall *et al.*, 2001). To date, none of these proteins have been shown to be regulated by Ras proteins.

It has been reported previously that RasG(G12T) expression induces tyrosine phosphorylation of a protein with the same apparent molecular weight as actin (Chen and Katz, 2000). In this thesis, I have identified actin as a RasG-regulated phosphoprotein, confirming the earlier report. In addition, I showed that actin was phosphorylated at more than one site in cells

expressing activated RasG by the detection of two spots via 2D electrophoresis (*Figure 12 and Table 1*). Both of the actin species exhibited increases in tyrosine phosphorylation, suggesting the possibility that two tyrosines are phosphorylated upon the activation of RasG, but the pI shift could also be explained by the phosphorylation of a threonine or serine residue.

Induction of actin phosphorylation on Tyr53 in *Dictyostelium* has been reported to occur upon oxygen depletion, inhibition of ATP stimulation, heat shock, azide treatment and the re-feeding of starved *Dictyostelium* cells (Schweiger *et al.*, 1992; Howard *et al.*, 1993; Jungbluth *et al.*, 1994; Jungbluth *et al.*, 1995), but a second phosphorylation site has not previously been reported. The phosphorylation of *Dictyostelium* actin has been correlated with cell-shape changes (Howard *et al.*, 1993; Rebstein *et al.*, 1993; Chen and Katz, 2000), although the functional significance of this phosphorylation is still not clear. Nevertheless, the phosphorylation of actin is potentially a mode of actin regulation. For example, in *Physarum polycephalum*, threonine actin phosphorylation in response to dry stress prevents its ability to polymerize (Furuhashi *et al.*, 1998). A kinase, actin-fragmin kinase (AFK), involved in actin phosphorylation in *P. polycephalum* has been identified (Gettemans *et al.*, 1993). AFK phosphorylates actin when in a complex with Fragmin P and thereby blocks the F-actin capping activity of the actin-Fragmin P complex (Gettemans *et al.*, 1995). In mammalian cells, EGF and insulin have been shown to induce serine phosphorylation of actin (Carrascosa and Wieland, 1985; van Delft *et al.*, 1995). More recently, actin was found to be phosphorylated in opossum kidney cells in response to opioids (Papakonstanti and Stournaras, 2002). This phosphorylation was regulated by PI3K and PAK1 and correlated with the redistribution of filamentous actin (Papakonstanti and Stournaras, 2002). More components involved in *Dictyostelium* actin phosphorylation need to be discovered before it will become clear how this phosphorylation affects cytoskeletal regulation, and whether RasG is directly involved.

4.5 Which RasGEF is the right RasGEF for RasG?

RasGEFs are well established as essential components of Ras signaling pathways (Shields *et al.*, 2000; Wilkins and Insall, 2001) and more than 20 putative RasGEFs have been identified from the *Dictyostelium* genome sequencing project (Wilkins and Insall, 2001). However, none of these have as yet been shown to act on any of the Ras proteins *in vitro*. The

identification of RasGEF-R as a putative component of the RasG signaling pathway is therefore of considerable interest.

A variety of RasGEFs, including yeast Cdc25, human Sos1 and human RasGRF1, have been found to be phosphorylated (Gross *et al.*, 1992; Douville and Downward, 1997; Yang *et al.*, 2003) and it has been speculated that phosphorylation can result in both negative (human Sos1) and positive (human RasGRF1) regulation. In fact, in the case of human Sos1, phosphorylation has been suggested as a mechanism for negative feedback of Ras stimulation, given that Ras-regulated components have been implicated in the phosphorylation of Sos1 (Douville and Downward, 1997). This negative feedback could potentially ensure tight regulation of Ras activation in response to stimulation. Since RasGEF-R was dephosphorylated in response to activated RasG (*Figure 12; Table 1*), RasGEF-R could be responsible for the activation of RasG and its de-phosphorylation could be a mechanism for the negative feedback of RasG stimulation. Although the phosphorylation of human Sos1 has been suggested to have a negative influence on its RasGEF activity (Douville and Downward, 1997), it has recently been shown to elicit RacGEF activity, leading to actin cytoskeleton remodeling (Sini *et al.*, 2004). If this model holds true for RasG and RasGEF-R, RasG-regulated dephosphorylation of RasGEF-R might result in effects on other *Dictyostelium* GTPases.

Further experimentation is required to determine if RasGEF-R can act as a specific exchange factor for RasG. However, even if this were shown to be the case, the lack of an observable mutant phenotype for *gefR* null cells (R. Insall, *unpublished observations*) as compared to the complex phenotype for *rasG* null cells (Tuxworth *et al.*, 1997) suggests that RasGEF-R is functionally redundant. The only other RasGEFs that have been partially characterized are RasGEF-A (also called AleA or Aimless) (Insall *et al.*, 1996) and RasGEF-B (Wilkins *et al.*, 2000a). In the case of *aleA* null strain, its failure to aggregate is dissimilar from the delay seen in the development of *rasG* null cells (Insall *et al.*, 1996; *Figure 25*). Both *aleA* and *rasG* nulls cells show impaired chemotaxis, reduced activation of adenylyl cyclase and reduced ERK2 phosphorylation in response to cAMP stimulation (Insall *et al.*, 1996; Tuxworth *et al.*, 1997; Lim, 2002). *gefB* null cells move rapidly, are impaired in macropinocytosis and exhibit significantly delayed aggregation (Wilkins *et al.*, 2000a). Although *rasG* null cells exhibit delayed aggregation, they do not exhibit the other properties, so it unlikely that RasGEF-B is the exchange factor for RasG. This complexity highlights the importance of the potential

RasG/RasGEF-R relationship, since such relationships have been difficult to elucidate by genetic methods alone. Recently, an assay to measure the activation state of *Dictyostelium* RasG has been developed (Kae *et al.*, 2004). With this development, it will be important to determine the activation state of RasG in the various *gef* null strains, although the potential redundancy of *Dictoystelium* RasGEF function could complicate such an investigation. Alternatively, the detailed analysis of protein phosphorylation in strains lacking genes for RasGEFs, using the techniques described in this thesis, could potentially provide information on the phosphorylation events regulated the actions of these proteins.

4.6 A role for RasG in regulating early developmental adhesion through the dephosphorylation of DdCAD-1

A role for RasG signal transduction affecting early development was suggested by the finding that the expression of RasG(G12T) blocked development (Khosla *et al*, 1996). The marked effect of activated RasG on *discoidin* gene expression (*Figure 3 and 8*; Secko *et al.*, 2001), a known molecular marker of the transition from growth to development (Zeng *et al.*, 2000; Primpke *et al.*, 2000), is consistent with such a role. The results described in Sections 3.3 suggest a new facet to the regulatory role of RasG in regulating early developmental adhesion through the phosphorylation of DdCAD-1.

The importance of adhesion during *Dictyostelium* development was recognized over 35 years ago (Gerisch, 1968) and the adhesion protein DdCAD-1 (also known as contact sites B [csB] and gp24) is one of the first proteins to be expressed at the cell surface at the onset of starvation (Beug *et al.*, 1973; Yang *et al.*, 1997). DdCAD-1 has been implicated in mediating initial side-to-side contacts during early aggregation (Coates and Harwood, 2001). A second adhesion molecule, termed gp80 or contact sites A (csA), is induced by cAMP as development proceeds (Faix *et al.*, 1992) and mediates a second type of contact in the aggregation stream (Choi and Siu, 1987). gp80 allows tight adhesion between cells after the initial adhesive events mediated by DdCAD-1. In addition to differences in temporal gene expression, gp80 and DdCAD-1 mediated contacts can also be distinguished by their sensitivity to EDTA, since DdCAD-1 forms EDTA-sensitive contacts and gp80 forms EDTA-insensitive contacts (Coates and Harwood, 2001).

Although DdCAD-1 has been long implicated as a major adhesion molecule during early development, the finding that it is phosphorylated in *Dictyostelium* is novel. Since DdCAD-1 was resolved into at least three spots by 2D electrophoresis, it is likely that it is phosphorylated at more than one site (*Figure 12*). Although these separated components were detected with a phosphothreonine antibody, the pI shift might be due to phosphorylation on alternative amino acid residues or other modifications. The most abundant DdCAD-1 species, based on intensity by immuno- and silver-staining (s57 or DdCAD-1a), showed a slight, but reproducible increase in phosphorylation upon the expression of RasG(G12T). The second and third DdCAD-1 spots (s56 or DdCAD-1b and s55 or DdCAD-1c) were resolved at lower pI values. DdCAD-1b and DdCAD-1c spots were lower in total protein abundance (as determined by their weaker silver staining intensity) as compared to DdCAD-1a. The levels of both the phosphorylated DdCAD-1b and DdCAD-1c species decreased in response to the expression of RasG(G12T) and this data was consistent with an overall decrease in DdCAD-1 phosphorylation in response to activated RasG. This conclusion was supported by 1D immunoblot analysis (*Figure 23*). Since, total DdCAD-1 protein levels were not significantly different between RasG(G12T) expressing and control cells (*Figure 16*), the changes in DdCAD-1 phosphorylation were not a result of changes in DdCAD-1 levels.

DdCAD-1 mediated adhesion is known to be homophilic (e.g. binding is through DdCAD-1/DdCAD-1 interactions) and Ca^{2+} requiring (Brar and Siu, 1993; Wong *et al.*, 1996). The work reported here suggests that DdCAD-1 may also be regulated by phosphorylation. Initial insight into the effect of phosphorylation on DdCAD-1 function was garnered from the observation that cells expressing RasG(G12T) became cohesive during vegetative growth (*Figure 19*). Constitutive gp80 overexpression in vegetative cells has been found to induce EDTA-stable contacts in suspension (Faix *et al.*, 1992). RasG(G12T)-induced cohesion was instead EDTA-sensitive and could be blocked with anti-DdCAD-1 antibodies (*Figure 20*), suggesting that it was DdCAD-1 mediated. The fact that the RasG(G12T) expressing cells appeared more cohesive and contained less phosphorylated DdCAD-1, suggests the possibility that dephosphorylation of DdCAD-1 is involved in mediating DdCAD-1 adherence function. It is important to point out, that in the experiments described in Section 3.3.3 and shown in Figure 20, cell-to-substratum adhesion may also have been affected. In fact, the expression of RasG(G12T) has previously been suggested to increase cell-to-substratum adhesion (Chen and Katz, 2000),

and therefore, these experiments are likely assessing a combination of cell-to-cell and cell-to-substratum interactions.

Although cells grown on bacteria do not express DdCAD-1 until the onset of starvation (Knecht *et al.*, 1987), axenically grown Ax2 cells express high levels of DdCAD-1 without being adhesive (*Figure 13*; Sesaki and Siu, 1996). This is presumably due to the sequestration of DdCAD-1 in the cytoplasm of vegetative cells (Brar and Siu, 1993). Cells expressing RasG(G12T) contained rings of DdCAD-1 localized on the cell surface (*Figure 19*), suggesting the possibility that RasG(G12T) levels regulate the movement of DdCAD-1 to the surface. Transport of DdCAD-1 to the cell surface has been shown to occur via a non-classical pathway involving contractile vacuoles (Sesaki *et al.*, 1997) and a considerable fraction of DdCAD-1 was found in the contractile vacuoles of 12 hr developed cells (Sesaki *et al.*, 1997). Contractile vacuoles containing DdCAD-1 are similar to the DdCAD-1 ring structures observed in RasG(G12T) expressing cells (*Figure 21*).

The location of DdCAD-1 on the surface of developing cells is proposed to allow cells chemotaxing towards cAMP to adhere to one another and enter cellular streams (Sesaki and Siu, 1996). If RasG(G12T) expression enhanced the localization of DdCAD-1 to the surface, one would expect cells expressing RasG(G12T) to be more cohesive; and as a result, potentially form larger cellular streams. In standard *in vitro* cell cohesion assays, developing RasG(G12T) expressing cells were more cohesive (*Figure 22*), but, the failure of RasG(G12T) expressing cells to initiate development (Khosla *et al.*, 1996) precluded studying the effect of increased cell surface DdCAD-1 on cellular streaming. Since *rasG* null cells do differentiate after a delay in initiating aggregation, it was possible to examine their aggregation in more detail. They produced disorganized streams that resembled those of *cadA* null cells (*Figure 25*). Since DdCAD-1 has been implicated in the initial formation of cellular streams (Sesaki and Siu, 1996), the streaming phenotypes of *rasG*, and *cadA*, null cells may be a result of these cells utilizing alternative adhesion systems during aggregation, a hypothesis consistent with the delay in aggregation and thicker, shorter, streams formed in these strains. *rasG* null cells also express lower levels of DdCAD-1 (*Figure 26*) consistent with a role for DdCAD-1 in adherence during streaming. It is interesting that *rasG* null cells express less DdCAD-1, since RasG(G12T) expression was found not to affect DdCAD-1 protein levels (*Figure 16*). This difference could be

due to the short time period used for expressing RasG(G12T) (e.g. three hrs) and longer induction times may result in increased DdCAD-1 expression.

It will be of interest to define the signaling pathway leading from RasG activation to DdCAD-1 dephosphorylation. DdCAD-1 shares some homology with the extracellular domain of metazoan cadherins (Wong *et al.*, 1996), which are involved in cell-cell adhesion and the formation of adherens junctions (Nelson and Nusse, 2004). Metazoan cadherins form complexes with catenins to allow the linking of cadherins to the actin cytoskeleton (Jamora and Fuchs, 2002). These complexes are regulated by phosphorylation. Tyrosine phosphorylation of ß-catenin by Src or Fer results in the disruption of the cadherins/ß-catenin complexes and decreased adhesion (Lilien *et al.*, 2002; Nelson and Nusse, 2004). It is possible that DdCAD-1 phosphorylation performs a similar function. It should be noted that cadherins/ß-catenin complexes are phosphorylated on serine/threonine residues, which results in increased stabilization of the complexes (Lickert *et al.*, 2000). Since DdCAD-1 also appears to be phosphorylated on several residues (*Figure 18*), its regulation by phosphorylation could be equally complex. Finally, an unidentified transmembrane linker has been postulated to bind to DdCAD-1 (Sesaki *et al.*, 1997), however the proteins that interact with DdCAD-1 are currently not known. Determining the pathway leading from RasG to DdCAD-1 will not only help in our understanding of *Dictyostelium* development, but could produce insights into the regulation of metazoan cell-cell adhesion.

4.7 Effect of RasG(G12T) on PKB phosphorylation

It has been suggested that *Dictyostelium* PKB has two threonine phosphorylation sites (T278 and T435) that are required for receptor-mediated activation of its kinase activity (Meili *et al.*, 1999). PKB activation does not occur in *pi3k1/pi3k2* null cells (lacking both PI3K1 and PI3K2), suggesting a requirement for PI3K activity for PKB activation (Meili *et al.*, 1999). Since PI3K is a known downstream effector for activated Ras in mammalian cells (Shields *et al.*, 2000) and RasG is known to bind to PI3K1 and PI3K2 in a yeast two-hybrid assay (Funamoto *et al.*, 2002), it is reasonable to hypothesize that RasG regulates *Dictyostelium* PKB activity through its activation of PI3K1 or PI3K2. The data presented here provides additional evidence that PKB phosphorylation is RasG-regulated.

PKB was detected during the search for vegetative proteins whose phosphorylation was altered in response to the expression of activated RasG (*Table 1*). PKB was detected with a polyclonal phosphothreonine antibody during the 2D immunoblot analysis, consistent with Meili *et al.*'s (1999) postulated phosphorylation of PKB on threonine residues. The 2D analysis revealed that PKB phosphorylation was reduced in an activated RasG strain (*Figure 12*). This was unexpected, since data from mammalian studies show increased PKB phosphorylation in response to an activated Ras protein (Campbell *et al.*, 1998), and it raised the possibility that in *Dictyostelium*, RasG negatively regulates PKB. An SH2-domain-containing kinase, SHK1, has recently been identified as a negative regulator of PKB activation in *Dictyostelium* cells, possibly reducing PtdIns(3,4,5)P_3 via the modulation of the activity of either PI3K or PTEN (Moniakis *et al.*, 2001), and RasG might act in a similar manner. However, a more plausible possibility for the reduction in PKB phosphorylation in response to RasG is that the removal of membrane proteins during 2D sample preparation resulted in a loss of membrane-bound phosphorylated PKB. Membrane fractions of cells overexpressing RasG(G12T) contained slightly more PKB than control cells (*Figure 29*) and more phosphorylated PKB was detected in RasG(G12T) expressing cells analyzed by 1D immunoblot analysis (*Figures 28*). To date, RasG activation of PI3K has not been directly demonstrated for any of the *Dictyostelium* PI3Ks nor have the levels of PtdIns(3,4,5)P_3 in *rasG* mutant strains been analyzed.

It is not clear how PI3K stimulation results in PKB phosphorylation. In mammalian cells, PI3K activation is associated with the translocation of some PKB and phosphoinositide-dependent kinase 1 (PDK1) to the membrane (Anderson *et al.*, 1998; Bellacosa *et al.*, 1998). PDK1 can phosphorylate threonine-308 in the kinase domain of this fraction of PKB and the translocation of PDK1 to the membrane is required for this phosphorylation (Filippa *et al.*, 2000; Vanhaesebroeck and Alessi, 2000). Full PKB activity requires this PDK1 phosphorylation and a secondary phosphorylation on serine-473 (Persad *et al.*, 2001). Although a PDK has yet to be identified in *Dictyostelium*, the observation that cAMP-stimulated PI3K activation induces the translocation of a fraction of PKB (Meili *et al.*, 1999), suggests that PKB may be translocated and then phosphorylated in response to chemoattractant stimulation. Since RasG(G12T) expressing cells contain more PKB in their membrane fractions (*Figure 29*), and the translocation of the PKB PH-domain fused to GFP to the membrane in response to cAMP is

reduced in *rasG* nulls cells (R. Firtel, *personal communication*), it is possible that RasG is regulating the translocation of PKB to the membrane.

PKB phosphorylation was also observed to increase upon stimulation by folate (*Figure 28*), a known chemoattractant in *Dictyostelium* (Blusch and Nellen, 1994). This phosphorlyation was detected by 1D immunoblot analysis of total cell lysates, a method that has successfully used to monitor the phosphorlyation of PKB in response to cAMP (Lim *et al.*, 2001; Lim, 2002). Folate signal reception requires the G proteins Gß and Ga4 (Hadwiger *et al.*, 1994; Nebl *et al.*, 2002) and results in the stimulation of ERK2 phosphorylation (Kosaka *et al.*, 1998). The increase observed in PKB phosphorylation upon folate stimulation suggests that PKB may be an additional component involved in the transmission of a folate signal and it would be of interest to determine the ability of *pkbA*$^-$ null cells to chemotax towards folate. Nevertheless, confirmation of the phosphorlyation of PKB in response to folate stimulation, for example through the immunoprecipation of tagged versions of PKB, will be required before initiating such studies.

The finding that RasG(G12T) expression increased the levels of PKB phosphorylation in cells stimulated by a chemoattractant indicates that RasG may be involved in the regulation of chemotaxis and the generation of cell polarity. RasG(G12T) expressing cells responded poorly in a spatial gradient of folate and exhibited reduced cell polarity (*Figure 30*). Since PKB has been implicated in proper orientation and chemotaxis to cAMP (Meili *et al.*, 1999), it is possible that the effects of RasG(G12T) expression on these properties are partially mediated through its role in the translocation and phosphorylation of PKB.

Dictyostelium has become an important organism for understanding the mechanisms involved in cell polarity and chemotaxis (Devreotes and Janetopoulos, 2003). In the current model, chemotaxis begins with the receptor-stimulated generation of PtdIns(3,4,5)P_3 by the reciprocal regulation of PI3K and PTEN at the leading edge of the cell (Devreotes and Janetopoulos, 2003; Williams and Harwood, 2003). Local concentrations of PtdIns(3,4,5)P_3 attract PH-containing proteins, and the formation of actin-filled projections. This localization results in cell polarity and subsequent movement toward a chemoattractant (Devreotes and Janetopoulos, 2003; Williams and Harwood, 2003). The results presented in this thesis suggest the possibility that RasG may be involved in the generation of PtdIns(3,4,5)P_3, and thus PH domain binding sites, through the activation of PI3K activity. The generation of PtdIns(3,4,5)P_3 in *Dictyostelium* wild type, *pi3k1*$^-$/*pi3k2*$^-$and *pten*$^-$ cells in response to cAMP stimulation was

recently studied by metabolically labeling cells with ^{32}P followed by TLC (Huang *et al.*, 2003) and similar experiments on *rasG* mutants strains would allow investigation of the above possibility.

4.8 Additional targets of RasG regulation

The significance of the changes in the phosphorylation of the other proteins identified as responding to RasG(G12T) expression (*Tables 1 and 3*) were not studied further. Nevertheless, it is anticipated that the cellular activity of these proteins will be affected by the changes in phosphorylation and a brief examination of some of their predicted functions is therefore in order.

One of the most intriguing proteins to be identified in this study was FtsZA. This protein is most closely related to the bacterial protein FtsZ (Gilson *et al.*, 2003), a bacterial tubulin homolog that is a component of the "Z ring" structure that constricts upon cell division (Romberg and Levin, 2003). In *Dictyostelium*, FtsZA and a related protein FtsZB have been implicated in mitochondrial division (Gilson *et al.*, 2003). Neither bacterial FstZ nor *Dictyostelium* FstZA have been previously shown to be phosphorylated, although the bacterial protein FstA, which binds to FstZ, is phosphorylated in *Escherichia coli* (Romberg and Levin, 2003). If the RasG-regulated phosphorylation of *Dictyostelium* FtsZA is confirmed, it will suggest a RasG signaling pathway that regulates mitochondrial division.

Another potentially important protein exhibiting changes in phosphorylation in response to activated RasG is the phosphatidylinositol transfer protein 1 (PITP1). In mammalian cells, PITPs are involved in exocytosis of secretory granules, PLC-mediated hydrolysis of PtdIns(4,5)P_2, and the PI3K pathway (Cockcroft, 2001). In *Dictyostelium*, two PITPs, PITP1 and PITP2, have been identified and their ability to stimulate phosphoinositide synthesis has been documented (Swigart *et al.*, 2000). In other organisms, the phosphorylation of PITP has been reported (Snoek *et al.*, 1993; Monks *et al.*, 2001), but this is the first report of the potential phosphorylation of *Dictyostelium* PITP1. PITPs have been shown to enhance PtdIns(3,4,5)P_3 production in human neutrophils (Kular *et al.*, 1997).

cAMP stimulation of aggregating *Dictyostelium* cells has been shown to induce the release of protons and this release is blocked by the vacuolar H^+-ATPase inhibitor concanamycin A (Flaadt *et al.*, 2000). This process could be regulated by the phosphorylation of

vacuolar H^+-ATPase components such as VatA, and RasG may be involved in this regulation. However, definitive proof of the phosphorylation of VatA was not obtained, due to the difficulties encountered in trying to express VatA proteins and the fact that VatA appears to be essential (see Section 3.5.5). The antibody used to identify VatA was specific for the doubly phosphorylated TXY motif of human ERK1/2 (Pearson *et al.*, 2001) and it can be assumed that reactive proteins are also phosphorylated on this motif. VatA does contain a TXY motif at position 547-549 (with the start codon labeled amino acid position 1), which could be the site of putative phosphorylation.

A component of the vacuolar H+-ATPase complex is phosphorylated in another organism (Myers and Forgac, 1993), but this is the first report of a component of vacuolar H+-ATPase complex being phosphorylated in *Dictyostelium*. New functions continue to be discovered for the vacuolar H^+-ATPase complex apart from its ability to pump protons (Nishi and Forgac, 2002). For example, in mammalian cells the overexpression the VatE subunit causes altered actin distribution potentially through it involvement in a mSos1-dependent Rac1 signaling pathway (Miura *et al.*, 2001) and the 16-kDa proteolipid c subunit of the V_0 domain has been suggested to play a role in cell growth through ß1-intergrin binding (Skinner and Wildeman, 1999). If VatA proves to be phosphorylated, it will of interest to define the pathway leading from chemoattractant stimulation to VatA phosphorylation through RasG.

4.9 Emerging themes of the RasG signaling pathway(s) and future prospects

The phenotypes of cells overexpressing RasG(G12T) have been difficult to probe. For example, a striking alteration in these cells is an unusual shape suggestive of altered actin regulation (Zhang *et al.*, 1999; Weeks and Spiegelman, 2003). However, as many cell properties are tied to the cytoskeleton, it is difficult to segregate the effects of RasG on actin from its effects on other cellular components. The work presented was initiated to begin to disentangle this problem, by revealing changes in protein phosphorylation, which may have effects on various regulatory networks. The specific changes in phosphorylation described in this thesis provide a first step towards mapping out how signals from RasG penetrate the regulatory networks of the cell.

The variety of different proteins whose phosphorylation has been shown to respond to activated RasG is large but not surprising, since RasG is known to affect several independent

cellular processes (Zhang *et al.*, 1999; Secko *et al.*, 2001). It has been suggested the mammalian Ras protein, H-Ras, interacts with at least eight effector proteins to thereby potentially eight distinct signaling pathways, which each contain three to eight (known) signaling components (Campbell *et al.*, 1998). The work presented in this thesis suggests that RasG will be no different, and it is thus dangerous at this point to make generalizations. Nevertheless, a body of evidence indicates that there are at least three distinct endpoints of RasG signaling: the actin cytoskeleton, the transition from growth to development and the reception of chemotactic signals leading to cell motility. All three are important to growth and differentiation in *Dictyostelium*, as well as the growth and differentiation of other organisms, and it will be important to understand the role that RasG plays in their regulation. The further identification of proteins lying between RasG and these physiological functions are needed to define how these pathways are being controlled.

The approach described in this thesis can also be used as a first step in examining a peculiarity of *Dictyostelium,* in that this organism has more Ras subfamily proteins than *Drosophila* or *C. elegans* (Chubb and Insall, 2001). Thus, for example vegetative *Dictyostelium* cells contain a minimum of four Ras subfamily proteins (RasB, RasC, RasG and RasS) and each appears to have a specific function. One fundamental question is whether, and to what extent, their signaling pathways interact. Identification of protein phosphorylation changes in response to the overexpression of other Ras proteins should help to answer this question.

BIBLIOGRAPHY

Anderson, K. E., Coadwell, J., Stephens, L. R. and Hawkins, P. T. (1998) Translocation of PDK-1 to the plasma membrane is important in allowing PDK-1 to activate protein kinase B. *Curr Biol*, **8**, 684-91.

Aubry, L., Maeda, M., Insall, R., Devreotes, P. N. and Firtel, R. A. (1997) The *Dictyostelium* mitogen-activated protein kinase ERK2 is regulated by Ras and cAMP-dependent protein kinase (PKA) and mediates PKA function. *J Biol Chem*, **272**, 3883-6.

Aubry, L. and Firtel, R. A. (1998) Spalten, a protein containing Galpha-protein-like and PP2C domains, is essential for cell-type differentiation in *Dictyostelium*. *Genes Dev*, **12**, 1525-38.

Aubry, L. and Firtel, R. (1999) Integration of signaling networks that regulate *Dictyostelium* differentiation. *Annu Rev Cell Dev Biol*, **15**, 469-517.

Barbacid, M. (1987) *ras* genes. *Annu Rev Biochem*, **56**, 779-827.

Bellacosa, A., Chan, T. O., Ahmed, N. N., Datta, K., Malstrom, S., Stokoe, D., McCormick, F., Feng, J. and Tsichlis, P. (1998) Akt activation by growth factors is a multiple-step process: the role of the PH domain. *Oncogene*, **17**, 313-25.

Bernards, A. (2003) GAPs galore! A survey of putative Ras superfamily GTPase activating proteins in man and *Drosophila*. *Biochim Biophys Acta*, **1603**, 47-82.

Beug, H., Katz, F. E., Stein, A. and Gerisch, G. (1973) Quantitation of membrane sites in aggregating *Dictyostelium* cells by use of tritiated univalent antibody. *Proc Natl Acad Sci USA*, **70**, 3150-4.

Biggs, W. H., Meisenhelder, J., Hunter, T., Cavenee, W. K., Arden, K. C. (1999) Protein kinase B/Akt-mediated phosphorylation promotes nuclear exclusion of the winged helix transcription factor FKHR1. *Proc Natl Acad Sci USA*, **96**, 7421-6.

Blaauw, M., Linskens, M. H. and van Haastert P. J. (2000) Efficient control of gene expression by a tetracycline-dependent transactivator in single *Dictyostelium discoideum* cells. *Gene*, **252**, 71-82.

Blusch, J., Morandini, P. and Nellen, W. (1992) Transcriptional regulation by folate: inducible gene expression in *Dictyostelium* transformants during growth and development. *Nucleic Acids Res,* **20,** 6235-6238.

Blusch, J.H. and Nellen, W. (1994) Folate responsiveness during growth and development of *Dictyostelium* - separate but related pathways control chemotaxis and gene regulation. *Mol Microbiol*, **11**, 331-335.

Blusch, J., Alexander, S. and Nellen, W. (1995) Multiple signal transduction pathways regulate discoidin I gene expression in *Dictyostelium discoideum*. *Differentiation*, **58**, 253-60.

Boguski, M. S. and McCormick, F. (1993) Proteins regulating Ras and its relatives. *Nature*, **366**, 643-54.

Bokoch, G. M. (2003) Biology of the p21-activated kinases. *Annu Rev Biochem*, **72**, 743-81.

Boriack-Sjodin, P. A., Margarit, S. M., Bar-Sagi, D. and Kuriyan, J. (1998) The structural basis of the activation of Ras by Sos. *Nature*, **394**, 337-43.

Bos, J. L. (1989) ras oncogenes in human cancer: a review. *Cancer Res*, **49**, 4682-9.

Bourne, H. R., Sanders, D. A. and McCormick, F. (1991) The GTPase superfamily: conserved structure and molecular mechanism. *Nature*, **349**, 117-27.

Brar, S. K. and Siu, C. H. (1993) Characterization of the cell adhesion molecule gp24 in *Dictyostelium discoideum*. Mediation of cell-cell adhesion via a Ca(2+)-dependent mechanism. *J Biol Chem*, **268**, 24902-9.

Buczynski, G., Grove, B., Nomura, A., Kleve, M., Bush, J., Firtel, R. A. and Cardelli, J. (1997) Inactivation of two *Dictyostelium discoideum* genes, DdPIK1 and DdPIK2, encoding proteins related to mammalian phosphatidylinositide 3-kinases, results in defects in endocytosis, lysosome to postlysosome transport, and actin cytoskeleton organization. *J Cell Biol*, **136**, 1271-86.

Burdine, V. and Clarke, M. (1995) Genetic and physiologic modulation of the prestarvation response in *Dictyostelium discoideum*. *Mol Biol Cell*, **6**, 311-325.

Burki, E., Anjard, C., Scholder, J. C., Reymond, C. D. (1991) Isolation of two genes encoding putative protein kinases regulated during *Dictyostelium discoideum* development. *Gene*, **102**, 57-65.

Burridge K. and Wennerberg, K. (2004) Rho and Rac take center stage. *Cell*, **116**, 167-79.

Bush, J., Nolta, K., Rodriguez-Paris, J., Kaufmann, N., O'Halloran, T., Ruscetti, T., Temesvari, L., Steck, T., Cardelli, J. (1994) Rab4-like GTPase in *Dictyostelium* discoideum colocalizes with V-H(+)-ATPases in reticular membranes of the contractile vacuole complex and in lysosomes. *J Cell Sci*, **107**, 2801-12.

Campbell, P. M. and Der, C. J. (2004) Oncogenic Ras and its role in tumor cell invasion and metastasis. *Semin Cancer Biol*, **14**, 105-14.

Campbell, S. L., Khosravi-Far, R., Rossman, K. L, Clark, G.J. and Der, C. J. (1998) Increasing complexity of Ras signaling. *Oncogene*, **17**, 1395-413.

Carpenter, G. (2000) The EGF receptor: a nexus for trafficking and signaling. *Bioessays*, **22**, 697-707.

Carrascosa, J. M. and Wieland, O. H. (1985) Evidence that (a) serine specific protein kinase(s) different from protein kinase C is responsible for the insulin-stimulated actin phosphorylation by placental membrane. *FEBS Lett*, **201**, 81-6.

Chen, M. Y., Long, Y. and Devreotes, P. N. (1997) A novel cytosolic regulator, Pianissimo, is required for chemoattractant receptor and G protein-mediated activation of the 12 transmembrane domain adenylyl cyclase in *Dictyostelium*. *Genes Dev*, **11**, 3218-31.

Chen, C. F. and Katz, E. R. (2000) Mediation of cell-substratum adhesion by RasG in Dictyostelium. *J Cell Biochem*, **79**, 139-49.

Choi, A. H. and Siu, C. H. (1987) Filopodia are enriched in a cell cohesion molecule of Mr 80,000 and participate in cell-cell contact formation in *Dictyostelium discoideum*. *J Cell Biol*, **104**, 1375-87.

Chubb, J. R., Wilkins, A., Thomas, G. M. and Insall, R. H. (2000) The *Dictyostelium* RasS protein is required for macropinocytosis, phagocytosis and the control of cell movement. *J Cell Sci*, **113**, 709-19.

Chubb, J. R. and Insall, R. H. (2001) *Dictyostelium*: an ideal organism for genetic dissection of Ras signalling networks. *Biochim Biophys Acta*, **1525**, 262-71.

Chubb, J. R., Wilkins, A., Wessels, D. J., Soll, D. R. and Insall, R. H. (2002) Pseudopodium dynamics and rapid cell movement in *Dictyostelium* Ras pathway mutants. *Cell Motil Cytoskeleton*, **53**, 150-62.

Chung, C. Y., Reddy, T. B., Zhou, K. and Firtel, R. A. (1998) A novel, putative MEK kinase controls developmental timing and spatial patterning in *Dictyostelium* and is regulated by ubiquitin-mediated protein degradation. *Genes Dev*, **12**, 3564-78.

Chung, C. Y. and Firtel, R. A. (1999) PAKa, a putative PAK family member, is required for cytokinesis and the regulation of the cytoskeleton in *Dictyostelium discoideum* cells during chemotaxis. *J Cell Biol*, **147**, 559-76.

Chung, C. Y., Potikyan, G. and Firtel, R. A. (2001) Control of cell polarity and chemotaxis by Akt/PKB and PI3 kinase through the regulation of PAKa. *Mol Cell*, **7**, 937-47.

Clarke, M. and Gomer, R. H. (1995) PSF and CMF, autocrine factors that regulate gene expression during growth and early development of *Dictyostelium*. *Experientia*, **51**, 1124-34.

Clarke, M., Kohler, J., Arana, Q., Liu, T., Heuser, J. and Gerisch, G. (2002) Dynamics of the vacuolar H(+)-ATPase in the contractile vacuole complex and the endosomal pathway of *Dictyostelium* cells. *J Cell Sci*, **115**, 2893-905.

Coates, J. C. and Harwood, A. J. (2001) Cell-cell adhesion and signal transduction during *Dictyostelium* development. *J Cell Sci*, **114**, 4349-4358.

Cockcroft, S. (2001) Phosphatidylinositol transfer proteins couple lipid transport to phosphoinositide synthesis. *Semin Cell Dev Biol*, **12**, 183-91.

Cozier, G. E., Carlton, J., Bouyoucef, D. and Cullen, P. J. (2004) Membrane targeting by pleckstrin homology domains. *Curr Top Microbiol Immunol*, **282**, 49-88.

Cross, D. A., Alessi, D. R., Cohen, P., Andjelkovich, M. and Hemmings, B. A. (1995) Inhibition of glycogen synthase kinase-3 by insulin mediated by protein kinase B. *Nature*, **378**, 785-9.

Cullen, P. J. (2001) Ras effectors: buying shares in Ras plc. *Curr Biol*, **11**, R342-4.

Cullen, P. J. and Lockyer, P. J. (2002) Integration of calcium and Ras signalling. *Nat Rev Mol Cell Biol*, **3**, 339-48.

Datta, S. R., Dudek, H., Tao, X., Masters, S., Fu, H., Gotoh, Y. and Greenberg, M. E. (1997) Akt phosphorylation of BAD couples survival signals to the cell-intrinsic death machinery. *Cell*, **91**, 231-41.

Daniel, J., Spiegelman, G. B. and Weeks, G. (1995) *Dictyostelium ras* gene. In Guidebook to small GTPases, M. Zerial and L. A. Huber, eds. NY, Oxford University Press, pp. 100-104.

Der, C. J., Krontiris, T. G. and Cooper, G. M. (1982) Transforming genes of human bladder and lung carcinoma cell lines are homologous to the ras genes of Harvey and Kirsten sarcoma viruses. *Proc Natl Acad Sci USA*, **79**, 3637-40.

Desbarats, L., Brar, S. K. and Siu, C. H. (1994) Involvement of cell-cell adhesion in the expression of the cell cohesion molecule gp80 in *Dictyostelium discoideum*. *J Cell Sci*, **107**, 1705-12.

Devreotes, P. and Janetopoulos, C. (2003) Eukaryotic chemotaxis: distinctions between directional sensing and polarization. *J Biol Chem*, **278**, 20445-8.

Douville, E and Downward, J. (1997) EGF induced SOS phosphorylation in PC12 cells involves P90 RSK-2. *Oncogene*, **15**, 373-83.

Downward J. (1996) Control of Ras activation. *Cancer Surv*, **27**, 87-100.

Egan, S. E. and Weinberg, R. A. (1993) The pathway to signal achievement. *Nature*, **365**, 781-3.

Ehrhardt, A., Ehrhardt, G. R., Guo, X. and Schrader, J. W. (2002) Ras and relatives--job sharing and networking keep an old family together. Exp Hematol, **30**, 1089-106.

Eichinger, L. and Noegel, A. A. (2003) Crawling into a new era-the *Dictyostelium* genome project. *EMBO J*, **22**, 1941-6.

Flaadt, H., Schaloske, R. and Malchow, D. (2000) Mechanism of cAMP-induced H(+)-efflux of *Dictyostelium* cells: a role for fatty acids. *J Biosci*, **25**, 243-52.

Faix, J., Gerisch, G. and Noegel, A. A. (1992) Overexpression of the csA cell adhesion molecule under its own cAMP-regulated promoter impairs morphogenesis in *Dictyostelium*. *J Cell Sci*, **102**, 203-14.

Feig, L. A. (2003) Ral-GTPases: approaching their 15 minutes of fame. *Trends Cell Biol*, **13**, 419-25.

Ficarro, S. B., McCleland, M. L., Stukenberg, P. T., Burke, D. J., Ross, M. M., Shabanowitz, J., Hunt, D. F. and White, F. M. (2002) Phosphoproteome analysis by mass spectrometry and its application to *Saccharomyces cerevisiae*. *Nat Biotechnol*, **20**, 301-5.

Filippa, N., Sable, C. L., Hemmings, B. A. and Van Obberghen, E. (2000) Effect of phosphoinositide-dependent kinase 1 on protein kinase B translocation and its subsequent activation. *Mol Cell Biol*, **20**, 5712-21.

Finbow, M. E. and Harrison, M. A. (1997) The vacuolar H+-ATPase: a universal proton pump of eukaryotes. *Biochem J*, **324**, 697-712.

Firtel, R.A. and Chung, C.Y. (2000) The molecular genetics of chemotaxis: sensing and responding to chemoattractant gradients. *BioEssays*, **22**, 603-615.

Fok, A. K., Clarke, M., Ma, L. and Allen, R. D. (1993) Vacuolar H(+)-ATPase of *Dictyostelium discoideum*. A monoclonal antibody study. *J Cell Sci*, **106**, 1103-13.

Fresno Vara, J. A., Casado, E., de Castro, J., Cejas, P., Belda-Iniesta, C. and Gonzalez-Baron, M. (2004) PI3K/Akt signalling pathway and cancer. *Cancer Treat Rev*, **30**, 193-204.

Fukui, Y., De Lozanne, A. and Spudich, J. A. (1990) Structure and function of the cytoskeleton of a *Dictyostelium* myosin-defective mutant. *J Cell Biol*, **110**, 367-78.

Fukui, Y., Yumura, S. and Yumura-Kitanishi, T. (1987) Agar-overlay immuno- fluorescence: high resolution studies of cytoskeletal components and their changes during chemotaxis. *Methods Cell Biol*, **28**, 347-356.

Funamoto, S., Milan, K., Meili, R. and Firtel, R.A. (2001) Role of phosphatidylinositol 3' kinase and a downstream pleckstrin homology domain-containing protein in controlling chemotaxis in *Dictyostelium*. *J Cell Biol*, **153**, 795-809.

Funamoto, S., Meili, R., Lee, S., Parry, L. and Firtel, R. A. (2002) Spatial and temporal regulation of 3-phosphoinositides by PI 3-kinase and PTEN mediates chemotaxis. *Cell*, **109**, 611-23.

Furuhashi, K., Ishigami, M., Suzuki, M. and Titani, K. (1998) Dry stress-induced phosphorylation of *Physarum* actin. *Biochem Biophys Res Commun*, **242**, 653-8.

Gamper, M., Howard, P. K., Hunter, T. and Firtel, R. A. (1996) Multiple roles of the novel protein tyrosine phosphatase PTP3 during *Dictyostelium* growth and development. *Mol Cell Biol*, **16**, 2431-44.

Gaskins, C., Maeda, M. and Firtel, R. A. (1994) Identification and functional analysis of a developmentally regulated extracellular signal-regulated kinase gene in *Dictyostelium discoideum*. *Mol Cell Biol*, **14**, 6996-7012.

Gaudet, P. and Tsang, A. (1999) Regulation of the ribonucleotide reductase small subunit gene by DNA-damaging agents in *Dictyostelium discoideum*. *Nucleic Acids Res*, **27**, 3042-8.

Gaudet, P., MacWilliams, H. and Tsang, A. (2001) Inducible expression of exogenous genes in *Dictyostelium discoideum* using the ribonucleotide reductase promoter. *Nucleic Acids Res*, **29**, E5.

Genot, E. and Cantrell, D. A. (2000) Ras regulation and function in lymphocytes. *Curr Opin Immunol*, **12**, 289-94.

Gerisch, G. (1968) Cell aggregation and differentiation in *Dictyostelium*. *Curr Top Dev Biol*, **3**, 157-197.

Gerisch, G. (1980) Univalent antibody fragments as tools for the analysis of cell interactions in Dictyostelium. *Curr Top Dev Biol*, **14**, 243-70.

Gettemans, J., De Ville, Y., Vandekerckhove, J. and Waelkens, E. (1993) Purification and partial amino acid sequence of the actin-fragmin kinase from *Physarum polycephalum*. Eur J Biochem, **214**, 111-9.

Gettemans, J., De Ville, Y., Waelkens, E. and Vandekerckhove, J. (1995) The actin-binding properties of the *Physarum* actin-fragmin complex. Regulation by calcium, phospholipids, and phosphorylation. *J Biol Chem*, **270**, 2644-51.

Geyer, M. and Wittinghofer, A. (1997) GEFs, GAPs, GDIs and effectors: taking a closer (3D) look at the regulation of Ras-related GTP-binding proteins. *Curr Opin Struct Biol*, **7**, 786-92.

Gharahdaghi, F., Weinberg, C. R., Meagher, D. A., Imai, B. S. and Mische, S. M. (1999) Mass spectrometric identification of proteins from silver-stained polyacrylamide gel: a method for the removal of silver ions to enhance sensitivity. *Electrophoresis*, **20**, 601-5.

Gilson, P. R., Yu, X. C., Hereld, D., Barth, C., Savage, A., Kiefel, B. R., Lay, S., Fisher, P. R., Margolin, W. and Beech, P. L. (2003) Two *Dictyostelium* orthologs of the prokaryotic cell division protein FtsZ localize to mitochondria and are required for the maintenance of normal mitochondrial morphology. *Eukaryot Cell*, **2**, 1315-26.

Godovac-Zimmermann, J., Soskic, V., Poznanovic, S. and Brianza, F. (1999) Functional proteomics of signal transduction by membrane receptors. *Electrophoresis*, **20**, 952-61.

Gomer, R. H., Yuen, I. S. and Firtel, R. A. (1991) A secreted 80x10(3) Mr protein mediates sensing of cell density and the onset of development in *Dictyostelium*. *Development,* **112,** 269-278.

Gorg, A., Obermaier, C., Boguth, G., Harder, A., Scheibe, B., Wildgruber, R. and Weiss, W. (2000) The current state of two-dimensional electrophoresis with immobilized pH gradients. *Electrophoresis*, **21**, 1037-53.

Graves, P. R. and Haystead, T. A. (2002) Molecular biologist's guide to proteomics. *Microbiol Mol Biol Rev*, **66**, 39-63.

Gross, E., Goldberg, D. and Levitzki, A. (1992) Phosphorylation of the *S. cerevisiae* Cdc25 in response to glucose results in its dissociation from Ras. *Nature*, **360**, 762-5.

Guerin, N. A. and Larochelle, D. A. (2002) A user's guide to restriction enzyme-mediated integration in *Dictyostelium*. *J Muscle Res Cell Motil*, **23**, 597-604.

Hadwiger, J. A., Lee, S. and Firtel, R. A. (1994) The G alpha subunit G alpha 4 couples to pterin receptors and identifies a signaling pathway that is essential for multicellular development in *Dictyostelium*. *Proc Natl Acad Sci USA*, **91**, 10566-70.

Harvey, J. J. (1964) An unidentified virus which causes the rapid production of tumors in mice. *Nature*, **204**, 1104-1105.

Harwood, A. J., Plyte, S. E., Woodgett, J., Strutt, H. and Kay, R. R. (1995) Glycogen synthase kinase 3 regulates cell fate in *Dictyostelium*. *Cell*, **80**, 139-48.

Herrmann, C. (2003) Ras-effector interactions: after one decade. *Curr Opin Struct Biol*, **13**, 122-9.

Heuser, J., Zhu, Q. and Clarke, M. (1993) Proton pumps populate the contractile vacuoles of *Dictyostelium* amoebae. *J Cell Biol*, **121**, 1311-27.

Hofer, F., Fields, S., Schneider, C. and Martin, G. S. (1994) Activated Ras interacts with the Ral guanine nucleotide dissociation stimulator. *Proc Natl Acad Sci USA*, **91**, 11089-93.

Hood, L. (2003) Systems biology: integrating technology, biology, and computation. *Mech Ageing Dev*, **124**, 9-16.

Howard, P. K., Sefton, B. M. and Firtel, R. A. (1992) Analysis of a spatially regulated phosphotyrosine phosphatase identifies tyrosine phosphorylation as a key regulatory pathway in *Dictyostelium*. *Cell*, **71**, 637-47.

Howard, P. K., Sefton, B. M. and Firtel, R. A. (1993) Tyrosine phosphorylation of actin in *Dictyostelium* associated with cell-shape changes. *Science*, **259**, 241-4.

Howard, P. K., Gamper, M., Hunter, T. and Firtel, R. A. (1994) Regulation by protein-tyrosine phosphatase PTP2 is distinct from that by PTP1 during *Dictyostelium* growth and development. *Mol Cell Biol*, **14**, 5154-64.

Huang, Y. E., Iijima, M., Parent, C. A., Funamoto, S., Firtel, R. A. and Devreotes, P. (2003) Receptor-mediated regulation of PI3Ks confines PI(3,4,5)P3 to the leading edge of chemotaxing cells. *Mol Biol Cell*, **14**, 1913-22.

Hughes, P. E., Renshaw, M. W., Pfaff, M., Forsyth, J., Keivens, V. M., Schwartz, M. A. and Ginsberg, M. H. (1997) Suppression of integrin activation: a novel function of a Ras/Raf-initiated MAP kinase pathway. *Cell*, **88**, 521-30.

Hunter, T. (2000) Signaling--2000 and beyond. *Cell*, **100**, 113-27.

Iijima, M. and Devreotes, P. (2002) Tumor suppressor PTEN mediates sensing of chemoattractant gradients. *Cell*, **109**, 599-610.

Insall, R., Kuspa, A., Lilly, P. J., Shaulsky, G., Levin, L. R., Loomis, W. F., Devreotes, P. (1994) CRAC, a cytosolic protein containing a pleckstrin homology domain, is required for receptor and G protein-mediated activation of adenylyl cyclase in *Dictyostelium*. *J Cell Biol*, **126**, 1537-45.

Insall, R. H., Borleis, J. and Devreotes, P. N. (1996) The aimless RasGEF is required for processing of chemotactic signals through G-protein-coupled receptors in *Dictyostelium*. *Curr Biol*, **6**, 719-29.

Insall, R., Muller-Taubenberger, A., Machesky, L., Kohler, J., Simmeth, E., Atkinson, S. J., Weber, I. and Gerisch, G. (2001) Dynamics of the *Dictyostelium* Arp2/3 complex in endocytosis, cytokinesis, and chemotaxis. *Cell Motil Cytoskeleton*, **50**, 115-28.

Jaffer, Z. M., Khosla, M., Spiegelman, G. B. and Weeks, G. (2001) Expression of activated Ras during *Dictyostelium* development alters cell localization and changes cell fate. *Development*, **128**, 907-16.

Jain, R., Yuen, I. S., Taphouse, C. R. and Gomer, R. H. (1992) A density-sensing factor controls development in *Dictyostelium*. *Genes Dev*, **6**, 390-400.

Jamora, C. and Fuchs, E. (2002) Intercellular adhesion, signalling and the cytoskeleton. *Nat Cell Biol*, **4**, E101-8.

Johnson, L., Greenbaum, D., Cichowski, K., Mercer, K., Murphy, E., Schmitt, E., Bronson, R. T., Umanoff, H., Edelmann, W., Kucherlapati, R. and Jacks, T. (1997) K-ras is an essential gene in the mouse with partial functional overlap with N-ras. *Genes Dev*, **11**, 2468-2481.

Jungbluth, A., von Arnim, V., Biegelmann, E., Humbel, B., Schweiger, A. and Gerisch, G. (1994) Strong increase in the tyrosine phosphorylation of actin upon inhibition of oxidative phosphorylation: correlation with reversible rearrangements in the actin skeleton of *Dictyostelium* cells. *J Cell Sci*, **107**,117-25.

Jungbluth, A., Eckerskorn, C., Gerisch, G., Lottspeich, F., Stocker, S. and Schweiger, A. (1995) Stress-induced tyrosine phosphorylation of actin in *Dictyostelium* cells and localization of the phosphorylation site to tyrosine-53 adjacent to the DNase I binding loop. *FEBS Lett*, **375**, 87-90.

Kang, R., Kae, H., Ip, H., Spiegelman, G. B. and Weeks, G. (2002) Evidence for a role for the *Dictyostelium* Rap1 in cell viability and the response to osmotic stress. *J Cell Sci*, **115**, 3675-82.

Katso, R., Okkenhaug, K., Ahmadi, K., White, S., Timms, J. and Waterfield, M. D. (2001) Cellular function of phosphoinositide 3-kinases: implications for development, homeostasis, and cancer. *Annu Rev Cell Dev Biol*, **17**, 615-75.

Kawata, T., Shevchenko, A., Fukuzawa, M., Jermyn, K. A., Totty, N. F., Zhukovskaya, N. V., Sterling, A. E., Mann, M. and Williams, J. G. (1997) SH2 signaling in a lower eukaryote: a STAT protein that regulates stalk cell differentiation in *Dictyostelium*. *Cell*, **89**, 909-16.

Kay, R. R., Flatman, P., Thompson, C. R. (1999) DIF signalling and cell fate. *Semin Cell Dev Biol*, **10**, 577-85.

Kessin, R. H. (2001) *Dictyostelium* – Evolution, cell biology, and the development of multicellularity. Cambridge, UK, Cambridge University Press.

Kae, H., Lim, C. J., Spiegelman, G. B. and Weeks, G. (2004) Chemoattractant induced Ras activation during *Dictyostelium* aggregation. *EMBO Reports*, in press.

Khosla, M., Robbins, S. M., Spiegelman, G. B. and Weeks, G. (1990) Regulation of DdrasG gene expression during *Dictyostelium* development. *Mol Cell Biol*, **10**, 918-22.

Khosla, M., Spiegelman, G. B., Weeks, G., Sands, T. W., Virdy, K. J., Cotter, D. A. (1994) RasG protein accumulation occurs just prior to amoebae emergence during spore germination in *Dictyostelium discoideum*. *FEMS Microbiol Lett*, **117**, 293-8.

Khosla, M., Spiegelman, G.B. and Weeks, G. (1996) Overexpression of an activated rasG gene during growth blocks the initiation of *Dictyostelium* development. *Mol Cell Biol*, **16**, 4156-4162.

Khosla, M., Spiegelman, G. B., Insall, R. and Weeks, G. (2000) Functional overlap of the *Dictyostelium* RasG, RasD and RasB proteins. *J Cell Sci*, **113**, 1427-34.

Kim, L., Liu, J. and Kimmel, A. R. (1999) The novel tyrosine kinase ZAK1 activates GSK3 to direct cell fate specification. *Cell*, **99**, 399-408.

King, J. and Insall, R. H. (2004) Parasexual genetics of *Dictyostelium* gene disruptions: identification of a ras pathway using diploids. *BMC Genet*, **4**, 12.

Kirsten, W. H. and Mayer, L. A. (1967) Morphologic responses to a murine erythroblastosis virus. *J Natl Cancer Inst*, **39**, 311-335.

Knecht, D. A., Fuller, D. L. and Loomis, W. F. (1987) Surface glycoprotein, gp24, involved in early adhesion of *Dictyostelium discoideum*. *Dev Biol*, **121**, 277-283.

Kobe, B. and Kajava, A. V. (2001) The leucine-rich repeat as a protein recognition motif. *Curr Opin Struct Biol*, **11**, 725-32.

Kosaka, C. and Pears, C. J. (1997) Chemoattractants induce tyrosine phosphorylation of ERK2 in *Dictyostelium discoideum* by diverse signalling pathways. *Biochem J*, **324**, 347-52.

Kosaka, C., Khosla, M., Weeks, G. and Pears, C. (1998) Negative influence of RasG on chemoattractant-induced ERK2 phosphorylation in *Dictyostelium*. *Biochim Biophys Acta*, **1402**, 1-5.

Kular, G., Loubtchenkov, M., Swigart, P., Whatmore, J., Ball, A., Cockcroft, S. and Wetzker, R. (1997) Co-operation of phosphatidylinositol transfer protein with phosphoinositide 3-kinase gamma in the formylmethionyl-leucylphenylalanine-dependent production of phosphatidylinositol 3,4,5-trisphosphate in human neutrophils. *Biochem J*, **325**, 299-301.

Kuwayama, H., Ishida, S. and Van Haastert, P. J. (1993) Non-chemotactic *Dictyostelium discoideum* mutants with altered cGMP signal transduction. *J Cell Biol*, **123**, 1453-62.

Laemmli, U. K. (1970) Cleavage of structural proteins during assembly of the head of the bacteriophage T4. *Nature*, **227**, 592-596.

Lam, T. Y., Pickering, G., Geltosky, J. and Siu, C. H. (1981) Differential cell cohesiveness expressed by prespore and prestalk cells of *Dictyostelium discoideum*. *Differentiation,* **20**, 22-28.

Larochelle, D. A., Vithalani, K. K. and De Lozanne, A. (1996) A novel member of the rho family of small GTP-binding proteins is specifically required for cytokinesis. *J Cell Biol*, **133**, 1321-9.

Lee, S., Parent, C. A., Insall, R. and Firtel, R. A. (1999) A novel Ras-interacting protein required for chemotaxis and cyclic adenosine monophosphate signal relay in *Dictyostelium*. *Mol Biol Cell*, **10**, 2829-45.

Lewis, T. S., Hunt, J. B., Aveline, L. D., Jonscher, K. R., Louie, D. F., Yeh, J. M., Nahreini, T. S., Resing, K. A. and Ahn, N. G. (2000) Identification of novel MAP kinase pathway signaling targets by functional proteomics and mass spectrometry. *Mol Cell*, **6**, 1343-54.

Li, W., Han, M. and Guan, K. L. (2000) The leucine-rich repeat protein SUR-8 enhances MAP kinase activation and forms a complex with Ras and Raf. *Genes Dev*, **14**, 895-900.

Lickert, H., Bauer, A., Kemler, R., and Stappert, J. (2000) Casein Kinase II Phosphorylation of E-cadherin Increases E-cadherin/ß-Catenin Interaction and Strengthens Cell-Cell Adhesion. *J Biol Chem*, **275**, 5090-5095.

Lilien, J., Balsamo, J., Arregui, C. and Xu G. (2002) Turn-off, drop-out: functional state switching of cadherins. *Dev Dyn*, **224**, 18-29.

Lim, C. J., Spiegelman, G. B and Weeks, G. (2001) RasC is required for optimal activation of adenylyl cyclase and Akt/PKB during aggregation. *EMBO J*, **20**, 4490-9.

Lim, C. J. (2002) The *ras* subfamily protein, RasC, is required for the aggregation of *Dictyostelium discoideum. Ph.D. Thesis, University of British Columbia.*

Lim, C. J., Spiegelman, G. B. and Weeks, G. (2003) Roles of the *Dictyostelium* Ras subfamily proteins in regulating vegetative and differentiating cell function. In "Recent Research Developments in Cell Research" (ed A. Gayathri), *Recent Devel Cell Res*, **1**, 131-143.

Liu, T., Williams, J. G. and Clarke, M. (1992) Inducible expression of calmodulin antisense RNA in *Dictyostelium* cells inhibits the completion of cytokinesis. *Mol Biol Cell*, **3**, 1403-13.

Liu, T., Mirschberger, C., Chooback, L., Arana, Q., Dal Sacco, Z., MacWilliams, H. and Clarke, M. (2002) Altered expression of the 100 kDa subunit of the *Dictyostelium* vacuolar proton pump impairs enzyme assembly, endocytic function and cytosolic pH regulation. *J Cell Sci*, **115**, 1907-18.

Loomis, W. F. (1998) Role of PKA in the timing of developmental events in *Dictyostelium* cells. *Microbiol Mol Biol Rev*, **62**, 684-94.

Louis, S. A., Spiegelman, G. B. and Weeks, G. (1997) Expression of an activated rasD gene changes cell fate decisions during *Dictyostelium* development. *Mol Biol Cell*, **8**, 303-12.

Ma, H., Gamper, M., Parent, C. and Firtel, R. A. (1997) The *Dictyostelium* MAP kinase kinase DdMEK1 regulates chemotaxis and is essential for chemoattractant-mediated activation of guanylyl cyclase. *EMBO J*, **16**, 4317-32.

Maeda, M., Aubry, L., Insall, R., Gaskins, C., Devreotes, P. N. and Firtel, R. A. (1996) Seven helix chemoattractant receptors transiently stimulate mitogen-activated protein kinase in *Dictyostelium*. Role of heterotrimeric G proteins. *J Biol Chem*, **271**, 3351-4.

Maeda, M. and Firtel, R. A. (1997) Activation of the mitogen-activated protein kinase ERK2 by the chemoattractant folic acid in *Dictyostelium. J Biol Chem*, **272**, 23690-5.

Malumbres, M. and Barbacid, M. (2003) RAS oncogenes: the first 30 years. *Nature Rev Cancer*, **3**, 7-13.

Mann, S. K., Yonemoto, W. M., Taylor, S. S. and Firtel, R. A. (1992) DdPK3, which plays essential roles during *Dictyostelium* development, encodes the catalytic subunit of cAMP-dependent protein kinase. *Proc Natl Acad Sci USA*, **89**, 10701-5.

Marinissen, M. J. and Gutkind, J. S. (2001) G-protein-coupled receptors and signaling networks: emerging paradigms. *Trends Pharmacol Sci*, **22**, 368-76.

Marshall, C. J. (1996) Ras effectors. *Curr Opin Cell Biol,* **8**, 197-204.

Meier, R., Alessi, D. R., Cron, P., Andjelkovic, M. and Hemmings, B. A. (1997) Mitogenic activation, phosphorylation, and nuclear translocation of protein kinase Bbeta. *J Biol Chem*, **272**, 30491-7.

Meili, R., Ellsworth, C., Lee, S., Reddy, T. B., Ma, H. and Firtel, R. A. (1999) Chemoattractant-mediated transient activation and membrane localization of Akt/PKB is required for efficient chemotaxis to cAMP in *Dictyostelium*. *EMBO J*, **18**, 2092-105.

Meili, R., Ellsworth, C. and Firtel, R. A. (2000) A novel Akt/PKB-related kinase is essential for morphogenesis in *Dictyostelium*. *Curr Biol*, **10**, 708-17.

Milburn, M. V., Tong, L., deVos, A. M., Brunger, A., Yamaizumi, Z., Nishimura, S. and Kim, S. H. (1990) Molecular switch for signal transduction: structural differences between active and inactive forms of protooncogenic Ras proteins. *Science*, **247**, 939-45.

Miura, K., Miyazawa, S., Furuta, S., Mitsushita, J., Kamijo, K., Ishida, H., Miki, T., Suzukawa, K., Resau, J., Copeland, T. D. and Kamata T. (2001) The Sos1-Rac1 signaling. Possible involvement of a vacuolar H(+)-ATPase E subunit. *J Biol Chem*, **276**, 46276-83.

Moniakis, J., Funamoto, S., Fukuzawa, M., Meisenhelder, J., Araki, T., Abe, T., Meili, R., Hunter, T., Williams, J. and Firtel, R.A. (2001) An SH2-domain-containing kinase negatively regulates the phosphatidylinositol-3 kinase pathway. *Genes Dev*, **15**, 687-698.

Monks, D. E., Aghoram, K., Courtney, P. D., DeWald, D. B. and Dewey, R. E. (2001) Hyperosmotic stress induces the rapid phosphorylation of a soybean phosphatidylinositol transfer protein homolog through activation of the protein kinases SPK1 and SPK2. *Plant Cell*, **13**, 1205-19.

Morrison, D. K. and Cutler, R. E. (1997) The complexity of Raf-1 regulation. *Curr Opin Cell Biol*, **9**, 174-9.

Myers, M. and Forgac, M. (1993) The coated vesicle vacuolar (H+)-ATPase associates with and is phosphorylated by the 50-kDa polypeptide of the clathrin assembly protein AP-2. *J Biol Chem*, **268**, 9184-6.

Nebl, T., Kotsifas, M., Schaap, P. and Fisher, P. R. (2002) Multiple signalling pathways connect chemoattractant receptors and calcium channels in *Dictyostelium*. *J Muscle Res Cell Motil*, **23**, 853-65.

Nellen, W., Datta, S., Reymond, C., Sivertsen, A., Mann, S., Crowley, T. and Firtel, R. A. (1987) Molecular biology in *Dictyostelium*: tools and applications. *Methods Cell Biol*, **28**, 67-100.

Nelson, W. J. and Nusse, R. (2004) Convergence of Wnt, beta-catenin, and cadherin pathways. *Science*, **303**, 1483-7.

Nishi, T. and Forgac, M. (2002) The vacuolar (H+)-ATPases--nature's most versatile proton pumps. *Nat Rev Mol Cell Biol*, **3**, 94-103.

Nolta, K. V. and Steck, T. L. (1994) Isolation and initial characterization of the bipartite contractile vacuole complex from *Dictyostelium discoideum*. *J Biol Chem*, **269**, 2225-33.

Nolta, K. V., Padh, H., Steck, T. L. (1993) An immunocytochemical analysis of the vacuolar proton pump in *Dictyostelium discoideum*. *J Cell Sci*, **105**, 849-59.

Oda, Y., Nagasu, T. and Chait, B. T. (2001) Enrichment analysis of phosphorylated proteins as a tool for probing the phosphoproteome. *Nat Biotechnol*, **19**, 379-382.

Palmieri, S. J., Nebl, T., Pope, R. K., Seastone, D. J., Lee, E., Hinchcliffe, E. H., Sluder, G., Knecht, D., Cardelli, J. and Luna, E. J. (2000) Mutant Rac1B expression in *Dictyostelium*: effects on morphology, growth, endocytosis, development, and the actin cytoskeleton. *Cell Motil Cytoskeleton*, **46**, 285-304.

Pandey, A., Podtelejnikov, A. V., Blagoev, B., Bustelo, X. R., Mann, M. and Lodish, H. F. (2000) Analysis of receptor signaling pathways by mass spectrometry: identification of vav-2 as a substrate of the epidermal and platelet-derived growth factor receptors. *Proc Natl Acad Sci USA*, **97**, 179-84.

Papakonstanti, E. A. and Stournaras, C. (2002) Association of PI-3 kinase with PAK1 leads to actin phosphorylation and cytoskeletal reorganization. *Mol Biol Cell*, **13**, 2946-62.

Parent, C.A. and Devreotes, P.N. (1996) Molecular genetics of signal transduction in *Dictyostelium*. *Annu Rev Biochem*, **65**, 411-440.

Parent, C.A., Blacklock, B.J., Froehlich, W.M., Murphy, D.B. and Devreotes, P.N. (1998) G protein signaling events are activated at the leading edge of chemotactic cells. *Cell*, **95**, 81-91.

Pawson, T. and Schlessinger, J. (1993) SH2 and SH3 domains. *Curr Biol*, **3**, 434-442.

Pawson, T. and Scott, J. D. (1997) Signaling through scaffold, anchoring, and adaptor proteins. *Science*, **278**, 2075-80.

Pearson, G., Robinson, F., Beers-Gibson, T., Xu, B. E., Karandikar, M., Berman, K. and Cobb, M. H. (2001) Mitogen-activated protein (MAP) kinase pathways: regulation and physiological functions. *Endocr Rev*, **22**, 153-83.

Perkins, D. N., Pappin, D. J., Creasy, D. M. and Cottrell, J. S. (1999) Probability-based protein identification by searching sequence databases using mass spectrometry data. *Electrophoresis*, **20**, 3551-67.

Persad, S., Attwell, S., Gray, V., Mawji, N., Deng, J. T., Leung, D., Yan, J., Sanghera, J., Walsh, M. P. and Dedhar, S. (2001) Regulation of protein kinase B/Akt-serine 473 phosphorylation by integrin-linked kinase: critical roles for kinase activity and amino acids arginine 211 and serine 343. *J Biol Chem*, **276**, 27462-9.

Perucho, M., Goldfarb, M., Shimizu, K., Lama, C., Fogh, J. and Wigler, M. (1981) Human-tumor-derived cell lines contain common and different transforming genes. *Cell*, **27**, 467-76.

Peterson, S. N., Trabalzini, L., Brtva, T. R., Fischer, T., Altschuler, D. L., Martelli, P., Lapetina, E. G., Der, C. J. and White, G. C. (1996) Identification of a novel RalGDS-related protein as a candidate effector for Ras and Rap1. *J Biol Chem*, **271**, 29903-8.

Plyte, S. E., O'Donovan, E., Woodgett, J. R. and Harwood, A. J. (1999) Glycogen synthase kinase-3 (GSK-3) is regulated during *Dictyostelium* development via the serpentine receptor cAR3. *Development*, **126**, 325-33.

Primpke, G., Iassonidou, V., Nellen, W. and Wetterauer, B. (2000) Role of cAMP-dependent protein kinase during growth and early development of *Dictyostelium discoideum*. *Dev Biol*, **221**, 101-11.

Pruitt, K and Channing D. J. (2001) Ras and Rho regulation of the cell cycle and oncogenesis. *Cancer Lett*, **171**, 1-10.

Rathi, A., Kayman, S. C. and Clarke, M. (1991) Induction of gene expression in *Dictyostelium* by prestarvation factor, a factor secreted by growing cells. *Dev Genet*, **12,** 82-87.

Rathi, A. and Clarke, M. (1992) Expression of early developmental genes in *Dictyostelium discoideum* is initiated during exponential growth by an autocrine- dependent mechanism. *Mech Dev,* **36,** 173-182.

Rebhun, J. F., Castro, A. F. and Quilliam, L. A. (2000) Identification of guanine nucleotide exchange factors (GEFs) for the Rap1 GTPase. Regulation of MR-GEF by M-Ras-GTP interaction. *J Biol Chem*, **275**, 34901-8.

Rebstein, P. J., Weeks, G. and Spiegelman, G. B. (1993) Altered morphology of vegetative amoebae induced by increased expression of the *Dictyostelium discoideum* ras-related gene rap1. *Dev Genet*, **14**, 347-55.

Reymond, C. D., Gomer, R. H., Nellen, W., Theibert, A., Devreotes, P. and Firtel, R. A. (1986) Phenotypic changes induced by a mutated ras gene during the development of *Dictyostelium* transformants. *Nature*, **323**, 340-3.

Rivero, F., Dislich, H., Glockner, G. and Noegel, A. A. (2001) The *Dictyostelium discoideum* family of Rho-related proteins. *Nucleic Acids Res*, **29**, 1068-79.

Robbins, S. M., Williams, J. G., Jermyn, K. A., Spiegelman, G. B. and Weeks G. (1989) Growing and developing *Dictyostelium* cells express different ras genes. *Proc Natl Acad Sci USA*, **86**, 938-42.

Rodriguez-Viciana, P., Warne, P. H., Khwaja, A., Marte, B. M., Pappin, D., Das, P., Waterfield, M. D., Ridley, A. and Downward, J. (1997) Role of phosphoinositide 3-OH kinase in cell transformation and control of the actin cytoskeleton by Ras. *Cell*, **3**, 457-67.

Romberg, L. and Levin, P. A. (2003) Assembly dynamics of the bacterial cell division protein FTSZ: poised at the edge of stability. *Annu Rev Microbiol*, **57**, 125-54.

Russell, M., Lange-Carter, C. A. and Johnson, G. L. (1995) Direct interaction between Ras and the kinase domain of mitogen-activated protein kinase kinase kinase (MEKK1). *J Biol Chem*, **270**, 11757-60.

Sambrook, J., Fritsch, E. F. and Maniatis, T. (1989) Molecular cloning—A laboratory manual 2 ed. Cold spring harbor, Cold spring harbor laboratory press.

Saran, S., Meima, M. E., Alvarez-Curto, E., Weening, K. E., Rozen, D. E. and Schaap, P. (2002) cAMP signaling in *Dictyostelium*. Complexity of cAMP synthesis, degradation and detection. *J Muscle Res Cell Motil*, 23, 793-802.

Schlessinger, J. (2000) Cell signaling by receptor tyrosine kinases. *Cell*, **103**, 211-25.

Schweiger, A., Mihalache, O., Ecke, M. and Gerisch, G. (1992) Stage-specific tyrosine phosphorylation of actin in *Dictyostelium discoideum* cells. *J Cell Sci*, **102**, 601-9.

Schulkes, C. and Schaap, P. (1995) cAMP-dependent protein kinase activity is essential for preaggregative gene expression in *Dictyostelium*. *FEBS Lett*, **368**, 381-4.

Scolnick, E. M., Rands, E., Williams, D. and Parks, W. P. (1973) Studies on the nucleic acid sequences of Kristen sarcoma virus: a model for formation of a mammalian RNA-containing sarcoma virus. *J Virol*, **12**, 458-463.

Secko, D. M., Khosla, M., Gaudet, P., Tsang, A., Spiegelman, G.B. and Weeks, G. (2001) RasG regulates discoidin gene expression during *Dictyostelium* growth. *Exp Cell Res*, **266**, 135-141.

Secko, D. M., Insall, R. H., Spiegelman, G.B. and Weeks, G. (2004) The identification of *Dictyostelium* phosphoproteins altered in response to the activation of RasG. *Proteomics*, in press.

Seddighzadeh, M., Linder, S., Shoshan, M. C., Auer, G. and Alaiya, A. A. (2000) Inhibition of extracellular signal-regulated kinase 1/2 activity of the breast cancer cell line MDA-MB-231 leads to major alterations in the pattern of protein expression. *Electrophoresis*, **21**, 2737-43.

Segall, J. E., Kuspa, A., Shaulsky, G., Ecke, M., Maeda, M., Gaskins, C., Firtel, R. A. and Loomis, W. F. (1995) A MAP kinase necessary for receptor-mediated activation of adenylyl cyclase in *Dictyostelium*. *J Cell Biol*, **128**, 405-13.

Sesaki, H. and Siu, C. H. (1996) Novel redistribution of the Ca(2+)-dependent cell adhesion molecule DdCAD-1 during development of *Dictyostelium discoideum*. *Dev Biol*, **177**, 504-16.

Sesaki, H., Wong, E. F. and Siu, C. H. (1997) The cell adhesion molecule DdCAD-1 in *Dictyostelium* is targeted to the cell surface by a nonclassical transport pathway involving contractile vacuoles. *J Cell Biol*, **138**, 939-51.

Shaulsky, G., Fuller, D. and Loomis, W. F. (1998) A cAMP-phosphodiesterase controls PKA-dependent differentiation. *Development*, **125**, 691-9.

Shevchenko, A., Wilm, M., Vorm, O. and Mann, M. (1996) Mass spectrometric sequencing of proteins silver-stained polyacrylamide gels. *Anal Chem*, **68**, 850-8.

Shields, J. M., Pruitt K., McFall, A., Shaub, A. and Der C. J. (2000) Understanding Ras: 'it ain't over 'til it's over'. *Trends Cell Biol*, **10**, 147-154.

Shih, C., Shilo, B. Z., Goldfarb, M. P., Dannenberg, A. and Weinberg, R. A. (1979) Passage of phenotypes of chemically transformed cells via transfection of DNA and chromatin. *Proc Natl Acad Sci USA*, **76**, 5714-5718.

Shou, W., Verma, R., Annan, R. S., Huddleston, M. J., Chen, S. L., Carr, S. A. and Deshaies, R. J. (2002) Mapping phosphorylation sites in proteins by mass spectrometry. *Methods Enzymol*, **351**, 279-96.

Sieburth, D. S., Sun, Q. and Han, M. (1998) SUR-8, a conserved Ras-binding protein with leucine-rich repeats, positively regulates Ras-mediated signaling in *C. elegans*. *Cell*, **94**, 119-30.

Simon, M. N., Pelegrini, O., Veron, M. and Kay, R. R. (1992) Mutation of protein kinase A causes heterochronic development of *Dictyostelium*. *Nature*, **356**, 171-2.

Sini, P., Cannas, A., Koleske, A. J., Di Fiore, P. P., Scita, G. (2004) Abl-dependent tyrosine phosphorylation of Sos-1 mediates growth-factor-induced Rac activation. *Nat Cell Biol*, **6**, 268-74.

Skinner, M. A. and Wildeman, A. G. (1999) beta(1) integrin binds the 16-kDa subunit of vacuolar H(+)-ATPase at a site important for human papillomavirus E5 and platelet-derived growth factor signaling. *J Biol Chem*, **274**, 23119-27.

Snoek, G. T., Westerman, J., Wouters, F. S. and Wirtz, K. W. (1993) Phosphorylation and redistribution of the phosphatidylinositol-transfer protein in phorbol 12-myristate 13-acetate- and bombesin-stimulated Swiss mouse 3T3 fibroblasts. *Biochem J*, **291**, 649-56.

Sobko, A., Ma, H. and Firtel, R. A. (2002) Regulated SUMOylation and ubiquitination of DdMEK1 is required for proper chemotaxis. *Dev Cell*, **2**, 745-56.

Sorensen, B. K., Hojrup, P., Ostergard, E., Jorgensen, C. S., Enghild, J., Ryder, L. R. and Houen, G. (2002) Silver staining of proteins on electroblotting membranes and intensification of silver staining of proteins separated by polyacrylamide gel electrophoresis. *Anal Biochem*, **304**, 33-41.

Soskic, V., Gorlach, M., Poznanovic, S., Boehmer, F. D. and Godovac-Zimmermann, J. (1999) Functional proteomics analysis of signal transduction pathways of the platelet-derived growth factor beta receptor. *Biochemistry*, **38**, 1757-64.

Souza, G. M., Lu, S. and Kuspa, A. (1998) YakA, a protein kinase required for the transition from growth to development in *Dictyostelium*. *Development*, **125**, 2291-302.

Souza, G. M., da Silva, A. M. and Kuspa, A. (1999) Starvation promotes *Dictyostelium* development by relieving PufA inhibition of PKA translation through the YakA kinase pathway. *Development*, **126**, 3263-74.

Sternberg, P. W. and Han, M. (1998) Genetics of RAS signaling in *C. elegans*. *Trends Genet*, **14**, 466-72.

Sutherland, B. W. (2001a) Investigation of the function of the *Dictyostelium discoideum* RasB protein, *Ph.D. Thesis, University of British Columbia*.

Sutherland, B. W., Spiegelman, G. B. and Weeks, G. (2001b) A Ras subfamily GTPase shows cell cycle-dependent nuclear localization. *EMBO Rep*, **2**, 1024-8.

Swigart, P., Insall, R., Wilkins, A. and Cockcroft, S. (2000) Purification and cloning of phosphatidylinositol transfer proteins from *Dictyostelium discoideum*: homologues of both mammalian PITPs and Saccharomyces cerevisiae sec14p are found in the same cell. *Biochem J*, **347**, 837-43.

Takai, Y., Sasaki, T. and Matozaki, T. (2001) Small GTP-binding proteins. *Physiol Rev*, **81**, 153-208.

Tall, G. G., Barbieri, M. A., Stahl, P. D. and Horazdovsky, B. F. (2001) Ras-activated endocytosis is mediated by the Rab5 guanine nucleotide exchange activity of RIN1. *Dev Cell*, **1**, 73-82.

Thomason, P. A., Traynor, D., Cavet, G., Chang, W. T., Harwood, A. J. and Kay R. R. (1998) An intersection of the cAMP/PKA and two-component signal transduction systems in *Dictyostelium*. *EMBO J*, **17**, 2838-45.

Thomason, P., Traynor, D. and Kay, R. (1999) Taking the plunge. Terminal differentiation in *Dictyostelium*. *Trends Genet*, **15**, 15-9.

Towbin, H., Staehelin, T. and Gordon, J. (1979) Electrophoretic transfer of proteins from polyacrylamide gels to nitrocellulose sheets: procedure and some applications. *Proc Natl Acad Sci USA*, **76**, 4350-4.

Tuxworth, R. I., Cheetham, J. L., Machesky, L. M., Spiegelmann, G. B., Weeks, G. and Insall, R. H. (1997) *Dictyostelium* RasG is required for normal motility and cytokinesis, but not growth. *J Cell Biol,* **138,** 605-614.

Vanhaesebroeck, B. and Alessi, D. R. (2000) The PI3K-PDK1 connection: more than just a road to PKB. *Biochem J*, **346**, 561-76.

van Delft, S., Verkleij, A. J., Boonstra, J. and van Bergen en Henegouwen, P. M. (1995) Epidermal growth factor induces serine phosphorylation of actin. *FEBS Lett*, **357**, 251-4.

van Es, S., Weening, K. E. and Devreotes, P. N. (2001) The protein kinase YakA regulates g-protein-linked signaling responses during growth and development of *Dictyostelium. J Biol Chem*, **276**, 30761-5.

Vercoutter-Edouart, A. S., Czeszak, X., Crepin, M., Lemoine, J., Boilly, B., Le Bourhis, X., Peyrat, J. P. and Hondermarck, H. (2001) Proteomic detection of changes in protein synthesis induced by fibroblast growth factor-2 in MCF-7 human breast cancer cells. *Exp Cell Res*, **262**, 59-68.

Vojtek, A. B., Hollenberg, S.M. and Cooper, J. A. (1993) Mammalian Ras interacts directly with the serine/threonine kinase Raf. *Cell*, **74**, 205-14.

Wang, J., Hou, L., Awrey, D., Loomis, W. F., Firtel, R. A. and Siu, C. H. (2000) The membrane glycoprotein gp150 is encoded by the lagC gene and mediates cell-cell adhesion by heterophilic binding during *Dictyostelium development. Dev Biol*, **227**, 734-45.

Wang, Y., Liu, J. and Segall, J. E. (1998) MAP kinase function in amoeboid chemotaxis. *J Cell Sci*, **111**, 373-83.

Wassarman, D. A., Therrien, M. and Rubin, G. M. (1995) The Ras signaling pathway in *Drosophila. Curr Opin Genet Dev*, **5**, 44-50.

Watts, D. and Ashworth, J. (1970) Growth of myxamoebae of the cellular slime mould *Dictyostelium discoideum* in axenic culture. *Biochem J*, **119**, 171-174.

Weeks, G. (2000) Signalling molecules involved in cellular differentiation during *Dictyostelium* morphogenesis. *Curr Opin Microbiol*, **3**, 625-30.

Weeks, G. and Spiegelman, G. B. (2003) Roles played by Ras subfamily proteins in the cell and developmental biology of microorganisms. *Cell Signal*, **15**, 901-9.

Wetterauer, B. W., Salger, K., Carballo-Metzner, C. and MacWilliams, H. K. (1995) Cell-density-dependent repression of discoidin in *Dictyostelium discoideum. Differentiation,* **59,** 289-297.

Wilkins, A., Chubb, J. R. and Insall, R. H. (2000a) A novel *Dictyostelium* RasGEF is required for normal endocytosis, cell motility and multicellular development. *Curr Biol*, **10**, 1427-37.

Wilkins, A, Khosla M, Fraser DJ, Spiegelman GB, Fisher PR, Weeks G, Insall RH. (2000b) *Dictyostelium* RasD is required for normal phototaxis, but not differentiation. *Genes Dev*, **14**, 1407-13.

Wilkins, A. and Insall, R. H. (2001) Small GTPases in *Dictyostelium*: lessons from a social amoeba. *Trends Genet,* **17**, 41-48.

Williams, H. P. and Harwood, A. J. (2003) Cell polarity and *Dictyostelium* development. *Curr Opin Microbiol*, **6**, 621-7.

Williams, R. L. (1999) Mammalian phosphoinositide-specific phospholipase C *Biochim Biophys Acta*, **1441**, 255-67.

Wilm, M., Shevchenko, A., Houthaeve, T., Breit, S., Schweigerer, L., Fotsis, T. and Mann, M. (1996) Femtomole sequencing of proteins from polyacrylamide gels by nano-electrospray mass spectrometry. *Nature*, **379**, 466-9.

Wolthuis, R. M. and Bos, J. L. (1999) Ras caught in another affair: the exchange factors for Ral. *Curr Opin Genet Dev*, **9**, 112-7.

Wong, E. F., Brar, S. K., Sesaki, H., Yang, C. and Siu C. H. (1996) Molecular cloning and characterization of DdCAD-1, a Ca2+-dependent cell-cell adhesion molecule, in *Dictyostelium discoideum*. *J Biol Chem*, **271**, 16399-408.

Wong, E., Yang, C., Wang, J., Fuller, D., Loomis, W. F. and Siu C. H. (2002) Disruption of the gene encoding the cell adhesion molecule DdCAD-1 leads to aberrant cell sorting and cell-type proportioning during *Dictyostelium* development. *Development*, **129**, 3839-50.

Yanagida, M., Miura, Y., Yagasaki, K., Taoka, M., Isobe, T. and Takahashi, N. (2000) Matrix assisted laser desorption/ionization-time of flight-mass spectrometry analysis of proteins detected by anti-phosphotyrosine antibody on two-dimensional-gels of fibrolast cell lysates after tumor necrosis factor-alpha stimulation. *Electrophoresis*, **21**, 1890-8.

Yang, C., Brar, S. K., Desbarats, L. and Siu, C. H. (1997) Synthesis of the Ca(2+)-dependent cell adhesion molecule DdCAD-1 is regulated by multiple factors during *Dictyostelium* development. *Differentiation*, **61**, 275-84.

Yang, H., Cooley, D., Legakis, J. E., Ge, Q., Andrade, R. and Mattingly, R. R. (2003) Phosphorylation of the Ras-GRF1 exchange factor at Ser916/898 reveals activation of Ras signaling in the cerebral cortex. *J Biol Chem*, **278**, 13278-85.

Yeung, Y. G., Wang, Y., Einstein, D. B., Lee, P. S. and Stanley, E. R. (1998) Colony-stimulating factor-1 stimulates the formation of multimeric cytosolic complexes of signaling proteins and cytoskeletal components in macrophages. *J Biol Chem*, **273**, 17128-37.

Yuan, X. and Desiderio, D. M. (2003) Proteomics analysis of phosphotyrosyl-proteins in human lumbar cerebrospinal fluid. *J Proteome Res*, **2**, 476-87.

Yuen, I. S., Jain, R., Bishop, J. D., Lindsey, D. F., Deery, W. J., Van Haastert, P. J. and Gomer, R. H. (1995) A density-sensing factor regulates signal transduction in *Dictyostelium*. *J Cell Biol*, **129**, 1251-62.

Zeng, C., Anjard, C., Riemann, K., Konzok, A. and Nellen, W. (2000) gdt1, a new signal transduction component for negative regulation of the growth-differentiation transition in *Dictyostelium discoideum*. *Mol Biol Cell*, **11**, 1631-43.

Zhang, T., Rebstein, P. J., Khosla, M., Cardelli, J., Buczynski, G., Bush, J., Spiegelman, G. B. and Weeks, G. (1999) A mutation that separates the RasG signals that regulate development and cytoskeletal function in *Dictyostelium*. *Exp Cell Res*, **247**, 356-66.

Zhang, N., Long, Y. and Devreotes, P. N. (2001) Ggamma in *Dictyostelium*: its role in localization of gbetagamma to the membrane is required for chemotaxis in shallow gradients. *Mol Biol Cell*, **12**, 3204-13.

Zhou, H., Watts, J. D. and R. Aebersold, R. (2001) A systematic approach to the analysis of protein phosphorylation. *Nat Biotechnol*, **19**, 375-378.

Zhou, K., Takegawa, K., Emr, S. D. and Firtel, R. A. (1995) A phosphatidylinositol (PI) kinase gene family in *Dictyostelium discoideum*: biological roles of putative mammalian p110 and yeast Vps34p PI 3-kinase homologs during growth and development. *Mol Cell Biol*, **15**, 5645-56.

Zhukovskaya, N. V., Fukuzawa, M., Tsujioka, M., Jermyn, K. A., Kawata, T., Abe, T., Zvelebil, M. and Williams, J. G. (2004) Dd-STATb, a *Dictyostelium* STAT protein with a highly aberrant SH2 domain, functions as a regulator of gene expression during growth and early development. *Development*, **131**, 447-58.